Fishery Manuscript Series No. 13-07

Evaluating Error in Sockeye Salmon Abundance Estimates from Salmon Traveling Outside the Sonar Beam at the Yentna, Copper, and Kenai Rivers

by

Suzanne L. Maxwell,

April V. Faulkner,

and

Theodore D. Hacklin

November 2013

Alaska Department of Fish and Game **Divisions of Sport Fish and Commercial Fisheries**

Symbols and Abbreviations

The following symbols and abbreviations, and others approved for the Système International d'Unités (SI), are used without definition in the following reports by the Divisions of Sport Fish and of Commercial Fisheries: Fishery Manuscripts, Fishery Data Series Reports, Fishery Management Reports, and Special Publications. All others, including deviations from definitions listed below, are noted in the text at first mention, as well as in the titles or footnotes of tables, and in figure or figure captions.

Weights and measures (metric)

centimeter	cm
deciliter	dL
gram	g
hectare	ha
kilogram	kg
kilometer	km
liter	L
meter	m
milliliter	mL
millimeter	mm

Weights and measures (English)

cubic feet per second	ft^3/s
foot	ft
gallon	gal
inch	in
mile	mi
nautical mile	nmi
ounce	oz
pound	lb
quart	qt
yard	yd

Time and temperature

day	d
degrees Celsius	°C
degrees Fahrenheit	°F
degrees kelvin	K
hour	h
minute	min
second	s

Physics and chemistry

all atomic symbols	
alternating current	AC
ampere	A
calorie	cal
direct current	DC
hertz	Hz
horsepower	hp
hydrogen ion activity (negative log of)	pH
parts per million	ppm
parts per thousand	ppt, ‰
volts	V
watts	W

General

Alaska Administrative Code	AAC
all commonly accepted abbreviations	e.g., Mr., Mrs., AM, PM, etc.
all commonly accepted professional titles	e.g., Dr., Ph.D., R.N., etc.
at	@
compass directions:	
east	E
north	N
south	S
west	W
copyright	©
corporate suffixes:	
Company	Co.
Corporation	Corp.
Incorporated	Inc.
Limited	Ltd.
District of Columbia	D.C.
et alii (and others)	et al.
et cetera (and so forth)	etc.
exempli gratia (for example)	e.g.
Federal Information Code	FIC
id est (that is)	i.e.
latitude or longitude	lat or long
monetary symbols (U.S.)	$, ¢
months (tables and figures): first three letters	Jan,...,Dec
registered trademark	®
trademark	™
United States (adjective)	U.S.
United States of America (noun)	USA
U.S.C.	United States Code
U.S. state	use two-letter abbreviations (e.g., AK, WA)

Mathematics, statistics

all standard mathematical signs, symbols and abbreviations	
alternate hypothesis	H_A
base of natural logarithm	*e*
catch per unit effort	CPUE
coefficient of variation	CV
common test statistics	(F, t, χ^2, etc.)
confidence interval	CI
correlation coefficient (multiple)	R
correlation coefficient (simple)	r
covariance	cov
degree (angular)	°
degrees of freedom	df
expected value	*E*
greater than	>
greater than or equal to	≥
harvest per unit effort	HPUE
less than	<
less than or equal to	≤
logarithm (natural)	ln
logarithm (base 10)	log
logarithm (specify base)	log_2, etc.
minute (angular)	'
not significant	NS
null hypothesis	H_O
percent	%
probability	P
probability of a type I error (rejection of the null hypothesis when true)	α
probability of a type II error (acceptance of the null hypothesis when false)	β
second (angular)	"
standard deviation	SD
standard error	SE
variance	
population	Var
sample	var

FISHERY MANUSCRIPT SERIES NO. 13-07

EVALUATING ERROR IN SOCKEYE SALMON ABUNDANCE ESTIMATES FROM SALMON TRAVELING OUTSIDE THE SONAR BEAM AT THE YENTNA, COPPER, AND KENAI RIVERS

by
Suzanne L. Maxwell, April V. Faulkner, and Theodore D. Hacklin
Alaska Department of Fish and Game, Division of Commercial Fisheries, Soldotna

Alaska Department of Fish and Game
Division of Sport Fish, Research and Technical Services
333 Raspberry Road, Anchorage, Alaska, 99518-1565

November 2013

This investigation was partially financed by the Federal Aid in NOAA grant No. 45913 RM&E. The report was prepared by Suzanne Maxwell, April Faulkner, and Theodore Hacklin under award #NAO8NMF4380597 from the National Oceanic and Atmospheric Administration, U.S. Department of Commerce, administered by the Alaska Department of Fish and Game. The statements, findings, conclusions, and recommendations are those of the authors and do not necessarily reflect the views of the National Oceanic and Atmospheric Administration, the U.S. Department of Commerce, or the Alaska Department of Fish and Game.

The Fishery Manuscript Series was established in 1987 by the Division of Sport Fish for the publication of technically-oriented results of several years' work undertaken on a project to address common objectives, provide an overview of work undertaken through multiple projects to address specific research or management goal(s), or new and/or highly technical methods, and became a joint divisional series in 2004 with the Division of Commercial Fisheries. Fishery Manuscripts are intended for fishery and other technical professionals. Fishery Manuscripts are available through the Alaska State Library and on the Internet: http://www.adfg.alaska.gov/sf/publications/ This publication has undergone editorial and peer review.

Suzanne L. Maxwell, April V. Faulkner, and Theodore D. Hacklin
Alaska Department of Fish and Game, Division of Commercial Fisheries,
43961 Kalifornsky Beach Rd. Suite B, Soldotna, Alaska, USA

This document should be cited as:
Maxwell, S. L., A. V. Faulkner, and T. D. Hacklin. 2013. Evaluating error in sockeye salmon abundance estimates from salmon traveling outside the sonar beam at the Yentna, Copper, and Kenai rivers. Alaska Department of Fish and Game, Fishery Manuscript Series No. 13-07, Anchorage.

The Alaska Department of Fish and Game (ADF&G) administers all programs and activities free from discrimination based on race, color, national origin, age, sex, religion, marital status, pregnancy, parenthood, or disability. The department administers all programs and activities in compliance with Title VI of the Civil Rights Act of 1964, Section 504 of the Rehabilitation Act of 1973, Title II of the Americans with Disabilities Act (ADA) of 1990, the Age Discrimination Act of 1975, and Title IX of the Education Amendments of 1972.

If you believe you have been discriminated against in any program, activity, or facility please write:
ADF&G ADA Coordinator, P.O. Box 115526, Juneau, AK 99811-5526
U.S. Fish and Wildlife Service, 4401 N. Fairfax Drive, MS 2042, Arlington, VA 22203
Office of Equal Opportunity, U.S. Department of the Interior, 1849 C Street NW MS 5230, Washington DC 20240

The department's ADA Coordinator can be reached via phone at the following numbers:
(VOICE) 907-465-6077, (Statewide Telecommunication Device for the Deaf) 1-800-478-3648,
(Juneau TDD) 907-465-3646, or (FAX) 907-465-6078

For information on alternative formats and questions on this publication, please contact:
ADF&G, Division of Sport Fish, Research and Technical Services, 333 Raspberry Rd, Anchorage AK 99518 (907) 267-2375

TABLE OF CONTENTS

Page

LIST OF TABLES iii

LIST OF FIGURES iii

LIST OF APPENDICES v

ABSTRACT 1

INTRODUCTION 1

OBJECTIVES 3

CHAPTER 1: YENTNA RIVER 3

Study Site 3

METHODS YENTNA RIVER 3

Cross-river Study 4

- Data Processing, Interpolation, and Expansion 5
- Comparing Fish Distributions 5
- Error in Range Calculations: The Problem with 2-dimensional Spatial Data 6
- Fish Range and Depth from the Mobile v-DIDSON 7
- Depth Values 9

Vertical Study 10

- Equipment and Deployment 10
- Data Collection and Processing 10
- Estimating Fish Outside the h-DIDSON Beam 10
  - Beam Mapping 11
  - Modeled Beam Method 11
  - Examining the Effect of Tilt Angle on Fish Detection 12
  - Count Comparison Method 12

RESULTS YENTNA RIVER 13

Cross-river Study 13

- Differences between h- and v-DIDSON Images 13
- Cross-river and Shore-based Fish Distributions 13
- Error in Range and Depth from Using Slant Measures 14
- Cross-river Fish Distributions: Adding Depth 15
  - Tilt-Depth Check 15

Vertical Study 15

- Beam Mapping 16
- Modeled Beam Method 16
- Count Comparison Method 17

DISCUSSION YENTNA RIVER 17

Cross-river Study 18

- Comparison of h- and v-DIDSONs for Mobile Surveys 18
- Comparison of Cross-river and Shore-based Fish Distributions 19
- Error in Range and Depth from Using Slant Measures 20
- Range and Depth from Mobile DIDSONs 21

Vertical Study 21

- The Effect of Changes in Tilt Angle on Fish Passage Estimates 22

RECOMMENDATIONS AND FUTURE WORK 22

CHAPTER 2: COPPER RIVER 23

TABLE OF CONTENTS (Continued)

Page

Study Site....23
METHODS COPPER RIVER....24
Cross-River Study....24
Data Processing....24
Interpolating and Expanding Fish Counts....24
Vertical Study....25
RESULTS COPPER RIVER....25
Cross-River Study....25
Vertical Study South Bank....25
DISCUSSION AND RECOMMENDATIONS COPPER RIVER....26
Cross-river Study....26
Vertical Study....27
Recommendations and Future Work....28
CHAPTER 3: KENAI RIVER....28
Study Site....28
METHODS KENAI RIVER....28
Cross-River Study....28
Data Processing and Interpolating....29
Vertical Study....29
RESULTS KENAI RIVER....29
Cross-river Study....29
Vertical Study....30
DISCUSSION AND RECOMMENDATIONS KENAI RIVER....31
Cross River Study....31
Vertical Study....32
Recommendations and Future Work....32
ACKNOWLEDGEMENTS....33
REFERENCES CITED....34
TABLES AND FIGURES....37
APPENDIX A: YENTNA RIVER EQUIPMENT SETUP....101
APPENDIX B: YENTNA RIVER WATER LEVEL CHANGES....107
APPENDIX C: CROSS-RIVER SURVEY INFORMATION....109
APPENDIX D: YENTNA RIVER FISH COUNTS FROM VERTICAL AND HORIZONTAL DIDSONS....111

LIST OF TABLES

Table **Page**

1 Specifications for the standard and long-range DIDSONs used in this study. 38
2 Differences between Yentna River fish counts from shore-based, horizontal DIDSONs and cross-river, mobile DIDSONs. 39
3 Yentna River bank to bank percentages from shore-based, horizontal DIDSONs and cross-river, mobile DIDSONs. 40
4 The error in Yentna River horizontal distance measurements from using slant range in place of the true range based on sampling ranges and tilt angles used in this study. 41
5 Yentna River percentages and 95% bootstrapped confidence limits of fish within the DIDSON's effective horizontal beam at the Yentna River if tilted at the traditional aim compared with percentages where the beam is raised 7°. 43
6 Depth and average tilt angle by bank and year for the shore-based, vertically and horizontally positioned DIDSONs, Yentna River. 44
7 Comparisons of Yentna River daily fish counts from horizontally and vertically positioned DIDSONs using total ratios, linear regression, and *t*-tests by year and bank. 44
8 Summary of expansion factors from 3 rivers to account for fish swimming outside the detection volume of shore-based, horizontal DIDSONs. 45
9 Percentages of fish from Copper River cross-river transects and a shore-based DIDSON in paired range bins from 2005 and 2006. 45
10 A comparison of the percentages of fish observed in paired range bins from the cross-river surveys and shore-based DIDSONs, Kenai River, 2006 and 2007. 46
11 Percentage of fish within the effective limits of a DIDSON horizontal beam assuming an effective beam width of 14° or 17° along with bootstrapped confidence limits, Kenai River south bank. 47
12 The depth of the vertical and horizontal transducers and average tilt angle, Kenai River south bank. 47

LIST OF FIGURES

Figure **Page**

1 The locations of the Alaska Department of Fish and Game's Yentna, Copper, and Kenai river sonar sites in Southcentral Alaska notated with a square and labeled with the name of the river. 48
2 Bathymetry map of the Yentna River at the sonar site located 9.2 km upriver from the confluence with the Susitna River. 49
3 River bottom profiles of the Yentna River site with the composite DIDSON beam positioned vertically and horizontally. 50
4 Images from a shore-based, horizontally oriented DIDSON showing reflective and non-reflective regions in the river bottom at the Yentna River. 51
5 Shore-based DIDSONs mounted horizontally and vertically using an aluminum H-mount and automated rotator. 52
6 Kenai River mobile DIDSONs mounted with the composite beam positioned horizontally and vertically. 53
7 The spacing between stations for the mobile surveys along the north and south banks of the Yentna River. 54
8 The outermost cross-river stations at the Yentna River illustrating the effective sampling regions, unsampled regions, and the variables used for interpolating the unsampled regions between stations. 55
9 The Yentna River setup used for mobile surveys and the variables used to calculate the distance from shore to a fish observed in DIDSON images. 56
10 As the DIDSON changes tilt angle, the depth of the lens changes 57
11 Diagram showing the change in depth of a DIDSON lens based on the tilt angle and length of the rotational arm. 58
12 Images from a mobile, horizontally oriented DIDSON at the Yentna River showing static river bottoms, likely composed of small gravel, with fish traces and the shadow of a fish. 59

LIST OF FIGURES (Continued)

Figure **Page**

13 Yentna River images from a DIDSON oriented vertically, aimed sideways and down from a boat at the south bank station closest to shore. 60
14 Undulating sand waves along the river bottom from a mobile DIDSON positioned horizontally, aimed sideways and down from a boat at the Yentna River. 61
15 Images of Yentna River fish detectable moving through clouds of silt from mobile DIDSONs positioned horizontally and vertically. 62
16 Cross-river fish distributions by year from mobile, cross-river surveys and a fixed, shore-based sonar, both using DIDSONs, north bank Yentna River. 63
17 Cross-river fish distributions by year from mobile, cross-river surveys and a shore-based sonar, both using DIDSONs, south bank Yentna River. 64
18 South bank frequency distribution of fish averaged across all years of the cross-river study overlaid onto a contour map of the river bottom, Yentna River. 65
19 North bank frequency distribution of fish averaged across all years of the cross-river study overlaid onto a contour map of the river bottom, Yentna River. 66
20 Yentna River range and depth of fish observed from a mobile, vertically positioned DIDSON, 2011 67
21 Yentna River range and depth of fish observed from a mobile, vertically positioned DIDSON, 2012 68
22 A comparison of measured and calculated values for the changes in depth of the DIDSON transducer due to tilt angle for the shore-based H-mount and mobile boat mount. 69
23 Images from the horizontal and vertical DIDSONs showing 3 fish in each image, Yentna south bank, July 27, 2012. 70
24 Modeled nominal and effective beams for the horizontally oriented Yentna River DIDSONs. 71
25 Modeled nominal beams for the vertically oriented Yentna River DIDSONs. 72
26 The effect of changing the tilt angle on the percentage of migrating fish detectable to a horizontally positioned DIDSON 73
27 Yentna River, 2010, density plots of randomly selected fish coordinates with modeled sonar beams illustrating the traditional DIDSON tilt angle used at fish-counting sites and the raised tilt angle that encompassed the largest number of fish. 74
28 Yentna River, 2011, density plots of randomly selected fish coordinates with modeled sonar beams illustrating the traditional DIDSON tilt angle used at fish-counting sites and the raised tilt angle that encompassed the largest number of fish. 75
29 Yentna River, 2012, density plots of randomly selected fish coordinates with modeled sonar beams illustrating the traditional DIDSON tilt angle used at fish-counting sites and the raised tilt angle that encompassed the largest number of fish. 76
30 Yentna River north bank paired daily fish counts from vertically and horizontally oriented DIDSONs. 77
31 Yentna River south bank paired daily fish counts from vertically and horizontally oriented DIDSONs. 78
32 Yentna River north bank paired hourly counts from vertically and horizontally oriented DIDSONs. 79
33 Yentna River south bank paired hourly counts from vertically and horizontally oriented DIDSONs. 80
34 A comparison of paired hourly fish counts from a DIDSON positioned horizontally and vertically by year and bank at the Yentna River. 81
35 The Copper River sonar sites, marked by square markers, below the Million Dollar Bridge at mile 48 of the Copper River Highway, May 15, 2002. 82
36 River bottom profile of the 5° north bank slope and 8.4° south bank slope with a model of the sonar beam, Copper River. 83
37 Bathymetry map of the areas around the north (top) and south bank (bottom) sonar sites at the Copper River. 84
38 Cross-river transects starting from the Copper River north and south banks illustrating the effective sampling regions, unsampled regions, and the variables used for interpolating the unsampled regions between stations. 85
39 A comparison of Copper River cross-river fish distributions from mobile and shore-based DIDSONs with vertical lines marking the approximate end ranges of the shore-based systems. 86
40 Copper River estimated salmon fish passage and water level for 2005 and 2006. 87
41 The effect of changing the tilt angle on the percentage of migrating fish detectable to a horizontally positioned DIDSON. 88

LIST OF FIGURES (Continued)

Figure **Page**

42 Copper River south bank, 2006, density plots of randomly selected fish coordinates with modeled sonar beams illustrating the traditional DIDSON tilt angle used at fish-counting sites and the raised tilt angle that encompassed the largest number of fish. 89
43 Paired 10 min fish counts by day and linear regression comparison obtained from DIDSONs, one with the composite beam positioned vertically and the other horizontally....90
44 Kenai River bathymetry of the sonar site showing locations of the shore-based DIDSONs, docks, and weirs. 91
45 The spacing between stations for the 2007 July to August cross-river surveys at the Kenai River using a mobile DIDSON. 92
46 Diagram of the end stations of the 12 cross-river transects starting from the north and south banks illustrating the effective sampling regions, unsampled regions, and variables used for interpolating the unsampled regions, Kenai River, 2007....93
47 Fish counts summed by range bin from 2 cross-river surveys on July 26, 2006. 94
48 Kenai River cross-river fish distributions from shore-based and mobile surveys showing the raw counts and the percent of total fish in each range bin. 95
49 Daily escapement and water level for the 2007 field season at the Kenai River with the cross-river sampling days marked with stars....96
50 Kenai River bottom profiles with modeled sonar beams representing horizontally positioned and vertically positioned DIDSONs and the results from mapping the vertical detection limits of the beams using a stainless steel sphere along the north bank and a BB-filled plastic sphere along south bank. 97
51 The effect of changing the tilt angle on the percentage of migrating fish detectable to a horizontally positioned DIDSON 98
52 Kenai River south bank, 2006, density plots of randomly selected fish coordinates with modeled sonar beams illustrating the traditional DIDSON tilt angle used at fish-counting sites and the raised tilt angle that encompassed the largest number of fish....99
53 Paired daily fish counts and linear regression comparison obtained from DIDSONs, one with the composite beam positioned vertically and the other horizontally. 100

LIST OF APPENDICES

Appendix **Page**

A1. Yentna River equipment setup for 2010....102
A2. Yentna River equipment setup for 2011....103
A3. Yentna River equipment setup for 2012....104
A4. Satellite view of Yentna River sonar site, 2012 setup. 105
B1. Yentna River water level changes at the sonar site, 2011–2012. 108
C1. The number of transects, time sampled, and fish counted during the cross-river study. 110
D1. Yentna River north bank daily fish counts from vertically and horizontally oriented DIDSONs. 112
D2. Yentna River south bank daily fish counts from vertically and horizontally oriented DIDSONs. 113
D3. Yentna River north bank hourly fish counts from vertically and horizontally oriented DIDSONs....114
D4. Yentna River south bank hourly fish counts from vertically and horizontally oriented DIDSONs. 115

ABSTRACT

Dual-frequency identification sonars (DIDSONs) are used at several sites in Alaska to assess Pacific salmon *Oncorhynchus* spp. escapement. This study examined one potential error source associated with this method, the number of fish migrating outside the ensonified region. We used a mobile DIDSON to assess fish migrating beyond the counting range and a shore-based DIDSON with the large composite beam positioned vertically in the water column to determine whether fish were migrating above or below the beam of the horizontal DIDSON. The main focus of this study was the Yentna River, where salmon escapement estimates appeared to be biased low based on results from a mark–recapture study. Along the north bank, 23% of fish were observed beyond the beam and 12.4% above it, and along the south bank, 1.8% of fish were beyond and the largest error, 42.6%, were above the beam. The north bank offshore component was likely due to the close proximity of a fish wheel used to apportion the sonar count to species. This may be remedied by switching to a new gear type. A modeling exercise showed that the number of fish passing above the beam would be reduced to less than 7% on both banks by raising the beam 7°.

Condensed versions of both studies were performed at the Copper and Kenai rivers. At the Copper River, 14.7% of north bank and 3.7% of south bank fish were observed beyond the shore-based sonar. At the Kenai River, 3.5% were observed mid-river outside the range of the shore-based sonar. Fewer than 3% of fish were observed above the sonar beams along the south shores at either river. No vertical data were collected along the north shores because shallow water columns left little room for fish to pass above the beams.

Key words: acoustics, Copper River, cross-river fish distributions, cross-river surveys, DIDSON, dual-frequency identification sonar, fish distributions, hydroacoustics, Kenai River, Miles Lake, Miles Lake sonar, *Oncorhynchus* spp., riverine acoustics, riverine sonar, salmon, salmon assessment, salmon escapement, sonar, vertical fish distributions, vertical sonar deployments, Yentna River

INTRODUCTION

Active sonar systems have been a primary tool in assessing adult sockeye salmon (*Oncorhynchus nerka*) escapement in large, turbid Alaska rivers for many years (Gaudet 1990; Maxwell 2007; Faulkner and Maxwell 2008; Brazil and Buck 2011; Westerman and Willette 2013). Fishery managers must balance conservation of these stocks and their harvest by commercial, sport, subsistence, and personal use fisheries that generate millions of dollars for local economies and basic food needs for many Alaskans. Daily management decisions require accurate and timely in season estimates. Because commercial fisheries take place in the ocean where fish are more dispersed and assessment is difficult, active sonar systems are often located in the lower reaches of rivers where large numbers of salmon migrate through more constricted regions.

Shallow, wide (>100 m), turbid rivers are challenging environments for sonar systems. Ideally, sonars are deployed at sites where the river bottom drops off evenly from shore with no shallow, slow current regions mid-river, and where current flows are strong enough to keep migrating salmon nearshore and near bottom at sites reasonably close to where the fishery takes place (Gaudet 1990). However, no site selection is perfect. Other logistical factors are also taken into account, such as access and a reasonable place to situate a field camp. At many of the large river sites, the sonar beams are unable to cover the entire width and depth of the river. To maximize sonar coverage where the majority of fish migrate, sonar beams are concentrated close to shore and near the river bottom based on the assumption that migrating salmon take advantage of slower current flows in these regions to conserve energy (Brett 1995; Hinch and Rand 1998, 2000). This assumption is not perfect, but ensonifying the entire width of large rivers is difficult and expensive. Dual-frequency identification sonars[1] (DIDSONs; Belcher et al. 2001) used to

[1] Product names used in this report are included for scientific completeness, but do not constitute a product endorsement.

assess passage rates of migrating salmon at the Yentna, Copper, and Kenai rivers ensonify only a portion of the river's width (24%, 18%, 67%, respectively; Maxwell et al. 2011).

Estimates of sockeye salmon abundance using DIDSON were shown to be accurate and precise when compared in a clear river against visual counts made by an observer at a weir site (Holmes et al. 2006) and a tower site (Maxwell and Gove 2004, 2007). Site-specific differences found in count comparisons between older, echo-counting Bendix sonars and DIDSONs led us to suspect that these same variables may affect salmon passage estimates generated by DIDSONs. The Bendix-DIDSON comparison showed that salmon passage estimates from the 2 sonars were statistically similar at the Copper River, but Bendix counts were substantially lower than DIDSON counts at the Kenai and Yentna rivers (Maxwell et al. 2011). Further comparisons at the Yentna River between apportioned DIDSON and Bendix estimates, upriver weir counts, and mark–recapture abundance estimates (Fair et al. 2009) suggested that both Bendix and DIDSON estimates were low; however, a confounding factor in these comparisons was the apportionment of the sonar-based estimates to species using fish wheels. The fish wheel apportionment method may be selective for smaller fish, i.e., pink salmon (*O. gorbuscha*), hence reducing estimates of sockeye salmon and inflating estimates of pink salmon.

To determine why the Yentna River's sonar counts were low compared to other sources, we first identified potential error sources in the sonar and fish wheel methods. Apportionment errors may result if one species, because of its behavioral tendencies, is more likely to be captured in the fish wheel than another. This error source is currently under investigation in a related study. Error sources related specifically to the sonar estimates include: 1) the sampling design, 2) observer counting errors, 3) fish migrating outside the sonar beam, 4) truncating the field season, and 5) reduced detection of fish within the sonar beam. Potential error from the sampling design was addressed by Becker (1962) and Siebel (1967), who examined the 10 min/h sampling design used at sites where fish are counted in clear streams from towers, the same sampling design adopted for DIDSON projects. The uncertainty in this sample design was further examined and estimated (Reynolds et al. 2007). Observer counting errors have been examined and were shown to be low (Holmes et al. 2006; Maxwell and Gove 2007; Westerman and Willette 2012, 2013). We are currently in the process of examining the potential error from truncating the field season. This study was designed to examine the third potential error source, estimating the numbers of fish migrating outside the sonar beam.

For fish to migrate outside the ensonified region, they have to travel under, over, or beyond the shore-based sonar beam. The DIDSON beam is positioned with the strongest energy of the beam (the beam's center) placed near the river bottom; therefore, fish traveling close to the river bottom will be detected as long as the slope is linear and the signal strength is adequate. We determined the characteristics of the river bottom by examining DIDSON images of it and creating range and depth profiles. To assess the numbers of fish traveling above the beams of shore-based DIDSONs, we deployed a second DIDSON along either shore with the multiple beams (composite beam) positioned vertically (i.e., rotated 90°) to take advantage of the large beam in this dimension and to obtain the depth of migrating fish. To assess the numbers of fish traveling beyond the range of the shore-based sonar, we set up a mobile system. Mobile sonar systems have been used in oceans (Krieger et al. 2001), lakes (Knudsen and Saegrov 2002; Taylor and Maxwell 2007), and rivers (Banneheka et al. 1995; Duncan and Kubecka 1996; Levy and Cadenhead 1995; Lyons 1998) to assess fish populations. Xie et al. (2008) discovered detection issues and disruption in migrating fish behavior in the Frasier River caused by boat

avoidance. For our study, we used a mobile setup with the DIDSON beam directed perpendicular to the current and angled slightly downward from horizontal, allowing us to sample away from the boat to reduce fish avoidance and cover a larger region of river. Fish detection from the DIDSON as compared to single or split-beam sonar should be an improvement because DIDSON's video-like images are easier to interpret than echograms from lower resolution sonars.

OBJECTIVES

Our objectives were to assess the numbers of fish traveling above and beyond sonar beams used to assess fish passage and generate an expansion factor to correct the sonar estimates based on this assessment. To improve the readability, we have separated this report into chapters by river. Although the bulk of this study took place at the Yentna River, similar methods were used to assess fish above and beyond the sonar beam at the Kenai and Copper Rivers, so data from these rivers have been included in separate chapters.

CHAPTER 1: YENTNA RIVER

STUDY SITE

The Yentna River sonar site is 9.2 km upriver from the confluence of the Yentna and Susitna rivers (Figure 1). The site is above tidal influence, the river is highly turbid (secchi disk readings 0.10–0.12 m, Westerman and Willette 2011b; 576 nephelometric turbidity units, Maxwell et al. 2011), and heavily influenced by upriver rains that can increase the water level by several decimeters within a few hours. Sonar deployment sites along both banks were selected because of strong current flows that minimize fish milling and mostly linear river bottom slopes in the region of highest fish passage. The north and south bank sonar sites are offset by ~980 m because suitable sites directly opposite each other could not be found. Shallow, low flow regions occur opposite the selected sites along both banks (Figure 2). We profiled the river bottom along both sides of the river within the range of the shore-based sonars using methods described by Maxwell and Smith (2007) and Faulkner and Maxwell (2009). The south bank river bottom sloped at a 15° angle out to 10 m, where it became relatively flat; the north bank slope was 13° out to 10 m, and 9° beyond (Figure 3). Images from shore-based, fish-counting DIDSONs along either bank show reflective river bottom regions, likely small gravel, interspersed with non-reflective regions, likely fine silt (Figure 4).

METHODS YENTNA RIVER

To determine the number of fish traveling beyond the range or above the beam of the fish-counting sonars, we divided this study into 2 components, mobile cross-river surveys and a fixed, shore-based vertical study. We used standard and long-range DIDSONs whose specifications are listed in Table 1. Describing the setup for each of the multiple configurations is confusing. For example, the DIDSONs were deployed with the composite beams positioned either horizontally or vertically, and in some cases it was necessary to refer to the vertical or horizontal dimension of a beam from either deployment. To simplify the descriptions, we used the following terminology throughout this report:

1) h-DIDSONs were deployed with the composite beam oriented horizontally, the orientation used at our fish-counting sites (Westerman and Willette 2010a, 2010b, 2011a, 2011b, 2012, 2013);
2) v-DIDSONs were deployed with the composite beam oriented vertically, the orientation used for profiling the river bottom (Maxwell and Smith 2007);
3) h-beam refers to the horizontal dimension of the sonar beam;
4) v-beam refers to the vertical dimension of the sonar beam;
5) shore-based DIDSONs were deployed at fixed locations near the shoreline (Figure 5); and
6) mobile DIDSONs were mounted to the side of a boat (Figure 6) and moved across the river from station to station.

We began the mobile surveys with an h-DIDSON and then switched to a v-DIDSON in the final 2 years because we found that it was easier to detect fish using the v-DIDSON. We diagrammed each equipment setup and the year-to-year changes (Appendix A).

CROSS-RIVER STUDY

For the cross-river surveys, we attached a DIDSON to a mount fixed to the side of a boat, motored to a position offshore, and directed the beam perpendicular to current flow at an angle that grazed the river bottom. Small tilt angles (in reference to level) were selected for shallow regions and steeper angles for deeper regions with the goal of ensonifying the region near the river bottom across as large a range as possible at each station. There were 2 reasons for sampling with the beam angled slightly down from horizontal rather than straight down. First, sampling at a shallow angle allowed us to sample away from the boat in regions of the river where fish would be less disturbed by the boat's presence and second, to avoid masking fish echoes with strong bottom reflections. Boat operators motored to fixed stations spaced across the river recording DIDSON data files at each station for 5 min.

We used a standard DIDSON set at high frequency (1.8 MHz) whenever possible because the higher resolution provided more distinct images of fish. When high turbidity scattered the signal and caused the image to fade before the end of the desired sampling range, we switched to low frequency (1.1 MHz). The window length was set based on the range needed to reach the river bottom.

Using a DIDSON for mobile transects required a new methodology compared to previous mobile surveys that used single, dual-beam, or split-beam sonars where data was often collected as the boat moved across the river (Levy and Cadenhead 1995; Lyons 1998). Moving cross-river while recording DIDSON files created blurry images, so we designated a series of fixed stations that spanned the river's width. At each station, the boat was pointed upriver and "held" in place keeping the throttle set at current speed for the length of the sample period. We initially tried anchoring the boat at each station but this proved difficult in the fast-moving current and very time intensive. Boat operators were able to keep the boat in place as long as the winds were low, large debris did not interfere, and there were no serious wakes from boat traffic. If these conditions were not met, samples were re-done or discarded. To maintain the cross-river line as the boat was held in the current, the boat operator used a fixed point along shore and a laser range-finder to measure the distance to shore. During periods of high water and high debris loads, transects were postponed until the water level dropped (which usually happened within a day or two).

Because of the large offset between sonar sites along either bank (Figure 2), we were unable to sample a single transect across the river. Instead, we set up a series of stations: 15, 25, 35, 50, 75, and 100 m measured from the north bank, and from the south bank measured out the same stations, adding a station at 125 m because of the wider river width (Figure 7). Additional stations were sampled, but we truncated the data near the half-way point, i.e., from the south shore where the river was approximately 240 m wide, fish were included out to 125 m; from the north shore, where the river was approximately 200 m wide, fish were included out to 100 m. This truncation may include a minor overlap between banks. Nearshore stations were positioned closer together than offshore stations to produce a finer distribution in the areas where we expected more fish to pass and to assist us with aligning the resulting cross-river distribution with the more limited range distribution from the shore-based sonars.

Data Processing, Interpolation, and Expansion

Staff visually counted fish in DIDSON images and for each sample logged the date, time, DIDSON file name, effective start (*sr*) and end range (*er*), the approximate tilt angle, and the fish image quality. Based on our assumption that fish travel near the river bottom, we determined that the effective sampling range encompassed only the portion of the beam that reached the river bottom, so for each sample, *sr* and *er* were based on the range where we first observed the river bottom image and where it ended. For each transect, fish counted within a station were assigned the mid-range of the effective sampling region for that station (Figure 8).

The sampling regions left portions of the river width unsampled. Because we assumed that fish migrate mostly near the river bottom, upriver and not cross-river, and it only takes a few seconds to travel across the beam, it was not necessary to account for the volume covered by the sonar beam, only the one-dimensional cross-river line between samples.

We interpolated counts for the unsampled range between stations and between shore and the first and last station. The variables used for the interpolation process are diagrammed and explained in Figure 8. To interpolate unsampled regions between middle stations, i.e., stations not along the edges, we first determined the effective sampling range (*eff*) and calculated fish density (*Fd*) using the fish count (*FC*) for each station (*i*),

$$Fd_i = \frac{FC_i}{eff_i}. \tag{1}$$

We then averaged Fd_i and Fd_{i+1} and multiplied by the unsampled distance ($us_{i,i+1}$) to obtain an interpolated fish count (*IFC*). To interpolate from the first station to shore, we averaged Fd_1 and 0 and then multiplied by the unsampled distance from er_1 to shore. To expand the count from the last station to the half-way point, we averaged Fd_{last} and 0 and multiplied by the unsampled distance from sr_{last} to the half-river point. We assigned the mid-ranges of the unsampled regions to interpolated values and inserted them into the cross-river fish distribution.

Comparing Fish Distributions

We aligned the cross-river and shore-based fish distributions to determine the percentage of fish beyond the range of the shore-based units. Shore-based, h-DIDSON counts were obtained from operations along both sides of the river that use the fish counts for estimating salmon escapement (Westerman and Willette 2011b, 2012, 2013). For this comparison, we extracted blocks of data from the shore-based sonars that were recorded while the cross-river transects were in progress

and obtained range distributions by marking fish traces on echograms produced using the Sound Metrics Corporation (SMC) Echogram program (*Processing/Echogram/View Echogram*). Time and range information were exported, and the range data were binned in increments that matched the cross-river data. Range bins from the cross-river data were a combination of the effective regions sampled and the unsampled, interpolated regions. Because the range sampled depended upon the river bottom coverage of each sample, the bin sizes were unequal.

The cross-river method referenced fish range to shore, while echogram range values were referenced to the transducer. To pair the datasets, the distance between shore and the shore-based transducer was added to the fish range obtained from the echograms, and the cross-river fish counts and interpolated values were expanded to match the time sampled in the shore-based blocks of data.

Error in Range Calculations: The Problem with 2-dimensional Spatial Data

Whether the DIDSON is oriented horizontally or vertically, each position lacks one spatial dimension of information. For the h-DIDSON, we can measure the angle of the fish from the beam center in the horizontal (upriver-downriver) plane θ_{fh} but not the angle of the fish from the beam center in the vertical plane, θ_{fv}. For the v-DIDSON, we can measure θ_{fv} but not θ_{fh}.

An important note is that a range measurement using the measure tool in the DIDSON software is the slant range (*Rslant*), or polar coordinate, which is the time it takes a ping to travel out, reflect off a target, and return to the transducer, multiplied by 2 × sound speed (for the round trip). The sound speed was calculated based on water temperature (Simmonds and MacLennan 2005) measured daily and input into the DIDSON.ini file if it changed more than 2° Celsius.

To determine the true horizontal distance of a fish from the transducer it is necessary to take into account the tilt angle of the transducer relative to level, θ_t, and the fish's off-axis angles in the horizontal and vertical dimensions, θ_{fh} and θ_{fv}. This applies to both h- and v-DIDSONs. To convert *Rslant* to the rectangular coordinate *Rrect*, the true horizontal distance, the following calculations (diagrammed in Figure 9) are needed:

$$Rrect_h = Rslant \times \cos(\theta_{fh}); \tag{2}$$

$$Rrect_v = Rslant \times \cos(\theta_t + \theta_{fv}); \text{ and} \tag{3}$$

$$Rrect = Rslant - [(Rslant - Rrect_h) + (Rslant - Rrect_v)]. \tag{4}$$

Because *Rslant* is the same from either perspective, Equation 4 simplifies to:

$$Rrect = Rrect_h + Rrect_v - Rslant. \tag{5}$$

In the Equations above, *h* and *v* subscripts refer to horizontal and vertical dimensions of the sonar beam within the river whether an h-DIDSON or v-DIDSON was used.

The effective start and end ranges from the cross-river surveys were *Rslant* values and so were range values output from the SMC echogram program. In the echogram data (shore-based, h-

DIDSONs) there is no information in the vertical dimension; i.e., θ_{fv} is unknown, and θ_{fh} values are not included in the calculation nor in the output. For the cross-river surveys, although we were able to mark every fish in the cross-river DIDSON images, interpolating the unsampled regions made it necessary to retain the data within bins, and those bins contained a range of tilt and fish angles, so no adjustments were made to *Rslant*. For both of these datasets, we can assume that the maximum error in the range value occurred when the transducer was tilted at its lowermost angle and fish were at the lowermost vertical and outermost horizontal edges of the sonar beam.

We calculated the maximum potential error from using *Rslant* (*Rslant* error) for determining range and depth values by inputting the maximum *Rslant* from detected fish, the lowermost tilt angle, and the maximum off-axis angles in both dimensions; i.e., the half-beam dimensions, into Equations 2–5 to obtain *Rrect*. We then determined the difference and percent error between *Rslant* and *Rrect* using *Rrect* as the reference value. Moving away from the center beam line lengthens a distance measure between 2 points, so *Rslant* values are always larger than *Rrect* values. The error in depth values was also determined based on the use of *Rslant*. This error was dependent only on the composite beam angle and maximum end range of the samples because the depth calculations (below) took into account both θ_t and θ_{fv} so the only error from using *Rslant* was from not knowing θ_{fh}.

Although both shore-based and cross-river systems used *Rslant*, the error from the two systems was not equivalent and therefore could not be discounted. *Rslant* error from the shore-based h-DIDSONs was reduced because the beam width for drawing the echogram was constricted to the center 4 beams, which essentially removed the error from $Rrect_h$ but not $Rrect_v$. The processing of the cross-river data did not exclude error from either dimension.

Fish Range and Depth from the Mobile v-DIDSON

By switching from a horizontal orientation to a vertical one for the mobile surveys, we were able to build a cross-river distribution that included both the range and depth of fish, but we had to give up θ_{fh}.

Processing the cross-river v-DIDSON data proved to be challenging. The first issue that we encountered was attaching the v-DIDSON to the mounting bracket, which could be attached to either the right- or left-hand side. We have the same problem when obtaining river bottom profiles from shore-based systems. When collecting profile data, we positioned the DIDSON on the right-hand side (with the mount facing offshore) so that the orientation was always the same. If the DIDSON is placed on the opposite side, it became confusing to process data. SMC's data processing algorithm produces a menu that states, *Bottom return should tilt toward right side (positive theta) with increasing range if depth is increasing. Use reverse control to flip image if necessary*. While this message makes sense when the DIDSON is placed in shallow water and directed offshore into deeper water, the correct orientation is more difficult to discern when the DIDSON is angled from the side of a boat and the river bottom slant is unknown. If oriented incorrectly or worse, inconsistently, the calculated depth values will be wrong (a negative θ_{fv} value is used rather than a positive one) and the user will have to re-process and plot the data in both configurations to determine the correct one. To ensure that we used the correct orientation, we marked the river bottom in each vertical cross-river file and determined the correct depth of

the bottom points by first inputting a positive value and then negative value for θ_{fv}, and then plotting each case to determine the correct angle. Plots made from incorrect angles did not line up between segments; instead, the incorrect points were arranged in a series of slanted diagonals.

To process the v-DIDSON data, Bill Hanot (Sound Metrics Corporation, Vice President) modified a program in the DIDSON software (*Processing/Special/Mark Depth Profile*) that was originally written to produce river bottom profiles from shore-based DIDSONs (Maxwell and Smith 2007). The original program required the user to input the transducer tilt angle and the distance from the center of the lens to the water's surface, and then mark along the river bottom in the image using marks that persisted until the user exited the program. Upon exiting, a text file was exported with the range and depth of each mark. In the new program (*Processing/Special/Mark Fish Profile*), marks persist for 1 s and then disappear so fish images can be marked throughout a file. The modified program exports date, time, range ($Rrect_v$) depth, theta (angle of the fish from the central beam), tilt angle (if the DIDSON contains an attitude sensor), and latitude and longitude (if a Global Positioning System, GPS, is used) for each marked fish along with the location and name of the source file and the depth and tilt input by the user. Prior to 2010, the *Mark Depth Profile* program exported *Rslant*; after July 2010, both programs were modified to export rectangular range, $Rrect_v$, based on the single transducer tilt angle input by the user.

This algorithm works well for profiling because the transducer is deployed at a fixed, stable location, but sampling from a boat created a new problem, an unstable platform where the tilt angle fluctuated during sampling. Because of this instability, we did not use the exported fish range or depth values, but instead, recalculated these variables using the exported tilt angle for the frame in which a fish was marked. The first step in this process was to convert $Rrect_v$ back to *Rslant* for each marked fish (i) using the single tilt angle input by the user, θ_t,

$$Rslant_i = \frac{Rrect_{vi}}{\cos(\theta_t + \theta_{fi})} \quad . \tag{6}$$

We then re-calculated a more accurate $Rrect_{vi}$ using θ_{ti} (the tilt angle recorded in the frame a fish was marked in). Determining the distance of each fish (i) to shore ($dist_f$) required 2 additional factors, the distance of the boat to shore ($dist_b$) and an offset (*x.offset*). Although the boat was aligned using points along both shores, and its position relative to shore was measured with a laser rangefinder, swirling currents occasionally moved the boat from its designated position. To obtain an *x.offset* and provide a ground truth for the final range (and depth) values, we exported a river bottom profile from each station of each transect from the cross-river data (mini profiles) and aligned these mini profiles and the fish that went with them with river bottom profiles from the shore-based DIDSONs in overlapping regions. With the boat oriented perpendicular to shore, pointed upriver, and the DIDSON beam pointed toward shore, the distance of each fish to shore was

$$dist_{fi} = dist_{bi} - Rrect_{vi} - x.offset_i \quad . \tag{7}$$

Depth Values

Determining the depth of each fish involved several steps. First, the distance of each fish relative to a level line drawn at the top of the transducer (dL_i) was determined,

$$dL_i = Rslant_i \times \sin(\theta_{fi} + \theta_{ti}) \quad . \tag{8}$$

As was mentioned earlier, the *Mark Fish Profile* program requires the user to input both the tilt angle *and* the distance of the transducer from the river's surface, but as the tilt angle changes, so does the depth of the lens; i.e., the farther down the transducer is tilted, the deeper the center of the lens. The DIDSON was equipped with an internal attitude sensor, so tilt angle was available for each frame, but measuring the lens depth for every fish was not possible. Instead, we calculated the lens depth based on the exported tilt angles. In order to make this work, we input 0 into the *Mark Fish Profile* program for the distance to the river's surface for all files during processing. After studying the mounting setup, we determined that as the transducer was tilted down from level, the length of the rotational arm caused the end of the lens to trace an elliptical arc rather than a circular one (Figure 10 illustrates variables for a circular arc). To take into account this more flattened ellipse, depth values *d1* and *d2* (diagrammed in Figure 11) were calculated for each fish using the tilt angle for the frame the fish was observed in θt_i,

$$d1_i = Lpivot \times \sin \theta t_i \text{, and} \tag{9}$$

$$d2_i = -Larm \times \cos \theta t_i \quad . \tag{10}$$

To determine whether these equations were accurate for the mounts used in this study, we set up the shore-based and mobile mounts in a lab and measured the change in depth at the end of the lens for a wide range of tilt angles and then compared the measured depths to calculated values.

The next depth variable, the distance from the river's surface to the pivot point (*d3*); i.e., the top of the transducer when level, was measured and kept constant between years. To compare transects across several days at this site where the water level was dynamic, a fourth depth variable, *d4*, the change in water level, was added. Water level was measured multiple times per day at the Yentna River using a staff gauge. We selected the measurement closest to the start time of each transect, setting *d4* to 0 for the first transect of each year and either subtracting or adding changes in water level, changes that varied from 0 to 0.911 m between transects (Appendix B).

The final adjustment, the *y.offset*, added to account for boat movement, was obtained from aligning the mini profiles with the shore-based river bottom profiles.

The final depth for each fish was the sum of all depth factors (Figure 11):

$$Dtotal = dL + d1 + d2 + d3 + d4 + y.offset \quad . \tag{11}$$

Using x-offsets makes sense if the boat drifts closer or farther from shore, while y-offsets make sense if the boat drifts up or downriver and ends up over a region with different river bottom topography. For our alignment, we attempted to align the river bottoms using x-offsets when

possible. For the cross-river work, we considered using a GPS instead of the laser rangefinder, but found that without a base station at the Yentna River, error levels were as high as 13 m.

VERTICAL STUDY

Equipment and Deployment

We deployed a v-DIDSON adjacent to the shore-based h-DIDSONs along either side of the river (Appendix A). Each DIDSON was attached to an automated rotator mounted to an aluminum stand that allowed us to pan and tilt remotely after deployment (Figure 5). In 2010 and 2011, we only had one standard DIDSON available to sample both sides of the river for the vertical study and perform the cross-river transects. We deployed the unit along the south bank for a period of 3 days, then pulled the system and attached it to the boat for the cross-river transects, re-deployed it along the north bank for an additional 3 days, and then performed a cross-river transect before returning it to the south bank. This sequence was repeated throughout the field season. In 2012, a second DIDSON became available, and we placed one on the north bank for the entire season and used the south bank unit for cross-river transects and vertical data. Shore-based h-DIDSONs used in 2010 were long-range units, but were changed to standard units in 2011–2012 because the long-range units did not substantially extend the sampling range.

Another change between years was the location of the south bank sonar site. In 2010, we deployed both shore-based systems adjacent to each other at the traditional site. In 2011, we moved the v-DIDSON to the new site (Figure 2; Appendix A2), leaving the h-DIDSON deployed at the traditional site, but by 2012, the traditional south bank site had degraded and it became necessary to move the h-DIDSON to the new site. The river topography had changed, bringing fast current close to shore that created problems for sonar deployment and operations. The new site had a longer, straighter shoreline with a small region of slow current nearshore that provided an easier place to deploy the sonars.

Data Collection and Processing

We recorded two 10-min samples, 1–10 m (nearshore) and 10–30 m (offshore), per hour for the h- and v-DIDSONs. The offshore strata were sampled using low frequency, while the nearshore strata were sampled using high or low frequency depending on water level and turbidity. If the river's turbidity significantly reduced the effective range of the high frequency beam in the nearshore strata, low frequency was used. To avoid cross-talk, only 1 sonar can transmit at a time, so recordings from the 2 systems were interleaved within each hour. The DIDSON sampling program (*Image/Capture/Timer Data Entry*) allows the user to set up timed samples at designated intervals to allow sampling of multiple strata with different settings for frame rate, receiver gain, sampling range, and frequency. Bill Hanot of SMC added a function to this program that allows the user to disable the transmitter when the unit is not recording to avoid crosstalk.

The *Mark Fish Profile* program used to process DIDSON files for the cross-river work was also used for the vertical data. The exported columns used for this study included the date, time, range and depth for each marked fish.

Estimating Fish Outside the h-DIDSON Beam

We estimated the percentage of fish observed outside the beam limits of the h-DIDSONs using a modeled beam method and a count comparison. For the modeled beam method, we used the

parameters of the effective beam determined from mapping out the beam edges using an artificial target, and the range and depth of fish observed with the v-DIDSONs to determine the percentage of fish that would have passed within the effective beam edges of the h-DIDSONs. This method allowed us to examine whether altering the transducer tilt angles would increase the percentage of fish that would have been observed by the h-DIDSONs. The second method was a direct comparison of the numbers of fish counted from the 2 systems.

Beam Mapping

For the modeled beam method, it was necessary to determine the vertical dimension of the effective beam for the h-DIDSON. The horizontal orientation of the DIDSON provides no information about the vertical position of a target in the beam, instead, the individual beams resemble single-beam sonars; i.e., the edges of the beam depend on the target's size and position. Small targets close to the beam edge reflect less energy and appear very faint or not at all in DIDSON images and turbidity reduces the echo energy, so the size of the beam in this dimension is target and site specific.

To estimate the vertical beam edges for a sockeye salmon at the Yentna River site, we used an artificial target similar in acoustic strength to a sockeye salmon (a 10.16 cm stainless steel sphere). The target was lowered into the river from the side of a boat, centered in the sonar beam visually using the target's image, and then moved from the river bottom to surface. The h-DIDSON was operated using the same settings that were used for normal fish counting. We determined the top and bottom depth of the effective beam by holding the target at the uppermost and lowermost position it was observed in the DIDSON image, pulling the target from the water and measuring the distance from the bottom of the target to the position where the line encountered the water's surface. The target was placed near the transducer and then moved offshore incrementally until we were unable to find the target in the DIDSON image.

We also mapped out the vertical dimension of the v-beam. In this dimension, the individual beams that make up the composite beam are stacked from the river bottom to surface. Theoretically, at 10 m the dimension of 1 individual beam (standard DIDSON, high-frequency 0.3° beam) is about half the size of the stainless steel target (5.26 cm). Moving the target through the beam in this dimension moves it through the region of strongest energy, the center, of each individual beam, so we expected to see the target across the entire 28° field of view even though the beam energy in the outer beams is less (Bill Hanot, Sound Metrics Corporation, Vice President, personal communication).

Modeled Beam Method

We determined whether each fish observed with the v-DIDSONs would have traveled within or outside the confines of the h-DIDSON beams by calculating the depth of the top (*t.bm*) and bottom (*b.bm*) beam edges using the effective size of the h-DIDSON beam (*bw.h*), its depth below the river's surface (*yoffset.h*), its tilt angle (*tilt.h*), and the range (*Rg*) of fish *i*:

$$t.bm_i = yoffset.h + Rg_i \times \sin(tilt.h + 0.5bw.h) \text{, and} \tag{12}$$

$$b.bm_i = yoffset.h + Rg_i \times \sin(tilt.h - 0.5bw.h) \text{.} \tag{13}$$

Next, we compared the depth of each fish to $t.bm_i$ and $b.bm_i$ to determine whether each fish was within or outside the effective beam. Once a list was made of fish outside the beam (*fob*), we determined the percentage of fish within the h-beam (*fib.p*) where *n* is the total number of fish observed,

$$fib.p = 100 - \frac{100 \times fob}{n} \quad . \tag{14}$$

Bootstrapping Equations 12–14 using 1,000 iterations gave us a mean, median, and 95% confidence intervals (CI) for *fib.p*.

We determined the dimensions of both the h- and v-beams using Equations 12 and 13, substituting the minimum and maximum fish ranges for *Rg*, and overlaid these modeled beams on top of the fish and river bottom coordinates to provide a visual look at the relationship between the fish coordinates and the beam's position. Because of the large number of fish detected, we randomly selected 2,000 fish coordinates for the plot. We then created a matrix of fish coordinates by range and depth and plotted a density plot by river bank and year.

Examining the Effect of Tilt Angle on Fish Detection

Prior to using DIDSON, a much narrower vertical beam was required to ensonify fish in rivers because the beam had to fit entirely within the river's surface and bottom boundaries (Gaudet 1990; Maxwell 2007). The DIDSON's video-like image allowed us to push excess beam into the river bottom and still detect fish, and the large beam made it less likely that fish would swim over the top of the beam. However, even the large dimension of the h-beam did not fill the water column at the Yentna River and a tilt angle had to be selected that would maximize fish detection along both banks. We have traditionally selected tilt angles that placed the central axis of the beam just above the river bottom following the aiming protocol outlined by Maxwell and Smith (2007). However, the DIDSONs were moved inshore and offshore as water levels changed and the aim did not remain constant between moves. With each move, it was impractical to redo profiles of the river bottom, so the technician visually determined a new aim based on river bottom images from the DIDSON, resulting in a range of tilt angles over the course of the field season, although typically technicians restricted new aims to a narrow band around the original tilt angle selected. To test the effect of tilt angle on the percentage of fish from the v-DIDSONs that would have been observed with the h-DIDSONs, we applied Equations 12–14 across a range of tilt angles.

Count Comparison Method

We compared the numbers of fish counted from the shore-based v- and h-DIDSONs. Although data were not recorded simultaneously, the 2 systems were sampled for 10 min within each hour. The h-DIDSONs were sampled along both banks throughout the field season for the purpose of obtaining an estimate of fish passage. The v-DIDSONs were sampled as described above. We paired the 10 min counts by hour for each hour both systems had data, calculated ratios from the total counts, performed linear regression by year and bank, and tested 2 hypotheses: 1) null hypothesis H_o: B_1 *(Slope)* = 0, alternative hypothesis H_A: $B_1 \neq 0$; and 2) null hypothesis H_o: $B_1 = 1$, alternative hypothesis H_A: $B_1 \neq 1$.

RESULTS YENTNA RIVER

CROSS-RIVER STUDY

Differences between h- and v-DIDSON Images

Fish were difficult to detect in the mobile, h-DIDSON images collected in 2010. Although the images more resembled actual fish, unless the range and angle of a fish relative to the transducer resulted in the image appearing separate from the river bottom, the echoes were masked by bottom reflections and it became necessary to count fish shadows rather than direct images (Figure 12). Although in still images, fish shadows were difficult to distinguish from rocks, in moving video, the dark, oval shapes moving across the beam were detectable. Most of the images counted were shadows. In rare instances, we were able to detect a fish and its shadow.

Fish images from the v-DIDSON were blob-shaped and not at all fish-like (Figure 13). They either appeared and disappeared in place or moved up and/or down range. Fish that moved up or down range were easier to identify. Fish images exhibited some persistence between frames. A small blob that appeared and disappeared within a single frame was not likely to be a fish and was not counted. The largest advantage of the v-DIDSON was that all fish were observed above and separate from the river bottom, which appeared as a diagonal line across the image.

The river bottom was relatively stable nearshore, but at stations farther offshore, sand and silt waves appeared in h-DIDSON images as shifting clouds, and in v-DIDSON images as oscillations of the river bottom that resembled twisting ribbons (Figure 14). We also observed clouds resembling tumbleweeds rolling up from the bottom and moving along it. In one transect from station 10 (a station near the opposite bank that was not used in the analyses), we observed 6 fish moving through this cloud. We were able to observe fish in these silt clouds in images from both h- and v-DIDSONs (Figure 15).

Cross-river and Shore-based Fish Distributions

Along the north side of the river, a relatively large percentage of fish observed during the cross-river surveys were beyond the effective range of the shore-based sonar, 43.3% in 2010, although in later years this number was substantially lower, 6.0% in 2011 and 19.7% in 2012 for an overall average of 23.0% (Table 2). Along the south bank, few fish were observed beyond the shore-based sonar, 1.8% on average, with a high of 4.9% in 2012 and a low of 0 in 2010. Expansion factors based on the percentage of offshore fish ranged from 1.00–1.05 along the south bank and 1.06–1.76 along the north bank.

Aligned and paired fish counts from the shore-based and cross-river methods within overlapping regions were not similar; more fish were counted with the shore-based system (Table 2). Larger differences between counts from the 2 methods were observed along the north bank where the percent error averaged 25.2% across the 3 years sampled, while the south bank percent error average was 16.4%. The south bank 2011 paired data were most similar, differing by a single fish. The largest difference occurred in the 2010 south bank counts where substantially more fish were counted with the shore-based system, a percent error of 41.7%.

Most fish were observed in the 2 range bins closest to shore (Figures 16 and 17). Fish migrated farther offshore of the north bank than the south bank and this behavior was most pronounced in 2010. Peak fish passage periods from the cross-river and shore-based distributions were aligned in 2011 and 2012 along both sides of the river. In 2010, fish extended out to the 100 m end range

along the north bank. The lumpiness of the 2010 cross-river distribution was caused by the interpolation and uneven size of the range bins, which were less than 3 m for the sampled regions and as large as 20 m in the unsampled regions. Expanding the fish/m density from the sampled region to the much wider unsampled region resulted in larger fish numbers in these unsampled regions. Along the south bank transect line, few fish were observed mid-river in any year. Fish distributions from the shore-based sonars were very similar during each year of the study along both sides of the river.

North to south bank ratios of fish counts from the cross-river methods were similar to the ratios from the shore-based method, differing by an average of -1.1% across the years sampled (Table 3). The similarity between the bank to bank ratios and counts in overlapping regions lend credibility to the cross-river method. Across the study years, fewer fish migrated along the north side of the river, 26% as observed from the shore-based method and 27% from the cross-river method. The north to south bank ratio of fish detected outside the effective range of the shore-based system percentage was more variable between study years, ranging from 23 to 59%.

As the river rose, increasing turbidity reduced the effective sampling range of the DIDSONs. The most distant fish observed from the extracted shore-based data was 21 m on the north side of the river and 25 m on the south side of the river (Table 2). We compared these ranges with the most visible extent of the river bottom in images from the shore-based v-DIDSONs and found that the visible range of the river bottom varied from 16.5–26.5 m on north bank and 13.0–26.5 m on south bank while the surveys were being conducted.

We aligned and overlaid the cross-river fish distributions over images of the river bottom topography for a visual perspective of river depth and fish passage (Figures 18 and 19). Note, these figures were made using the range of individual fish and not binned fish, so interpolated data were not included, and all fish in the south bank line were included rather than cutting the distribution at the half-range. From these figures, we were able to determine that fish migration paths extended into the deepest portion of the river along the north bank, but not along the south bank.

The few fish observed during feasibility work in 2009 were not included in these results nor were transects in which no fish were observed (August 11, 2010, and July 7 and 10, 2011). Excluding the no-fish transects named above, we documented the number of transects, time sampled, and total fish counted by site and year (Appendix C).

Error in Range and Depth from Using Slant Measures

The maximum potential error from using *Rslant* rather than *Rrect* to determine the horizontal distance of a fish from the transducer was larger for the cross-river dataset because of the steeper tilt angles used in the deeper portions of the river. The *Rslant* error averaged 2.8 m (32.1% error) along the north bank and 2.2 m (23.0% error) along the south bank (Table 4). Since most fish were observed close to shore where shallower tilt angles were used, we also examined *Rslant* error based on the minimum tilt angles, which was considerably less, averaging 0.6 m (4.9%) on north bank and 0.5 m (4.6%) on south bank (Table 4).

The maximum potential *Rslant* error for the shore-based data averaged 1.3 m (7.6%) along the north bank and 1.9 m (10.1%) along the south bank (Table 4). All error was from the vertical dimension because the constricted 4° beam used for processing echograms reduced the error in the horizontal dimension close to 0.

The *Rslant* error inherent in fish depth calculations, 0.2 m (3.1%), was consistent between years and banks because it depended only on the composite beam angle and maximum end range of the samples, neither of which changed during the study (Table 4). Although the *Rslant* error was small for the depth values, because the river depth was considerably smaller than the width, error in this variable has a larger effect on depth than range.

Cross-river Fish Distributions: Adding Depth

With the addition of the depth dimension to the plotting of individual fish positions, we were able to determine that beyond 15 m, fish were close to the river bottom, but in the nearshore region, they were spread throughout more of the water column (Figures 20 and 21). Many of the station 1 DIDSON images extended past shore, and we were able to measure the points where the river's surface and bottom came together and use those measures to align the cross-river and shore-based bottom profiles. Typically, *x.offsets* were in the range of 0 to 5 m. However, in the July 28, 2011 north bank transect, fish and bottom points required an *x.offset* of -6.5 m for station 1 and -12 m for station 2 because the boat had drifted close to shore during the station 1 recording and into station 1 for the station 2 recording.

A fish's depth was occasionally plotted below the river bottom of its paired profile. Usually, we were able to alleviate this problem by creating a new profile either in the same frame of the observed fish or close to the frames where most fish were marked. For the south bank August 6, 2012, station 1 data, all points remained below the bottom of the bottom profile even after creating a new profile and remarking fish. Although we created profiles for each station within each transect, it was not practical to create a new profile and re-align each profile for individual fish.

The *y.offsets* used to align cross-river bottom profiles with shore-based were occasionally larger than expected after adjusting for changes in water level. In 2011, the *y.offset* was zero most of the time, but in 2012 ranged from -0.8 to 2.5 m. The first 2 transects of 2012, July 13 and July 16 matched the shore-based river bottom profiles with no depth adjustment, but as the season progressed, more depth adjustments were needed to align them. Because the changes in water level were included in the adjustments, we had no information as to why the additional adjustments were needed.

Tilt-Depth Check

The calculations used to determine the depth of the DIDSON lens based on the tilt angle (Equations 9 and 10) proved to be valid based on measured and calculated values in the lab study. The study showed that the outer edge of the v-DIDSON lens traced an elliptical arc as the transducer was tilted down from level, and measured and calculated values compared well, with R^2 values of 0.996 for the shore-based mount and 0.998 for the boat mount. The shorter rotational arm of the boat mount (5 cm) traced an arc that was closer to the circular arc illustrated in Figure 10 compared to the shore-mount with its 21.6 cm rotational arm (Figure 22).

VERTICAL STUDY

The v-DIDSON videos from the shore-based and cross-river systems were similar, but the fixed systems created more stable images. In shore-based h-DIDSON videos, fish swimming across the beam appeared similar to real fish, while fish in v-DIDSON videos were blob-shaped and rapidly appeared and disappeared in the beam, all appearing above the river bottom line (Figure 23). Rocks and gravel along the river bottom were visible in h-DIDSON images. In v-DIDSON

images, the river bottom appeared as a thick line that ran from the first range the sonar beam encountered the bottom to the end of the effective detection range with large boulders appearing as bumps along this line.

Beam Mapping

We experienced difficulties with the beam mapping. For the most part, within the first 10 m from the transducer, we were able to find the target in the beam, slowly lower it from surface to the river bottom, and determine the portion of the water column where the target was observed. Beyond 10 m, we encountered strong current that pulled the target sideways, rendering physical depth measures in this region unusable. Substituting a larger, heavier target would have been unacceptable because it would be considerably larger acoustically than a salmon. We found that when we set the target on the river bottom, we were able to view it in DIDSON images out to 15 m. Once the target was raised off the bottom, the usable range was shortened to less than 10 m. Along the south bank, the target image was visible at the uppermost beam edge when close to the transducer, but as it was moved offshore, the region of visibility was reduced (Figure 24). We visually drew a line through the target points and determined that the size of this narrower beam was 14°. Along the north bank, we were only able to obtain 3 target points, and all were above the nominal beam edge. Because this data were less convincing, we used both 14° and 17° vertical beam dimensions for the effective beam width when estimating which v-DIDSON fish were above the beam of the h-DIDSON.

Mapping the v-DIDSON beam was simpler. We had fewer problems with the target being pulled sideways, likely because the beam was much closer to the surface and very little line was needed for the target to reach the beam's top edge. The uppermost detection limits of the target followed the modeled composite beam very well for both banks (Figure 25).

Modeled Beam Method

Using the modeled beam approach, we observed large numbers of fish with the v-DIDSON that were outside the confines of the h-beam, and these numbers were higher along the south bank. Only 57.4% (54.4–60.3 CI) of south bank's v-DIDSON fish were observed within the modeled 14° h-beam and 70.2% (67.4–72.9 CI) within the modeled 17° beam. For the north bank, 87.6% (85.8–89.5 CI) of fish were within the modeled 14° h-beam and 93.4% (91.9–94.8 CI) within the 17° beam (Table 5). The depth and tilt angle of the h- and v-DIDSON's, factors that have a large effect on what portion of the water column is ensonified, varied between years, but on average, the difference between the tilt angle used and the best h-beam tilt angle based on the modeling exercises was -6.3° along the north bank and -7.7° along the south bank (Table 6).

Because the majority of fish outside the beam were above rather than below the beam, raising the beam to a higher tilt angle increased the numbers of fish within the modeled beam (Figure 26). The north bank was less sensitive to changes in tilt as indicated by the more flattened curves. In the modeling exercise, the numbers of fish observed within the beam along the south bank dropped off more steeply for all 3 years as the DIDSON was raised or lowered beyond the optimal tilt angle. Although there were differences in the optimal tilt angle per year, raising the beam 7° better encompassed the high fish region and resulted in higher percentages of fish within the modeled beam, increasing to 99% along north bank in every year, and along the south bank to 95% in 2010, 93% in 2011, and 90% in 2012 (Table 5).

Density plots by bank and by year illustrate the regions where fish were most concentrated in relation to the river bottom and in relation to the vertical and horizontal beam positions (Figures 27–29). Along the south bank, large concentrations of fish extended above the position of the h-beams out to approximately 10 m from the transducer. In 2011, the year with the highest percentage of fish within the h-beam, the v-beam was angled lower than in 2010 or 2012, and it is likely that the v-DIDSON detected fewer fish. Along the north bank, fewer fish extended above the h-beams and beyond 6–7 m, almost all fish were within the confines of the h-beams. In each case, raising the h-beam better ensonified the fish distributions. The tilt angle for the h-beam was more consistent between years. The v-beam tilt angle, although similar in 2010 and 2012, was aimed lower in 2011; the same year a higher percentage of fish was observed within the h-beam.

Count Comparison Method

Daily counts from the shore-based h- and v-DIDSONs were very similar for both banks during each year of the study (Figures 30–31). Along the north bank, the h-DIDSON counts were slightly higher each year and this was most notable during peak periods. Along the south bank, counts from the 2 systems were similar in 2010, but in 2011 and 2012, the v-DIDSON counts were slightly higher during several days of the field season. In an unpublished study from 2011, sonar fish counts from the h-DIDSON at the new, downriver site (Appendix A) were higher than counts from the traditional site and may compare more favorably to the v-DIDSON counts. We included the daily counts from the h- and v-DIDSONs (Appendices D1–D2) and the counts by hour of the day (Appendices D3–D4). Counts displayed by hour showed low points at 0600 and 2300 hours for both systems (Figures 32–33). The 2 sets of counts followed each other well but were offset due to differences in sampling times. The 2011 south bank data showed the largest differences between counts from the 2 systems, which was the year they were located at separate sites.

Regression slopes comparing the h-DIDSON (independent variable) and v-DIDSON counts showed strong linear relationships (Figure 34) that were significantly different from 0 ($p<0.01$), with all north bank regression slope values below 1, ranging from 0.83–0.89, while south bank slope values were closer to 1 (0.96–1.02) (Table 7). The slope value for the north bank combined dataset was 0.88 (± 0.015 SE) with an intercept of 10.8 (± 9.5 SE; $p>0.05$). For the 2010-2012 north bank datasets, the null hypothesis H_o: B_o (intercept) = 0 could not be rejected ($p>0.05$). For these same datasets, the slope values were not equivalent to 1 (i.e., the alternate hypothesis H_A: $B_1 \neq 1$ was true, $p<0.01$). The regression slope for the south bank combined dataset was 1.00 (± 0.018 SE) with an intercept of 145.2 (± 35.783 SE; $p<0.01$). For the individual years, the slope values were not significantly different from 1 ($p>0.05$), and intercept values were not equivalent to 0 in 2011, 2012 and the combined datasets at the 95% significance level (Table 7).

The total ratio from all years (v-DIDSON/h-DIDSON) was 0.90 (north bank) and 1.13 (south bank).

DISCUSSION YENTNA RIVER

We found that significant numbers of fish traveled above and beyond the effective ensonified volume of the shore-based fish-counting sonars at the Yentna River. Because accurate, daily sockeye salmon escapement estimates are critical for management of the Upper Cook Inlet commercial fisheries (Shields and Dupuis 2012), action is needed to improve the accuracy of

these estimates. This study agreed with independent studies that suggested escapement estimates produced from the Yentna River sonar program were low (Mark Willette, Commercial Fisheries Biologist, ADF&G, Soldotna, personal communication), but disproved our earlier hypothesis, that most of the error would be found in the species apportionment program. Along the south bank, the largest error was from fish traveling over the beam, while along the north bank, the larger error was from fish traveling beyond the beam. We recommend that either averaged or more conservative expansion factors be used to adjust the historical data from this river (Table 8), but not future data. The accuracy of future data will be improved by raising the sonar beam to ensonify more of the water column (Figure 26) and changing the fish wheel operations along the north bank to reduce the numbers of fish moving offshore.

CROSS-RIVER STUDY

Comparison of h- and v-DIDSONs for Mobile Surveys

Based on the count comparison within overlapping regions (Table 2), the v-DIDSON performed better than the h-DIDSON for the mobile surveys. In 2010, the year the h-DIDSON was used, we observed the largest difference between the shore-based and mobile systems. Potential reasons for observing fewer fish with the h-DIDSON could have come from fish being occluded by the river bottom image or differences in beam size which may have improved the sampling efficiency of the v-DIDSON. We knew going into the study that if the h-DIDSON was pointed straight down, strong river bottom reflections would mask fish images. Although shallow river bottoms can mask fish in shore-based systems, SMC's bottom subtraction algorithm removes static bottom echoes leaving moving fish echoes highly visible against a dark background. The bottom subtraction algorithm was not usable for the mobile DIDSON due to the instability of the boat, which was why we angled the DIDSON sideways away from the boat and downward, tilting enough for the sonar beam to reach the river bottom. We discovered that even at the shallower tilt angles, moving fish images were often invisible against the strong bottom reflections unless a fish was at an angle where it appeared at a range above the river bottom.

Although counting fish shadows appeared to be a viable alternative, the lower numbers of fish observed in the 2010 south bank dataset suggested that it may not be. The differences may have also been due to reduced sampling efficiency of the h-DIDSON. The h-DIDSON's vertical beam covered a smaller footprint along the river bottom compared to the v-DIDSON. With low fish passage, less coverage could mean zero fish counted, and therefore, no expansion for the larger unsampled regions. Another possibility is that some of the fish shadows may have been cast at angles where they did not move across the river bottom in the captured image. The better separation of fish from the river bottom in v-DIDSON images and better coverage by the composite beam along the river bottom gave the v-DIDSON an advantage over the h-DIDSON for the mobile surveys. This advantage was less apparent in the north bank data, where there was little difference between the h- and v-DIDSON count comparisons.

Images from the h- and v-DIDSONs gave us a better insight into the movement of the sand waves along the river bottom. The most severe sand waves were observed beyond the mid-range of the river at stations that were not used in the analyses. The sand waves were fascinating to watch in video mode, and we were surprised to find that we could detect fish passing through them. However, without an independent verification, it was impossible to know fish detection rates within these regions.

Comparison of Cross-river and Shore-based Fish Distributions

There are many factors that can affect the alignment and pairing of the cross-river and shore-based systems; *Rslant* error, the instability of the boat's position, changing tilt angle, limited range at high turbidity levels, etc. In spite of these factors, the relationships between counts within overlapping regions was better than expected, especially along the south bank when the v-DIDSON was used. The similarities between the bank to bank ratios from the shore and mobile units provided further evidence that the cross-river method was a viable method for assessing the cross-river fish distribution with a v-DIDSON.

The cross-river fish distributions showed that more fish were observed beyond the range limits of the shore-based DIDSONs along the north shore compared to the distribution along the south shore (Figures 16 and 17). The river topography (Figures 18 and 19) did not provide an explanation for this fish behavior since fish passage extended into the deepest portion of the river along the north bank. The most obvious reason for fish to swim offshore along the north bank was the site's close proximity to the fish wheel. From the bathymetry of the region (Figure 2), we can see that the north sonar site is located at the first place the thalweg is deep and close to shore. Below this site, the river is wider, shallower, and along the shore, the current is sluggish. The thalweg swings from the south bank to the north bank in the offset between sites. Because fish wheels require strong current flows to push the baskets around, they cannot be placed in low flow regions, so the north fish wheel is located less than 50 m downriver from the sonar, while the south fish wheel is 340 m downriver from the traditional sonar site and 175 m from the new site (Figure 2). The current is exceptionally strong where the north fish wheel is located and the moving baskets generate a lot of acoustic noise. Field staff noted that when the fish wheel was running, fish backed up behind the wheel and waited until it stopped before pushing through, and this observation was further verified by dramatically reduced fish passage in shore-based h-DIDSON images.

While this study was in progress, additional studies at this same site extended fish wheel operations to 16–18 h daily (Mark Willette, Commercial Fisheries Biologist, ADF&G, Soldotna, personal communication). Because of this extended sampling time, the fish wheel was always running when the cross-river transects were in progress leaving us no opportunity to compare surveys from when the fish wheel was operating and when it was stopped. If the fish wheel continues to run at this site for species apportionment, the beyond-range expansion factor for north bank (Table 8) will need to be taken into account. If researchers decide to replace the wheel with an alternative method, a new cross-river assessment along this side of the river will be needed. Gillnetting is one of the methods being tested as an alternative to the fish wheel. This method may also interfere with fish movement, but in a different way. The fish wheels move continuously for 16–18 hours, while gillnets will be drifted in short drifts according to a schedule that involves moving from one side of the river to the other. This may push fish offshore during the netting, but there will be more frequent gaps between net sweeps that will allow fish to move through their normal migration regions, and we anticipate that fewer fish will move offshore.

When aligning and pairing the data, another level of uncertainty comes from the end range of the shore-based system. Because fish passage can be sporadic, monitoring the end range of the river bottom image from the shore-based system can provide information on the effective sampling range; i.e., as the river bottom recedes, so does the effective sampling range. However, anecdotal evidence suggests that high water pushes fish closer to shore, so making adjustments to fish passage based on this information would be premature. The dataset collected was not broad

enough to tease out and compare high and low turbidity periods. In the future, if more cross-river surveys are completed, it may be possible to determine the relationship between fish distribution and high turbidity at this site.

Fish observed mid-river may be in the process of crossing from one side to the other. Typically, sonar sites are located in strong current regions which tend to keep fish on one side of the river or the other. The offset between the sonar sites and the slower current region separating them provide opportunity for fish to cross-over. However, since few fish were observed mid-river, we concluded that cross-over was not a major issue at this site.

Cross-river surveys are time-intensive, but this method may be used to expand shore-based counts when fish move outside of the ensonified regions of the fish-counting sonars and alert staff to changes in fish behavior that result from unseen environmental changes such as shifting sand bars and altered current flows or from changes to the project such as new sampling regimes, gear types, or site locations.

Error in Range and Depth from Using Slant Measures

The biggest lesson we learned from examining the *Rslant* error was how large the error grew with large tilt angles (Table 4). The 47.6% error in the 2010 north bank data was alarming; however, the error translated to meters (1.3–3.9 m) was only large when considering the small, effective sampling ranges. This error was relatively small when compared to the large distances between the cross-river stations. Range accuracy became important for aligning the cross-river and shore-based fish distributions and determining where to draw the line between cross-river fish observed within the effective sampling limits of the shore-based sonar and fish observed outside of this line. In spite of our inability to reduce *Rslant* error in this study, we found good agreement between paired and aligned counts from the 2 methods in overlapping regions (Table 2), and the north to south bank ratios were similar (Table 3), both results gave us confidence in the line that was drawn. However, in future cross-river surveys, an alternate method of interpolating using individual rather than binned fish should be sought to minimize *Rslant* error. If situations occur where fish are more clumped around the outermost shore-based sonar range, drawing an accurate line between within and beyond-range fish would be necessary, and reducing *Rslant* error, as well as other range error sources, would become a priority.

At our fish-counting sonar sites, *Rslant* error is ignored. For most of the fish-counting, fish range is less important other than to note how the range distribution drops off within the effective sampling range of the sonar. Profiling the river bottom using DIDSON is one situation where the range becomes more important. During profiling it is often necessary to align segments of river bottom from different video files where different tilt angles were used. Normally, the *Rslant* error is insignificant because changes in tilt angles are small; however, at sites like the Yentna River which have a steeper river bottom slant nearshore, this error should be examined more closely. In addition, SMC produces a lens attachment that reduces the beam width to 1°, eliminating the error due to θ_{fh} (in the v-DIDSON this is the 14° beam, not the composite beam). The error in the vertical dimension is removed by measuring θ_{fv} for the depth determination, but not for the range measures. To improve the accuracy of the profiling procedure (Maxwell and Smith 2007), researchers should consider using the 1° lens attachment and converting *Rslant* to $Rrect_v$, especially when larger tilt angles are used.

For any study where an accurate range determination is required, it is important to take into account the tilt angle and either θ_{fh} or θ_{fv} (depending on the DIDSON's orientation) when determining range. The range of error for the unknown value can then be determined based on the minimum and maximum sampling ranges. Currently, θ_f is not exported when marking fish on SMC echograms, and echograms may be drawn from the full beam instead of a restricted one. Full beam echograms are advantageous if fish, or other targets, are not present in the beam's center. If the entire width of beam is used in the echograms, the *Rslant* error is significant and SMC should consider the possibility of exporting θ_f so that $Rrect_h$ may be determined (Equation 2), minimizing *Rslant* error.

Range and Depth from Mobile DIDSONs

Obtaining depth data from the mobile v-DIDSONs proved to be more difficult than anticipated. Each depth component illustrated in Figure 11 had to be determined separately. Using depth measures to determine river bottom profiles was simpler because the mounts were placed at one location and kept stationary. All needed values could be measured. Adding the instability of the boat created a host of new variables. The first problem that arose came from determining the correct orientation for the v-DIDSON; i.e., whether the DIDSON was mounted on the right or left side of the bracket. Flipping the DIDSON from one side to the other confuses the resulting data. A procedure should be determined at the start of the season and rigidly followed for all remaining data collection. The next problem was from the change in the depth of the transducer lens (i.e., distance from the mid-lens to the water's surface) due to tilt angle (Equations 9–10). With a shore-based system, this was easily measured for every tilt angle used, and only a couple angles were needed to profile the river bottom from shore. In the mobile system, because the absolute tilt angle was constantly changing, it was necessary to calculate the change in the depth of the transducer's lens for every new tilt angle. We were able to accurately determine this depth value based on known tilt angles (Figure 22). More difficult determinations came from the x and y offsets. Small changes in range (x offsets) due to boat drift have less effect on the overall results because of the large width of the river. Because the river is fairly shallow, depth changes have a much greater effect. Aligning the cross-river and shore-based bottom profiles showed that in some cases relatively large depth offsets were needed.

VERTICAL STUDY

There was a disparity between the modeled beam method and count comparisons used to compare the numbers of fish observed from the h- and v-DIDSONs. Although the results from the count comparison indicated that fish counts from the 2 systems were either similar or in some cases the h-DIDSON counts were higher (Table 7; Figure 34), the modeled beam method showed that the h-beam was not adequately ensonifying the vertical distribution of fish, especially in the nearshore regions. This disparity between methods may in part be due to the difficulty of detecting and marking fish on v-DIDSON images. Because the v-DIDSON field of view is narrower, and the beam in that dimension provides no horizontal information, the shape of the image is ill defined and images disappear quickly, in some cases before it is possible to distinguish them as fish. In h-DIDSON images, fish resembled actual swimming fish and were simpler to identify (Figure 23). We also found that it was more difficult to count fish when stopping the video to mark them.

Another reason to suspect that the v-DIDSON's vertical fish distribution was more accurate than the count it produced comes from an earlier study, the DIDSON-Bendix comparison, where an h-DIDSON at this site produced counts more than 1.5 times higher than a Bendix system, which has a very narrow beam (4° nearshore and 2° offshore; Maxwell et al. 2011). Range distributions from the 2 sonars showed that the primary count differences occurred within 10 m from the transducer, indicating the DIDSON's larger vertical beam (17°) was the reason for the differences. Based on this earlier study, we expected few fish to travel above the DIDSON beam, but because of the relatively steep river bottom slope, even this beam did not fill the water column (Figure 24). Turning the DIDSON sideways with the composite beam positioned vertically filled the water column on the north bank and the beam came much closer to the surface on the south bank (Figure 25). Even with the v-DIDSON's larger, vertical beam, a handful of fish were still observed near the beam's top edge (Figures 27–29).

High turbidity levels at the Yentna River cause the beam to scatter, reducing the intensity as it travels away from the transducer and thereby reducing the sampling range. We expected the height of the sonar beam to be compromised for the same reason. The beam mapping component of the study showed that the effective h-beam was 14°. Although DIDSON specifications originally listed the vertical dimension of the beam as 14°, later beam pattern plots showed the size to be closer to 17° (Bill Hanot, Sound Metrics Corporation, Vice President, personal communication). The most likely cause of the reduced effective beam is scattering due to turbidity. Because the vertical fish distribution extended so far above the h-beam, knowing the effective beam size became important. There was a considerable difference between the percentages of fish that would be found within the limits of a 14° beam compared to a 17° degree beam, especially along the south bank (Table 5).

The Effect of Changes in Tilt Angle on Fish Passage Estimates

According to the modeled beam results, the h-beam was tilted down too far during sampling. Raising the beam (Figure 26) would have resulted in a higher percentage of fish ensonified along both banks. Fish traveling along the north bank were observed closer to the river bottom, so small changes in the tilt angle had less effect on the numbers of fish observed, whereas along the south bank, the vertical distribution of fish extended much higher (Figures 27–29), so raising the beam made a substantial difference.

We were less concerned about fish traveling underneath the DIDSON beam. Because our goal in aiming the DIDSON was to put the maximum response axis of the beam (the beam's center) just above the river bottom where we expected most fish to travel, a large portion of the beam penetrated or was reflected off from the river bottom making it highly unlikely a fish could travel underneath the beam. A fish could potentially be "hidden" from the sonar if it passed on the offshore side of a large rock; however, to completely escape detection the rock would have to extend from one side of the beam to the other. At 2 m from the transducer, the beam is already 1 m wide, considerably wider than the boulders observed at the site.

RECOMMENDATIONS AND FUTURE WORK

Based on the cross-river results from this study, we recommend:

1) Reducing the hours of fish wheel operations along the north bank to allow more breaks for fish to pass or expanding future north bank fish estimates based on expansion factors obtained in this study (Table 8).

2) Continuing cross-river surveys to alert staff to changes in fish behavior due to project or environment changes using a v-DIDSON.
3) Expanding the historical data during the years of enhanced fish wheel operations by the beyond-beam expansion factors (Table 8) using either average values or a more conservative expansion derived from the standard error.

Based on the vertical results from this study, we recommend:

1) Continuing to use h-DIDSONs for future fish-counting because the v-DIDSON fish counting was less accurate, but raising the h-beam 7° above the traditional tilt angle along both banks.
2) Studying the effects of raising the fish-counting sonar beam. The most direct study would be to sample 2 h-DIDSONs side-by-side, one with the higher tilt angle and the second with the traditional tilt to determine whether the higher angle ensonifies a greater proportion of fish.
3) Expanding the historical data by the above-beam expansion factors (Table 8) using either average values or a more conservative expansion derived from the upper confidence interval.

The future of the Yentna River sonar project depends on how effective this and other studies are in measuring the error in escapement estimates. A study of the final error source in escapement estimates from this river (the error from the species apportionment component of the project is in progress. One study is examining the selectivity of the fish wheel and another is examining the potential use of fish length measures from DIDSON in combination with the fish wheel for apportionment. Results from these studies may turn out to be the deciding factor in whether to continue this project.

CHAPTER 2: COPPER RIVER

STUDY SITE

The Copper River sonar site is approximately 100 m downriver from the Million Dollar Bridge below the outlet of Miles Lake (Figure 35). Here, the river is a single channel approximately 380 m wide and is influenced by Childs Glacier downriver and Miles Glacier upriver. Because the south bank's natural substrate is composed of large cobble and boulders, a concrete substrate (30 m long, 5 m wide) was constructed in 2001 that provides a uniform 8.4° slope for the acoustic beam. The north bank sonar was deployed on the natural substrate of sand and small cobble with a 5° slope (Figure 36). Bathymetry of the regions along either shore, conducted in 2000, showed a more gradual drop off along the north bank and steeper drop off along the south bank (Figure 37). Using the river bottom image as a gauge to determine the DIDSON's effective ensonification range, the south bank river bottom image was visible out to 20 m during low water levels (1.1 MHz, standard DIDSON), but on rare occasions of extreme high waters, the visible range was reduced to 7 m, and along the north bank, the visible range varied from 12 to 35 m (0.7 MHz, long-range DIDSON). Of the 3 rivers in this study, the Copper River was the most turbid (0.5–2.2 kg/m^3 with corresponding discharges of 1,119–10,394 m^3/s; Brabets 1997). In 2002, turbidity measures along the south bank were highly variable but remained above 800 nephelometric turbidity units (Maxwell and Gove 2007).

METHODS COPPER RIVER

CROSS-RIVER STUDY

We conducted a series of cross-river transects at the Copper River sonar site using a horizontally positioned, standard DIDSON (h-DIDSON). This was the first site we attempted to use a mobile DIDSON for cross-river surveys. One transect was done in 2005 to test the new method and 8 were performed in 2006 between May 26 and June 21. We began sampling at each station for 15 min in 2005 and then reduced the sampling time to 10 and then 5 min per station in 2006.

During periods of high water, strong current velocities created a disturbance at the face of the transducer that prevented signal detection and caused the DIDSON image to disappear completely. If we throttled the boat engine down to below current speed, the DIDSON images reappeared. We selected a throttle speed that improved the clarity of the DIDSON images. In partial drift mode, boat operators kept the boat at the designated range from shore using the laser range-finder. We used a combination of fixed and partial-drift sampling at this site.

We spaced the sampling stations closer together in the nearshore regions to make it easier to align data from the stations with range data from the shore-based units. In 2005, the river width of 355 m was divided into 13 stations measured from the south shore at 10, 20, 30, 50, 70, 90, 110, 130, 262, 387, 317, 328, and 340 m. In 2006, transects were performed across 3 days in May when the water level was increasing daily. The river width changed from 340 to 360 m and 18 stations were sampled: 10, 20, 30, 40, 60, 80, 100, 140, 180, 220, 260, 280, 300, 310, 320, 330, and 340 m. In June 2006, the river width was 383 m and the 17 stations sampled from the south shore included: 10, 15, 20, 30, 40, 60, 80, 100, 140, 180, 220, 260, 300, 320, 340, 350, 360, and 370 m (Figure 38).

Data Processing

For each station, the following data were recorded: date, transect no., station no., method (stationary or drift), minutes sampled (*t*), DIDSON file name, boat range (*br*) measured from the south shore, start range (*sr*) the range where the sonar beam first encountered the river bottom, and end range (*er*) the range where the river bottom ended. We counted fish visually from the DIDSON videos. All fish counted from one station were binned into a single range group, the mid-range (*mr*) of the station measured from the south bank shore,

$$mr = br - (sr + \frac{er - sr}{2}). \tag{15}$$

Raw fish counts (fc_{raw}) were expanded to equalize counts from different sampling times,

$$fc_{\exp} = fc_{raw} \times \frac{5}{t} \quad . \tag{16}$$

Interpolating and Expanding Fish Counts

The cross-river stations left much of the river width unsampled. We interpolated and expanded counts based on methods described for the Yentna River (*Data Processing, Interpolation, and Expansion*; Equation 1). The setup and unsampled regions at the Copper River site are diagrammed and explained in Figure 38. Unsampled regions between middle stations and

between the first and last station and shore were accounted for. Interpolated counts and their assigned ranges were added to the cross-river fish distribution.

For fish-counting, a standard DIDSON was used along the south bank sampling a single stratum from 1–20 m on low frequency, and a long-range DIDSON was used along the north bank sampling from 1–20 m on high frequency, and 15–35 m on low frequency (i.e., the images were counted from 15–35 m because the DIDSON software does not allow a 20–35 m window length). The methods used for fish-counting during this year were documented by Faulkner and Maxwell (2008).

VERTICAL STUDY

To obtain a vertical fish distribution at the Copper River site, we used the same methods described for Yentna River except that no beam mapping was performed. A standard v-DIDSON was placed on the south bank's concrete substrate adjacent to the h-DIDSON used for fish-counting. No vertical sampling was done on the north side of the river.

RESULTS COPPER RIVER

CROSS-RIVER STUDY

Fish migrated farther offshore of the north bank than the south bank (Figure 39) and even though the long-range DIDSON on this bank sampled farther offshore, more fish were observed beyond the range of the shore-based sonar, 14.7%, compared to only 3.7% observed offshore of the south bank DIDSON (Table 9). Of the 18 stations spaced across the river, no fish were observed mid-river, i.e., in stations 6–13. Although we occasionally observed fish in station 5, the occurrences were rare.

A much larger percentage of fish were observed on the south side of the river. After equalizing all samples to 5 min per sample, a total of 330 fish (93%) were observed along the south bank, and only 25 along the north bank during the course of the transects. Fish counts extracted from the shore-based DIDSONs operating at the same time transects were being conducted had a ratio of 95% south to north bank fish (Faulkner and Maxwell 2008).

Although the river width and effective sampling range of the shore-based DIDSONs was dynamic, overall approximately 6% of the river was ensonified along the south bank and 10% along the north bank. The effective river width sampled during the mobile surveys was approximately 23%, varying from 11 to 38%. Less range was sampled when steeper tilt angles were used. Tilt angles ranged from 0; i.e., where the center of the beam was level, to a slant of -52°, the steepest tilt angle used in the deepest portion of the river.

From the shore-based DIDSON, daily fish passage was estimated at 13,637 salmon on June 2, the day of the 2005 transect and ranged from 2,690 to 17,884 salmon on the days of the 2006 transects (Figure 40). Water level ranged from 40.7 to 43.2 m (Figure 40) and water temperature from 5 to 8°C (sound speeds of 1426–1439 m/s).

VERTICAL STUDY SOUTH BANK

Data were collected during 2 evenings after the cross-river transects were finished, from June 20, 2200 through June 21, 0700 and from June 21, 1900 through June 22, 0800, on the south side of the river only. Using the modeled beam approach, few fish were observed with the v-DIDSON outside the confines of the h-DIDSON's beam, assuming a 14° beam. A total of 2,530 fish were

observed with the v-DIDSON and of these fish 98.6% were within the h-beam, with bootstrapped 95% confidence limits of 98.1–99.2%. Raising the beam 3° would encompass 100% of the observed fish. The flattened curves show that tilt angles ranging from -5° to -7° would ensonify 100% of the observed fish, and that the angle selected for sampling was on the low side of the curve (Figure 41). Density plots show that fish were observed throughout the h-beam out to a range of 8 m, and beyond were concentrated closer to the river bottom (Figure 42).

Count comparisons between the v- and h-DIDSONs were very similar with a regression slope of 0.99 and an R^2 value of 0.776 (Figure 43). The minor differences between the paired hourly counts were in part due to the offset in sampling times that was necessary to eliminate cross-talk between the 2 sonars.

DISCUSSION AND RECOMMENDATIONS COPPER RIVER

CROSS-RIVER STUDY

The Copper River was the first site where we used a DIDSON for mobile surveys. We discovered many challenges with this method. The first problem is that DIDSON images become blurry when the boat is moving, so rather than motoring back and forth across the river while sampling, we set up fixed sampling stations. We considered anchoring at each station, but the strong current at this site makes it very difficult to hold a boat in place and with the large numbers of icebergs floating downriver throughout the summer, anchoring is dangerous. We did attempt to anchor a buoy with the idea we would mark the spot, drop a buoy, and then keep the nose of the boat at the buoy while sampling. This worked for the first station closest to shore, but when we tried it at the next station, the current pulled the buoy under and it was never seen again. We settled for holding the boat in place with the outboard engine and using a second person in the boat to measure the shoreline with the laser rangefinder. The boat captain eyeballed a fixed point along either shore in an attempt to hold the boat in place. We also used the bridge, lining up the boat with flagged points along the bridge for each new station.

We initially started sampling at each station for 15 min, but found it to be too time consuming, and holding the boat in place for that time period was difficult. In 2005, we sampled while holding the boat in a stationary position pointed upriver, but in 2006, the conditions (stronger current, high water, and larger boat and motor) were such that the image degraded. To get a visible image it was necessary to let the boat drift slowly downriver, parallel to shore while using the motor just enough to keep the boat at the same distance from shore. This procedure created a usable DIDSON image.

The cross-river fish distribution showed that more fish migrated beyond the range of the shore-based DIDSON along the north bank. Along the south bank, the strong current forced fish closer to shore. We have often observed fish in DIDSON images struggling to move upriver against the current within the 10 m nearshore stratum, so it was surprising to observe fish traveling farther offshore. Along the north shore, the current is slower. These surveys were completed after bridge work was done to raise the fallen portion of the Million Dollar Bridge (Figure 35). This work required crews to build a gravel work pad in the river along the north bank to work from. The work pad created a back eddy that moved fish offshore. Faulkner and Maxwell (2008) described the problems associated with this work pad. We do not know the erosion rate of the pad since the construction was finished, and the Bendix system used prior to the bridge work to assess fish passage provided limited information regarding fish migration pathways.

There are many uncertainties associated with cross-river surveys using DIDSON. The strong similarity between the north to south bank fish ratios from the cross-river and shore-based systems was very encouraging (93% and 95%, respectively) lending credibility to the cross-river method. The largest error was likely from aligning the range distributions and determining where to draw the line for the end range of the shore-based sonar. High turbidity at this site has a large effect on the maximum sampling range of the shore-based system, sometimes reducing it to half, but at the same time, the associated rising water and stronger current forces fish closer to shore, so adjusting the data based on the maximum sampling range would not be appropriate. Because of the turbidity effects, which always shorten the sampling range, the expansion factors (Table 8) are likely to be conservative and thus should be incorporated into the historical and future Copper River estimates until better information can be obtained.

There are also uncertainties in measuring the distance of the boat to shore and holding the boat in place. A few meters on either side of the overlapping stations can make a large difference, especially along the north bank where the first range bin outside the shore-based sonar contained the majority of offshore fish (Table 9). Using a GPS is one option for improving the range accuracy, but without a base station, there is large error associated with this method. The laser rangefinder was the better choice at the time of this study.

The mobile transects took place on mostly average fish passage days, based on the shore-based system (Figure 40). If future mobile surveys are done at this site, we recommend spreading them across the field season to encompass a broad range of fish densities.

VERTICAL STUDY

The modeled beam and count comparison methods were in good agreement. Unlike the Yentna River, where the 2 systems seemed to disagree, at the Copper River, both methods led to the same conclusion that a very small percentage of fish traveled above the beam. Examining the effect of varying tilt angles showed that a wide range of tilt angles would ensonify most of the observed fish. For fish migrating near the river bottom occupying a small vertical region, the tilt sensitivity curves will be relatively flat. However, the tilt angle selected for sampling was on the low side of the curve. Raising the beam 3° above the normal sampling aim would ensure that the region of fish passage is well covered.

Data from both the Yentna and Kenai rivers showed that staff had more difficulty detecting fish from v-DIDSON images. The images from the 2 orientations are very different from each other. While the h-DIDSON produces fish images that resemble actual fish swimming across the beam, the v-DIDSON creates blob-like images that rapidly appear and disappear within the beam. The v-data from the Copper River was easier to count for 2 reasons. First, daily fish passage at this site is usually lower (except during occasional peak days) and lower fish densities were easier to count. Second, the strong current along the Copper River's south shore slowed the fish movement, preventing them from darting through the beam. This created a greater persistence in the images and made it easier to detect fish.

No beam mapping was performed at this site. This is one of the more difficult sites to put a boat in and hold in place, and the strong current makes it impossible to find a usable target that is both heavy enough to sink in the current and acoustically similar in size to a salmon. We used the 14° beam for the vertical analysis. With the high turbidity at this site, we would expect some reduction in beam width.

No vertical data were collected along the north bank. Because the current is considerably slower along this side of the river, fish may travel higher above the river bottom; however, the shallow river bottom leaves little room for fish to travel above the DIDSON beam (Figure 36).

RECOMMENDATIONS AND FUTURE WORK

Based on the cross-river results, we recommend expanding the historical and future fish counts at this site for fish beyond the shore-based sonars (Table 8) and repeating the cross-river surveys to assess whether the work pad for the bridge is still affecting fish migration and to determine the variability between years. Although the fish we observed beyond the ensonified regions may be Chinook salmon *O. tshawytscha*, which also travel this river (Baird Canyon Chinook passage estimates for 2005 and 2006 were 30,333 and 67,789), because they are removed from the sockeye salmon estimates postseason (Steve Moffitt, Commercial Fisheries Biologist, ADF&G, Cordova, personal communication), they should be included in the count.

For future cross-river surveys, we recommend condensing the survey to exclude the mid-river stations, orienting the DIDSON vertically (v-DIDSON), and positioning the DIDSON right-handed; i.e., the lens on the right side when standing behind the mount. Omitting the mid-river stations would save considerable time, and the consistent lack of fish at these stations provided strong evidence that fish do not migrate there. Stations out to 60 m from the north shore and 50 m from the south shore should be adequate.

Based on the vertical results, we recommend expanding the historical counts for fish above the south bank shore-based sonar (Table 8). For future operations, rather than expanding the count, we recommend raising the beam 3° after following aiming protocols described by Maxwell and Smith (2007).

CHAPTER 3: KENAI RIVER

STUDY SITE

The Kenai River sonar site is located 30.6 km (River Mile 19) from the river mouth where the river is a single channel approximately 127 m wide. The river bottom substrate is a mixture of cobble with occasional boulders and is relatively flat along the north side, a smooth 1° slope out to 55 m, and much steeper along the south bank, a 12° slope out to 9 m before it flattens (Figure 44). The river bottom is visible in DIDSON images to the end range of 30 m for the south bank (1.1 MHz, standard DIDSON) and 50 m for the north bank (0.7 MHz, long-range DIDSON). At this site, water level at the start of the field season is often low, rises as snow melts in the mountains and upriver rains add to the flow, peaks in late July or early August, and then declines in mid-August. Although the pattern is typical, the low and high levels can be highly variable. Turbidity at this site was considerably lower than the other rivers in this study, measuring between 21 and 28 nephelometric turbidity units in a prior study (Maxwell and Gove 2004).

METHODS KENAI RIVER

CROSS-RIVER STUDY

We conducted a series of cross-river transects at the Kenai River sonar site using a horizontally oriented, standard DIDSON (h-DIDSON). We ran 2 transects in 2006 to work out the logistics of this method at the new site, and in 2007, completed 22 transects, sampling approximately every

other day between 7/16 and 8/8, the time period when the majority of adult sockeye salmon migrated through the sonar site. At this site, a dock is installed each year along both sides of the river. We set up 12 cross-river stations and sampled the 2 stations closest to each shore from the docks, one with the transducer facing shore, and the second, with the transducer facing offshore (Figure 45). A line was strung above the river and flagged at the location of each sampling station to assist in positioning the boat.

Data Processing and Interpolating

For the abbreviated 2006 survey, we summed the fish counts by station and plotted the results with no additional processing. The 2007 cross-river survey data were processed following methods described for Copper River and interpolated for unsampled regions following methods described for Yentna River (*Data Processing, Interpolation, and Expansion*; Equation 1). We diagrammed the setup and variables used for interpolation at this site (Figure 46). No expansion of data from the first and last stations to shore was needed because the effective range of the mobile DIDSON extended to shore along both sides of the river.

For the shore-based fish-counting sonar, a standard DIDSON was used along the south bank to sample 2 strata: 1–10 m, high frequency (HF), and 10–30 m low frequency (LF). Along the north bank, a long-range DIDSON with a condenser lens (a lens that reduces the vertical size of the DIDSON beam by one-half) was used to sample from 1–10 HF, 10–50 m LF through July 25, and then the sampling regime was changed to 3 strata: 1–10 m HF, 10–30 HF, 25–65 LF (counting from 30–65 m of this last stratum). The methods used for fish-counting in 2007 were documented by Westerman and Willette (2010a).

VERTICAL STUDY

We mapped out the vertical dimensions of the shore-based sonar beams along both sides of the river following methods described for the Yentna River. We started this work along the north shore of the Kenai River using the same type of target, a 10.16 cm stainless steel sphere suspended from a rod with a monofilament line and wrapped in a monofilament bag. When we began the target work on the south bank, drag caused by the strong current broke the line, and we were unable to retrieve the target. We substituted a plastic sphere of the same dimension filled with BB shot.

To obtain a vertical fish distribution, we used the same methods described for the Yentna River. A standard v-DIDSON was placed next to the south bank h-DIDSON used for fish-counting. Data were collected from July 6 to August 23, 2007. No vertical sampling was done on the north side of the river.

RESULTS KENAI RIVER

CROSS-RIVER STUDY

For the 2006 transects, the vast majority of fish were observed at the station closest to shore along either side of the river with a small number of fish observed at all but the center station (Figure 47).

In 2007, fish were observed at each of the 12 cross-river stations, although the percentages of fish in the mid-river stations were low (Table 10). A total of 3.5% of fish were observed offshore of the shore-based sonars dispersed fairly evenly across the river with a slightly larger percentage

offshore of the south bank DIDSON. We observed a total of 2,588 fish (including interpolated counts) with the cross-river system and 5,954 fish with the shore-based sonar. The shore-based dataset contained 39 full-range samples 10-min each for a total sampling time of 390 minutes, the cross-river survey consisted of 22 transects 5-min each for a full-range sampling time of 110 minutes. Expanding the cross-river survey data to match the sampling time of the shore-based system (a ratio of 3.55) resulted in a total of 9,177 fish, a higher fish count from the cross-river survey.

Most fish were observed within the first 2 range bins along either shore (Figure 48). Along the south bank, cross-river fish were more spread out between 3 range bins, while the shore-based sonar showed fish concentrated within a single range bin.

The effective range sampled during the cross-river survey was, on average, 48%, while the shore-based sonar sampled 23% of the river along the south shore and 32% along the north shore, a total of 55%. The effective sampling range of the shore-based sonar was based on the maximum range that fish were observed in the paired dataset.

The cross-river surveys were conducted across the field season and included a wide range of fish passage rates including the peak passage day on July 27, 2007 (Figure 49). Water level fluctuated 0.28 m during the surveys, and water temperature ranged from 12 to 16 °C (sound speed 1455–1469 m/s). Transducer tilt angles during the cross-river surveys ranged from -43° in the deepest regions of the river to 0° in shallow, nearshore regions.

VERTICAL STUDY

The beam mapping exercise worked well along the north bank, but we experienced difficulties along the south bank. The results from both banks are shown in Figure 50. Along the north bank, the stainless steel sphere was visible in the shore-based DIDSON images from the river bottom to the upper edge of the nominal 8° beam (condensed from 17° using an SMC condenser lens). Once the beam encountered the water's surface, the sphere was visible from river bottom to surface. But along the south bank, where the plastic sphere was substituted, the target detection range was well below the upper edge of both the 17° and 28° beams, which may have been due to a combination of factors, the poor quality of the substituted target and the stronger current along this shore.

Along the south bank, the modeled beam approach showed few fish above the h-DIDSON beam, assuming a 14° beam. We observed a total of 9,119 fish with the v-DIDSON during this study, and of these fish, 97.6% were within the h-beam, with bootstrapped 95% confidence limits of 96.6–98.4% (Table 11). Raising the beam 3° would have encompassed 99.8% of observed fish (Figure 51). The flattened curves showed that tilt angles ranging from -4° to -7° would ensonify over 99% of observed fish, and that the angle selected for sampling (Table 12) was on the low side of the curve. Density plots showed that fish were more concentrated in the first 4 m from the transducer, and although their vertical distribution covered more of the water column in this region, the majority of fish were within the confines of the h-beam throughout their observed range (Figure 52).

Fish counts from the h-DIDSON were consistently higher than counts from the v-DIDSON, resulting in a linear regression slope of 0.55 and an R^2 value of 0.861 (Figure 53). Some of the variability may have come from the offset in sampling times that was necessary to eliminate cross-talk between the 2 sonars, but technicians observed that counting fish at high passage rates

was considerably more difficult on v-DIDSONs, especially since it was necessary to continually stop the video to mark the fish traces.

DISCUSSION AND RECOMMENDATIONS KENAI RIVER

CROSS RIVER STUDY

Fish were observed all the way across the Kenai River, but the percentage of fish beyond the range of the shore-based sonars was low (3.5%). The purpose of the sonar project at this site (upriver site) is to estimate daily fish passage of sockeye salmon for management of the Upper Cook Inlet commercial fishery. While the primary species of interest for this project was sockeye salmon, Chinook, pink, and coho *O. kisutch* salmon also migrate this river. Pink and coho salmon begin to show up near the tail-end of the sockeye salmon run, while Chinook and sockeye salmon runs overlap. Studies have shown that Chinook salmon, because of their larger size, tend to migrate offshore of the band of migrating sockeye salmon (Miller et al. 2011). In 2007, 36,950 Chinook salmon were estimated for the late run at the River Mile 8.5 (Fleischman and McKinley 2013) and 872,153 total fish, of which 868,000 were sockeye salmon (99.5%), were estimated at the upriver site (Westerman and Willette 2010a). If we assumed that none of the Chinook salmon were counted (i.e., apportioned) at the upriver site and all of these fish were beyond the end range of the shore-based sonars, the total fish count would become 915,132 fish and Chinook salmon would make up 4.7% of that total. This suggests that most of the fish observed during the cross-river study were likely Chinook salmon. We have observed large fish in DIDSON images at the upriver site that were obviously Chinook salmon, so not all migrated mid-river.

Chinook salmon tend to swim farther offshore and are captured less frequently in fish wheels used for apportioning the sonar estimates. In 2007, no Chinook salmon were captured in the fish wheel until August 15, but beyond this date, their numbers made up 1.8–3.8% of the daily apportioned count (Westerman and Willette 2010a). Another confounding factor is that an unknown component of Chinook salmon counted by Miller et al. (2011) spawn downriver from the sockeye salmon site, so although their passage rates were estimated at the lower river site, it is unknown what percentage passed through the upriver site. The low percentage of offshore fish and the strong indication that most mid-river fish may be Chinook salmon confirms our assumption that sockeye salmon migrate nearshore to avoid strong current areas at the upriver site.

We do not recommend expanding the shore-based fish count for the offshore component of fish because if this component is comprised mostly of Chinook salmon, without a mid-river apportionment program, these extra fish would be apportioned incorrectly to sockeye salmon.

This cross-river study was mostly conducted during a single field season and does not provide information about inter-year variability in fish migration behavior. The most likely variables that affect the migratory pathways of fish are water level and fish density. At low current flows fish are more likely to move offshore to avoid land predators and reduce energy costs due to wave drag (Hughes 2004), while at higher flows, stronger currents force fish nearshore to conserve energy. High fish densities may also force fish farther offshore to avoid congested regions. Based on images from the shore-based DIDSON, fish are typically farther offshore at the start and end of the field season when fish densities are low, and move closer to shore mid-season. Whether

this is due to water level or fish density is unknown because peak water levels often coincide with peak fish densities. Likely the offshore movement is a combination of both factors.

The expanded cross-river fish count was larger than the shore-based count, and a higher percentage of fish were observed along the north bank (Figure 48). Along the south side of the river, the largest component of fish was very close to shore. Either the cross-river method of having the transducer offshore with the beam pointed toward shore was not as effective at covering the zone of high fish passage or the difference in sample times was responsible. A direct comparison of counts or percentages can only be considered a crude comparison because the 2 methods sampled different regions of the river at different time periods.

VERTICAL STUDY

Although the beam mapping plots for the north bank (Figure 50) showed that the artificial target was visible through the entire width of the sonar beam, the results from the south bank were disappointing. The poor results were likely due to a combination of factors: the target, the stronger current flow on the south side of the river, and the dimension of the sonar beam. The BB-filled plastic sphere turned out to be a poor substitute for the stainless steel sphere. It was lighter in weight and more affected by the pull of the stronger current along this side of the river, making it difficult to measure the target's depth, and the slant in the line made it difficult to center the target in the up-downriver plane of the sonar beam. The differences in results from the 2 sides of the river were also partly due to the vertical dimensions of the sonar beams. The north bank DIDSON had a condenser lens that halved the vertical beam to better fit the narrow water column. This half-beam has the same energy as the full beam, but since it is concentrated within a smaller volume, a higher energy beam is created. We also found that the reflectivity of the stainless steel sphere was superior to the plastic sphere. Although the plastic sphere was filled with reflective metal (i.e., copper coated BB shot), the images created from this sphere even at close range under the best of circumstances were not as clear as images from the stainless steel sphere.

Although the beam modeling showed that a small percentage of fish (1.02%) may have traveled above the h-beam, the Kenai River h-DIDSON counts were consistently higher than v-DIDSON counts (Figure 53). The most plausible explanation for the discrepancy is that the poorer image quality from the v-DIDSONs made it more difficult to detect fish. At high passage rates, marking v-DIDSON videos using the SMC software is difficult because the fish move in and out of the beam quickly. Although the v-DIDSON was a good tool for building vertical fish distributions, the images produced were more difficult for technicians to count at high fish passage densities making the h-DIDSON the more effective system for estimating fish passage.

RECOMMENDATIONS AND FUTURE WORK

We do not recommend expanding either the historical or future shore-based DIDSON counts based on the cross-river results (Table 8) because of the unknown component of Chinook salmon in the estimate and the lack of a mid-river species apportionment program to account for them. The cross-river study merits repeating under a wider range of environmental conditions to better understand migratory fish behavior at this site. If a new study is conducted, we recommend positioning the DIDSON vertically on the mobile mount and always mounting the DIDSON right-handed; i.e., the lens on the right side when standing behind the mount.

Few fish were observed above the limits of the sonar beam along the south bank (2.4%). The expansion factor from Table 8 may be applied to historical data from the site, but rather than expanding future fish passage estimates, we recommend following the established aiming protocol to aim the DIDSON beam (Faulkner and Maxwell 2009; Maxwell and Smith 2007) and then raising the beam 3° to improve coverage of the water column. For the north bank, a vertical study is not necessary. The condensed DIDSON beam fills most of the narrower water column along this side of the river and it is unlikely that a significant percentage of fish pass above the detection limits of the sonar beam.

ACKNOWLEDGEMENTS

The Yentna Sonar crew monitored sonar systems and assisted with cross-river surveys. Chris Brown assisted with sonar operations and cross-river surveys at both the Yentna and Kenai rivers. Paul Ruesch operated sonar equipment at the Kenai River site. Steve Moffitt, Glenn Hollowell, and Jeremy Botz operated the boat for the cross-river surveys at the Copper River. Lowell Fair and Mark Willette provided editorial comments for the manuscript.

REFERENCES CITED

Becker, C. D. 1962. Estimating red salmon escapements by sample counts from observation towers. Fishery Bulletin 192: Volume 61. Fish and Wildlife Service, Washington.

Belcher, E. O., B. Matsuyama, and G. M. Trimble. 2001. Object identification with acoustic lenses. Pages 6–11 [*In*] Conference proceedings MTS/IEEE Oceans, volume 1, session 1. Honolulu Hawaii, November 5 – 8.

Banneheka, S. G., R. D. Routledge, I. C. Guthrie, and J. C. Woodey. 1995. Estimation of in-river fish passage using a combination of transect and stationary hydroacoustic sampling. Canadian Journal of Fisheries and Aquatic Sciences 52:335–343.

Brabets, T. P. 1997. Geomorphology of the Lower Copper River, Alaska. U.S. Geological Survey Professional Paper 1581:89.

Brazil, C., and G. B. Buck. 2011. Sonar enumeration of Pacific salmon escapement into the Nushagak River, 2006. Alaska Department of Fish and Game, Fishery Management Report No. 11-23, Anchorage.

Brett, J. R. 1995. Energetics. Pages 3-68 [*In*] C. Groot, L. Margolis, and W. C. Clarke, editors. Physiological Ecology of Pacific Salmon. University of British Columbia Press, Vancouver, BC.

Duncan, A., and J. Kubecka. 1996. Patchiness of longitudinal fish distributions in a river as revealed by a continuous hydroacoustic survey. ICES Journal of Marine Science 53:161–165.

Fair, L. F., T. M. Willette, and J. Erickson. 2009. Escapement goal review for Susitna River sockeye salmon, 2009. Alaska Department of Fish and Game, Fishery Manuscript Series No. 09-01, Anchorage.

Faulkner, A. V., and S. L. Maxwell. 2008. Copper River hydroacoustic salmon enumeration studies, Miles Lake sonar project, 2005–2006. Alaska Department of Fish and Game, Fishery Data Series No. 08-37, Anchorage.

Faulkner, A. V., and S. L. Maxwell. 2009. An aiming protocol for fish-counting sonars using river bottom profiles from a dual-frequency identification sonar (DIDSON). Alaska Department of Fish and Game, Fishery Manuscript No. 09-03, Anchorage.

Fleischman, S. J., and T. R. McKinley. 2013. Run reconstruction, spawner–recruit analysis, and escapement goal recommendation for late-run Chinook salmon in the Kenai River. Alaska Department of Fish and Game, Fishery Manuscript Series No. 13-02, Anchorage.

Gaudet, D. M. 1990. Enumeration of migrating salmon populations using fixed-location sonar counters. Rapports et Proces-Verbaux des Reunions, Conseil International pour l'Exploration de la Mer 189:197–209.

Hinch, S. G., and P. S. Rand. 1998. Swim speeds and energy use of upriver-migrating sockeye salmon (*Oncorhynchus nerka*): role of local environment and fish characteristics. Canadian Journal of Fisheries and Aquatic Sciences 55:1821–1831.

Hinch, S. G., and P. S. Rand. 2000. Optimal swimming speeds and forward-assisted propulsion: energy-conserving behaviors of upriver-migrating adult salmon. Canadian Journal of Fisheries and Aquatic Sciences 57:2470–2478.

Holmes, J. A., M. W. Cronkite, H. J. Enzenhofer, and T. J. Mulligan. 2006. Accuracy and precision of fish-count data from a Dual-frequency identification sonar (DIDSON) imaging system. ICES Journal of Marine Science 63:543–555.

Hughes, N. 2004. The wave-drag hypothesis: an explanation for the size-based lateral segregation during the upstream migration of salmonids. Canadian Journal of Fisheries and Aquatic Sciences 61:103–109.

Knudsen, F. R., and H. Saegrov. 2002. Benefits from horizontal beaming during acoustic survey: application to three Norwegian lakes. Fisheries Research 56:205–211.

Krieger, K., J. Heifetz, and D. Ito. 2001. Rockfish assessed acoustically and compared to bottom-trawl catch rates. Alaska Fishery Research Bulletin 8(1):71–77.

Levy, D. A., and A. D. Cadenhead. 1995. Selective tidal stream transport of adult sockeye salmon (*Oncorhynchus nerka*) in the Fraser River Estuary. Canadian Journal of Fisheries and Aquatic Sciences 52:1–12.

REFERENCES CITED (Continued)

Lyons, J. 1998. A hydroacoustic assessment of fish stocks in the River Trent, England. Fisheries Research, 35:83-90.

Maxwell, S. L. 2007. Hydroacoustics: Rivers. Pages 133–151 [*In*] D. H. Johnson, B. M. Shrier, J. S. O'Neal, J. A. Knutzen, X. Augerot, T. A. O'Neil, and T. N. Pearsons. Salmonid field protocols handbook: techniques for assessing status and trends in salmon and trout populations. American Fisheries Society, Bethesda, Maryland.

Maxwell, S. L., and N. E. Gove. 2004. The feasibility of estimating migrating salmon passage rates in turbid rivers using a dual-frequency identification sonar (DIDSON) 2002. Alaska Department of Fish and Game, Division of Commercial Fisheries, Regional Information Report 2A04–05, Anchorage.

Maxwell, S. L., and N. E. Gove. 2007. Assessing a dual-frequency identification sonar's fish counting accuracy, precision, and turbid river range capability. Journal of the Acoustical Society of America 122(6):3364–3377.

Maxwell, S. L., and A.V. Smith. 2007. Generating river bottom profiles with a dual-frequency identification sonar (DIDSON). North American Journal of Fisheries Management 27:1294–1309.

Maxwell, S. L., A. V. Faulkner, L. Fair, and X. Zhang. 2011. A comparison of estimates from 2 hydroacoustic systems used to assess sockeye salmon escapement in 5 Alaska Rivers. Alaska Department of Fish and Game Fishery Manuscript Series No. 11-02, Anchorage.

Miller, J. D., D. L. Burwen, and S. J. Fleischman. 2011. Estimates of Chinook salmon passage in the Kenai River using split-beam sonar, 2007. Alaska Department of Fish and Game Fishery Data Series No. 11-52, Anchorage.

Reynolds, J. H., C. A. Woody, N. E. Gove, and L. F. Fair. 2007. Efficiently estimating salmon escapement uncertainty using systematically sampled data. American Fisheries Society Symposium 54:121–129.

Seibel, M. C. 1967. The use of expanded ten-minute counts as estimates of hourly salmon migration past counting towers on Alaskan rivers. Alaska Department of Fish and Game, Division of Commercial Fisheries, Informational Leaflet 101, Juneau.

Simmonds, E. J., and D. N. MacLennan. 2005. Fisheries acoustics: theory and practice. Blackwell Science Ltd., Oxford, UK.

Shields, P., and A. Dupuis. 2012. Upper Cook Inlet commercial fisheries annual management report, 2011. Alaska Department of Fish and Game, Fishery Management Report No. 12-25, Anchorage.

Taylor, J. C., and S. L. Maxwell. 2007. Hydroacoustics: lakes and reservoirs. Pages 153–172 [*In*] D. H. Johnson, B. M. Shrier, J. S. O'Neal, J. A. Knutzen, X. Augerot, T. A. O'Neil, and T. N. Pearsons. Salmonid field protocols handbook: techniques for assessing status and trends in salmon and trout populations. American Fisheries Society, Bethesda, Maryland.

Westerman, D. L., and T. M. Willette. 2010a. Upper Cook Inlet salmon escapement studies, 2007. Alaska Department of Fish and Game, Fishery Data Series No. 10-14, Anchorage.

Westerman, D. L., and T. M. Willette. 2010b. Upper Cook Inlet salmon escapement studies, 2008. Alaska Department of Fish and Game, Fishery Data Series No. 10-16, Anchorage.

Westerman, D. L., and T. M. Willette. 2011a. Upper Cook Inlet salmon escapement studies, 2009. Alaska Department of Fish and Game, Fishery Data Series No. 11-33, Anchorage.

Westerman, D. L., and T. M. Willette. 2011b. Upper Cook Inlet salmon escapement studies, 2010. Alaska Department of Fish and Game, Fishery Data Series No. 11-66, Anchorage.

Westerman, D. L., and T. M. Willette. 2012. Upper Cook Inlet salmon escapement studies, 2011. Alaska Department of Fish and Game, Fishery Data Series No. 12-83, Anchorage.

Westerman, D. L., and T. M. Willette. 2013. Upper Cook Inlet salmon escapement studies, 2012. Alaska Department of Fish and Game, Fishery Data Series No. 13-30, Anchorage.

REFERENCES CITED (Continued)

Xie, Y., C. J. G. Michielsens, A. P. Gray, F. J. Martens, and J. L. Boffey. 2008. Observations of avoidance reactions of migrating salmon to a mobile survey vessel in a riverine environment. Canadian Journal of Fisheries and Aquatic Sciences 65:2178–2190.

TABLES AND FIGURES

Table 1.–Specifications for the standard and long-range DIDSONs used in this study.

DIDSON Model		Frequency (MHz)	Start Ranges (m)	Window Lengths (m)	Number of beams	Individual beam width
Standard (SR)	High	1.8	0.42–26.1	1.25, 2.5, 5, 10	96	0.3°
	Low	1.1	0.83–52.3	5, 10, 20, 40	48	0.4°
Long Range (LR)	High	1.2	0.42–26.1	2.5, 5, 10, 20	48	0.7°
	Low	0.7	0.83–52.3	10, 20, 40, 80	48	0.8°

Note: Both models have a 28° composite beam made up of individual beams, each 17° in the vertical plane (nominal beam size).

Table 2.–Differences between Yentna River fish counts from shore-based, horizontal DIDSONs and cross-river, mobile DIDSONs.

	Year	h-shore fish counts[a]	In Range Cross-river fish counts[b]	% Fish within shore sonar	% Error[c]	Outside Range Cross-river fish counts[d]	% Fish beyond shore sonar	Expansion factor	Max fish range[e] of shore sonar (m)
North Bank									
	2010	278	220	56.7	20.9	168	43.3	1.76	19
	2011	504	366	94.0	27.4	23	6.0	1.06	15
	2012	298	379	80.3	27.2	93	19.7	1.25	21
Total		1,080	965	231.0	10.6	284	22.8		
Average		360	322	77.0	25.2	95	23.0	1.30	18
Std Error								0.21	
South Bank									
	2010	1,137	663	100.0	41.7	0	0.0	1.00	25
	2011	1,287	1,288	99.4	0.1	7	0.6	1.01	17
	2012	2,116	1,958	95.1	7.5	101	4.9	1.05	19
Total		4,540	3,909	294.6	13.9	108	2.7		
Average		1,513	1,303	98.2	16.4	35.9	1.8	1.02	20
Std Error								0.02	

Note: In 2010, the composite beam of the cross-river DIDSON was oriented horizontally, in 2011 and 2012, the beam was oriented vertically.

[a] From DIDSON files collected while the cross-river transects were in progress.

[b] The number of fish observed in range bins that overlapped the horizontal, shore-based DIDSONs expanded to equalize sampling time and interpolated for unsampled regions between stations.

[c] Using the horizontal, shore-based counts as the reference.

[d] The number of fish observed beyond the effective range of the shore-based units, using the same interpolation and expansion methods.

[e] The range of the most distant fish observed in the shore-based data from this comparison. (Fish may have been observed farther offshore during normal sampling operations.)

Table 3.–Yentna River bank to bank percentages from shore-based, horizontal DIDSONs and cross-river, mobile DIDSONs.

	Shore-based		Cross-river (in rge)		Cross-river (all fish)		Shore	Cross -in rge	Difference	Cross-all
Year	North	South	North	South	North	South	NB:SB %	NB:SB %	(%)	NB:SB %
2010	278	1,137	220	663	389	663	24.5	33.2	-8.7	58.7
2011	504	1,287	366	1,288	389	1295	39.2	28.4	10.7	30.0
2012	298	2,116	379	1,958	472	2059	14.1	19.4	-5.3	22.9
Avg	360	1,513	322	1,303	417	1,339	25.9	27.0	-1.1	37.2
Total	1,080	4,540	965	3,909	1,250	4,017	23.8	24.7	-0.9	111.6

Note: The cross-river counts were interpolated for regions between stations and expanded to match the sampling time of the shore-based counts.

Table 4.–The error in Yentna River horizontal distance measurements from using slant range in place of the true range based on sampling ranges and tilt angles used in this study.

Cross-river Range Maximum Error Values									
		Maximum	Tilt angle (degrees)						
Bank	Year	Slant Range	lowermost	uppermost	*Rrect h*	*Rrect v*	*Rrect*	Diff. (m)	% error
North	2010	12	-7	-38	11.6	8.5	8.1	3.9	47.6
	2011	12	1	-14	11.6	11.2	10.8	1.2	10.6
	2012	12	-2	-34	11.6	9.1	8.7	3.3	37.9
NB Avg			*-3*	*-29*				*2.8*	*32.1*
South	2010	12	-3	-29	11.6	9.7	9.4	2.6	28.3
	2011	12	-4	-16	11.6	11.0	10.7	1.3	12.3
	2012	12	1	-29	11.6	9.7	9.4	2.6	28.3
SB Avg				*-25*				*2.2*	*23.0*
Cross-river Range Minimum Error Values									
		Maximum	Tilt angle (degrees)						
Bank	Year	Slant Range	lowermost	uppermost	*Rrect h*	*Rrect v*	*Rrect*	Diff. (m)	% error
North	2010	12	-7	-38	11.6	11.6	11.3	0.7	6.3
	2011	12	1	-14	11.6	11.9	11.5	0.5	4.1
	2012	12	-2	-34	11.6	11.9	11.5	0.5	4.4
NB Avg			*-3*	*-29*				*0.6*	*4.9*
South	2010	12	-3	-29	11.6	11.8	11.5	0.5	4.7
	2011	12	-4	-16	11.6	11.8	11.4	0.6	5.1
	2012	12	1	-29	11.6	11.9	11.5	0.5	4.1
SB Avg				*-25*				*0.5*	*4.6*

-continued-

Table 4.–Page 2 of 2.

Shore-based Range using the h-DIDSON								
Bank	Year	Maximum Slant Range	Avg Tilt (degrees)	*Rrect h*	*Rrect v*	*Rrect*	Diff. (m)	% error
North	2010	19	-13.8	19.0	17.8	17.8	1.2	7.0
	2011	15	-15.7	15.0	13.8	13.8	1.2	8.4
	2012	21	-14.3	21.0	19.6	19.6	1.4	7.4
NB Avg			-14.6				1.3	7.6
South	2010	25	-18.1	25.0	22.6	22.6	2.4	10.5
	2011	17	-17.8	17.0	15.4	15.4	1.6	10.2
	2012	19	-17.2	19.0	17.3	17.3	1.7	9.7
SB Avg			-17.7				1.9	10.1

Cross-river Depth									
		Maximum	Tilt angle (degrees)			Depth	Depth		
Bank	Year	Slant Range	lowermost	uppermost	*Rrect h*	w/*Rslant*	w/*Rrect h*	Diff. (m)	% error
North	2010	12	-7	-38	11.6	9.5	9.2	0.3	3.1
	2011	12	1	-14	11.6	5.6	5.5	0.2	3.1
	2012	12	-2	-34	11.6	8.9	8.7	0.3	3.1
NB Avg		12		-29				0.2	3.1
South	2010	12	-3	-29	11.6	8.2	7.9	0.2	3.1
	2011	12	-4	-16	11.6	6.0	5.8	0.2	3.1
	2012	12	1	-29	11.6	8.2	7.9	0.2	3.1
SB Avg				-25				0.2	3.1

Table 5.–Yentna River percentages and 95% bootstrapped confidence limits of fish within the DIDSON's effective horizontal beam at the Yentna River (assuming a 14° or 17° beam) if tilted at the traditional aim compared with percentages where the beam is raised 7°.

Year	*n* [a]	% Fish in 14° beam	Expansion factor	Mean	Lower Quantile	Upper Quantile	Raising beam 7°	% Fish in 17° beam	Expansion factor	Mean	Lower Quantile	Upper Quantile
North Bank												
2010	6,974	87	1.15	87	85	89	99	93	1.08	93	91	94
2011	6,361	92	1.08	92	91	94	99	95	1.05	95	94	96
2012	17,766	84	1.19	84	82	86	99	92	1.08	92	91	94
Average		88	1.14	88	86	90	99	93	1.07	93	92	95
South Bank												
2010[b]	20,963	60	1.66	60	57	63	95	74	1.35	74	71	77
2011[c]	22,566	66	1.51	66	63	69	93	77	1.30	77	74	79
2012[d]	65,571	46	2.20	46	43	49	90	60	1.67	60	57	63
Average		57	1.74	57	54	60	93	70	1.42	70	67	73

[a] Number of fish observed with the shore-based vertically positioned DIDSON.

[b] Vertical and horizontal DIDSONs at the original sonar site.

[c] Horizontal DIDSON at original site, vertical DIDSON at new site.

[d] Both DIDSONs at new site.

Table 6.–Depth and average tilt angle by bank and year for the shore-based, vertically (v-beam) and horizontally (h-beam) positioned DIDSONs, Yentna River.

	v-beam		h-beam		Best	
Year	Depth (m)	Tilt (deg)	Depth (m)	Tilt (deg)	h-beam tilt	Difference
North Bank						
2010	-0.32	-13.0	-0.52	-13.8	-7.8	-6.0
2011	-0.38	-18.0	-0.50	-15.7	-10.7	-5.0
2012	-0.32	-12.0	-0.43	-14.3	-6.3	-8.0
Average						-6.3
South Bank						
2010	-0.33	-15.2	-0.51	-18.1	-11.1	-7.0
2011	-0.21	-19.0	-0.44	-17.8	-10.8	-7.0
2012	-0.34	-18.2	-0.74	-17.2	-8.2	-9.0
Average						-7.7

Table 7.–Comparisons of Yentna River daily fish counts from horizontally (*h*) and vertically (*v*) positioned DIDSONs using total ratios, linear regression (with *h* as the independent variable), and *t*-tests by year and bank.

	Hours	*df*	Ratio		Slope		Intercept		$Ho:B_1 = 1$		$H_o:B_o = 0$	
Year	Sampled	(days)	*v/h*	R^2	(B_1)	SE	(B_o)	SE	*t*	*p*	*t*	*p*
North Bank												
2010	342	18	0.86	0.993	0.85	0.017	6.0	9.5	9.14	<0.01	0.63	0.54
2011	316	18	0.87	0.993	0.83	0.017	13.8	9.3	10.10	<0.01	1.48	0.16
2012	834	35	0.93	0.975	0.89	0.024	18.2	17.7	4.36	<0.01	1.03	0.31
All Years	1,492	75	0.90	0.980	0.88	0.015	10.8	9.5	8.44	<0.01	1.14	0.26
South Bank												
2010	392	22	1.02	0.995	1.02	0.015	-1.7	17.6	1.22	>0.2	-0.95	0.93
2011	429	21	1.45	0.816	0.96	0.074	331.4	90.4	0.59	>0.5	3.67	<0.01
2012	825	35	1.08	0.987	1.01	0.019	117.4	50.3	0.54	>0.5	2.33	0.03
All Years	1,646	82	1.13	0.975	1.00	0.018	145.2	35.8	0.01	>0.5	4.06	<0.01

Table 8.–Summary of expansion factors from 3 rivers to account for fish swimming outside (beyond and above) the detection volume of shore-based, horizontal DIDSONs.

		Beyond			Above		
River	Bank	Beyond %	Expansion Factor	Expansion Based on SE	Above %	Expansion Factor	Expansion Based on CI
Yentna[a]	NB	23.0	1.30	1.09	12.4	1.14	1.12
Yentna[a]	SB	1.8	1.02	1.00	42.6	1.74	1.66
Copper	NB	14.7	1.17	na	na	na	na
Copper	SB	3.7	1.04	na	1.4	1.01	na
Kenai	NB	na	na	na	na	na	na
Kenai	SB	na	na	na	2.4	1.02	na
Kenai	both	4.2	1.04	na	na	na	na

[a] Yentna River data were averaged from 2010 to 2012 and more conservative expansion factors were included based on subtracting the standard error (SE) from the average (Beyond fish) and using the upper 95% confidence interval (CI) to determine the expansion factor (Above fish).

Table 9.–Percentages of fish from Copper River cross-river transects and a shore-based DIDSON in paired range bins from 2005 and 2006.

	South Bank		North Bank	
Range Bins (m)	Cross-River % of total	Shore-Based % of total	Cross-River % of total	Shore-Based % of total
2.5	34.1	19.6	0.9	5.0
7.5	37.6	65.2	29.9	21.3
12.5	11.5	12.4	5.2	27.7
17.5	11.9	2.5	15.1	16.4
22.5	1.2	0.3	8.2	13.5
27.5	1.4		10.5	6.3
32.5	0.5		8.6	6.6
37.5	1.1		6.8	3.2
42.5	0.7		10.1	
47.5			2.0	
57.5			2.6	
Fish offshore of the South Shore Sonar:			3.7%	
Fish offshore of the North Shore Sonar:			14.7%	

Table 10.–A comparison of the percentages of fish observed in paired range bins from the cross-river surveys and shore-based DIDSONs, Kenai River, 2006 and 2007.

Range Bins (m)	Mid-Range (m)	Bin Gaps[a] (m)	% of total Cross-river	% of total Shore-based	Difference
(North to South Bank)					
0–5	2.51		0.00	0.02	-0.02
6–8	7.08	4.57	9.59	8.99	0.60
9–16	12.67	5.59	32.96	29.83	3.13
17–18	17.57	4.91	8.08	1.90	6.18
19–25	21.89	4.32	7.22	3.41	3.82
26–30	28.15	6.26	5.34	0.42	4.92
31–36	34.45	6.30	2.32	0.10	2.22
37–41	39.58	5.13	0.93	0.02	0.91
42–47	44.32	4.74	0.23[b]		0.23
48–51	49.37	5.05	0.20[b]		0.20
52–57	54.40	5.03	0.19[b]		0.19
58–66	62.23	7.83	0.27[b]		0.27
67–73	70.14	7.91	0.08[b]		0.08
74–87	80.58	10.44	1.71[b]		1.71
88–93	90.43	9.85	0.85[b]		0.85
94–97	95.43	5.01	0.74	0.13	0.60
98–103	100.55	5.12	0.19	0.25	-0.06
104–107	105.29	4.74	0.28	0.10	0.18
108–112	110.24	4.95	0.31	0.57	-0.26
113–118	115.27	5.04	11.47	4.22	7.26
119–123	121.15	5.88	10.42	50.03	-39.61
124–127	125.44	4.29	6.61	0.02	6.59

[a] The size of each range bin was based on the sampled range and distance between sampling stations from the cross-river surveys.

[b] Fish beyond the range of the shore-based DIDSONS. The percentages in this region total 3.5%.

Table 11.–Percentage of fish within the effective limits of a DIDSON horizontal beam assuming an effective beam width of 14° or 17° along with bootstrapped confidence limits, Kenai River south bank.

Year	*n* [a]	% Fish in 14° beam	Mean	Lower Quantile	Upper Quantile	% Fish in 17° beam	Mean	Lower Quantile	Upper Quantile
South Bank									
2007	9,119	97.6	97.6	96.6	98.4	99.5	99.5	99.1	99.9

[a] Number of fish observed with the vertically positioned DIDSON.

Table 12.–The depth of the vertical and horizontal transducers and average tilt angle, Kenai River south bank.

	Vertical Beam		Horizontal Beam		Best	
Year	Depth (m)	tilt (deg)	Depth (m)	tilt (deg)	Aim	Diff.
South Bank						
2007	-0.35	-4.9	-0.35	-8.2	-5.20	-3.0

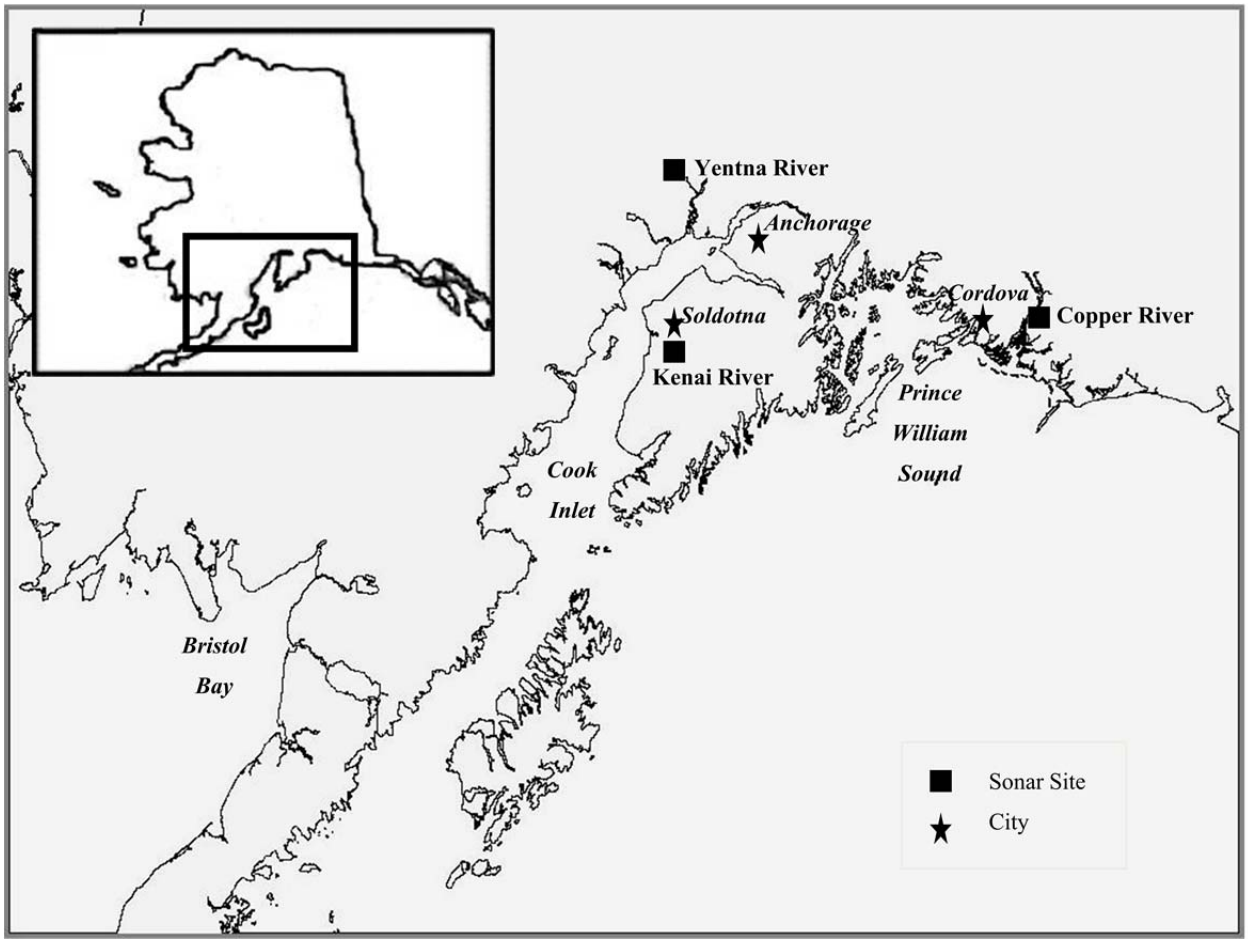

Figure 1.–The locations of the Alaska Department of Fish and Game's Yentna, Copper, and Kenai river sonar sites in Southcentral Alaska notated with a square and labeled with the name of the river.

Note: The dark, cross-river line at the north site is 200 m long; the line at the south site is 243 m long. The north site is 980 m upriver from the south site.

Figure 2.–Bathymetry map of the Yentna River at the sonar site located 9.2 km upriver from the confluence with the Susitna River.

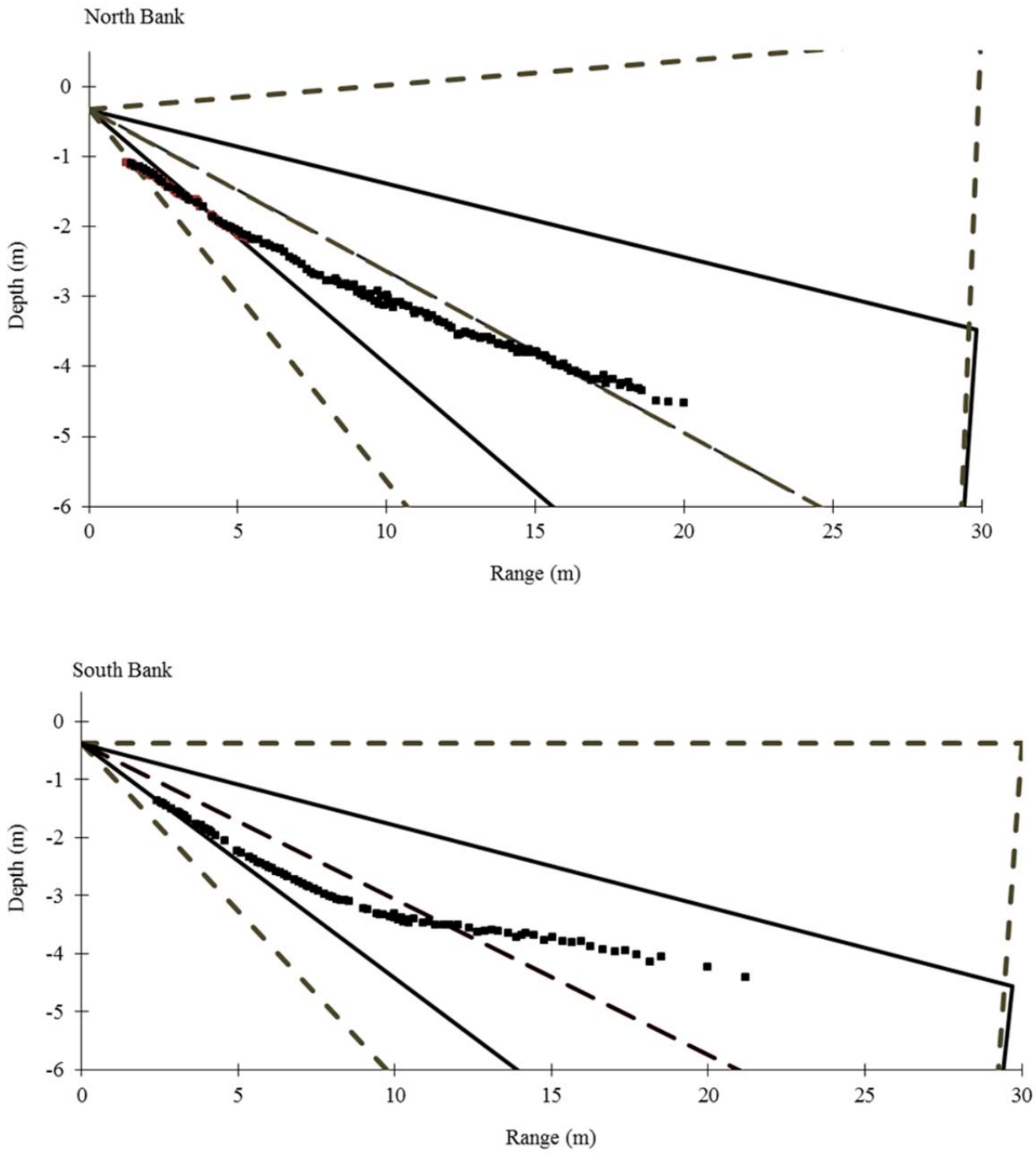

Figure 3.–River bottom profiles of the Yentna River site with the composite DIDSON beam positioned vertically (dotted line) and horizontally (solid line).

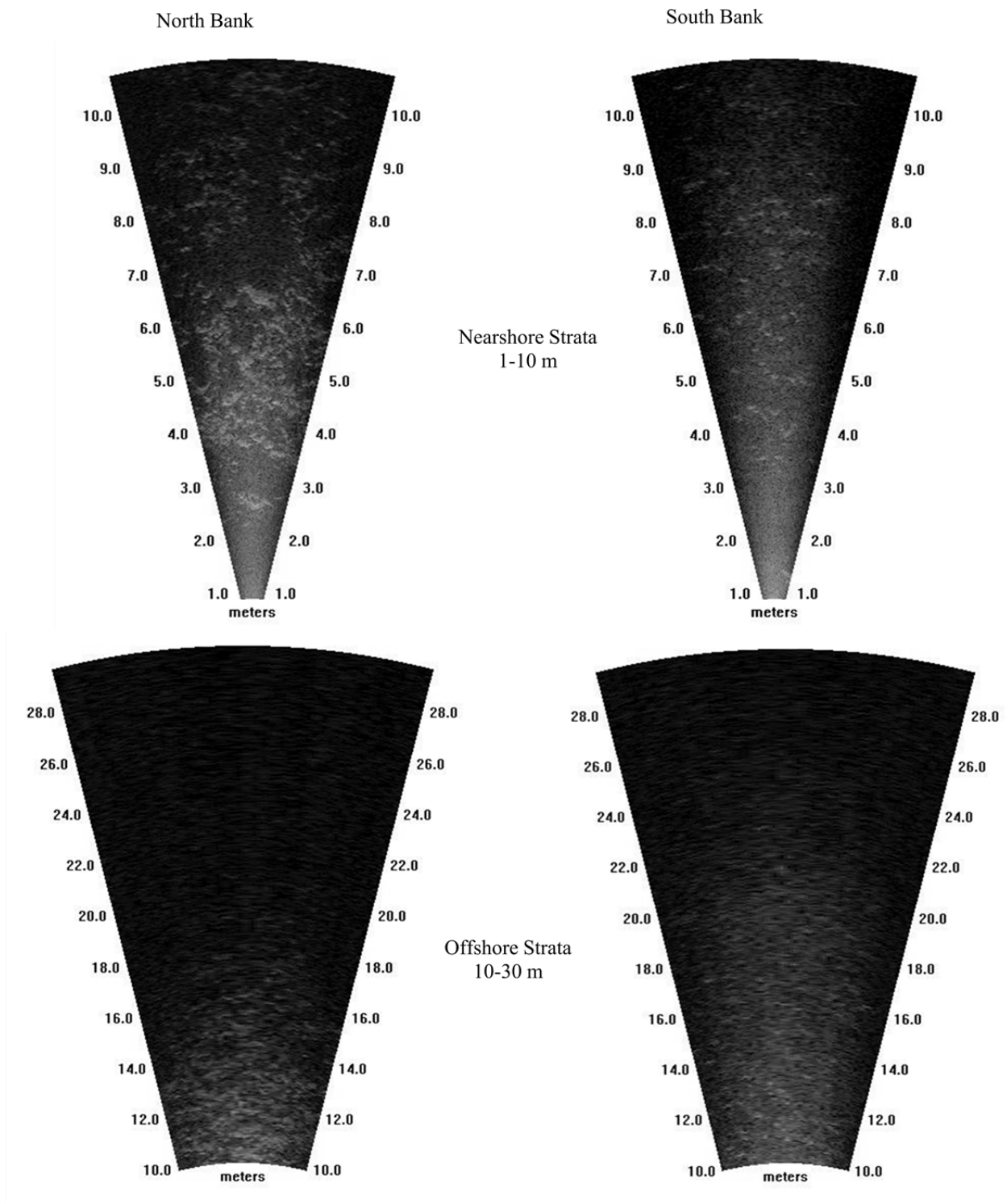

Figure 4.–Images from a shore-based, horizontally oriented DIDSON showing reflective and non-reflective regions in the river bottom at the Yentna River.

Figure 5.–Shore-based DIDSONs mounted horizontally (left) and vertically (right) using an aluminum H-mount and automated rotator.

Note: The mount allows the user to manually tilt, and if needed, to pan the DIDSON.

Figure 6.–Kenai River mobile DIDSONs mounted with the composite beam positioned horizontally (left) and vertically (right).

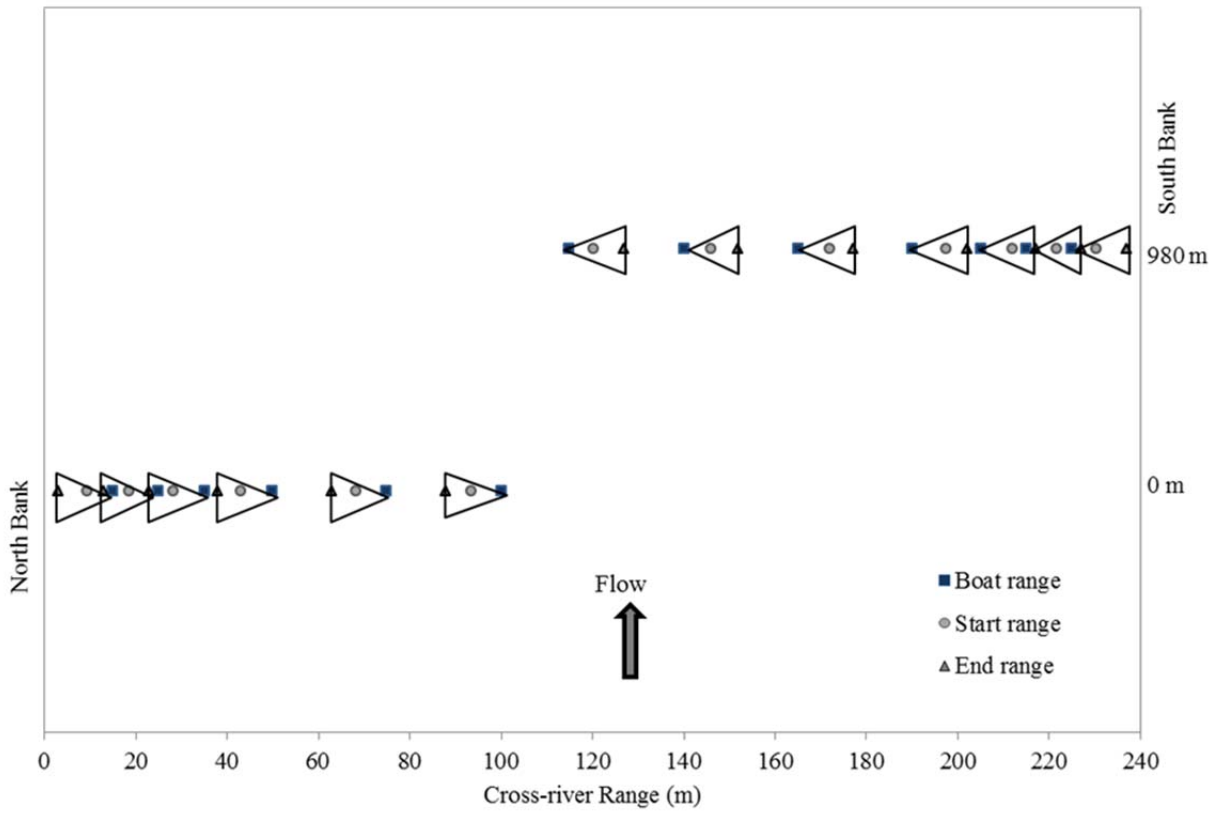

Figure 7.–The spacing between stations for the mobile surveys along the north and south banks of the Yentna River.

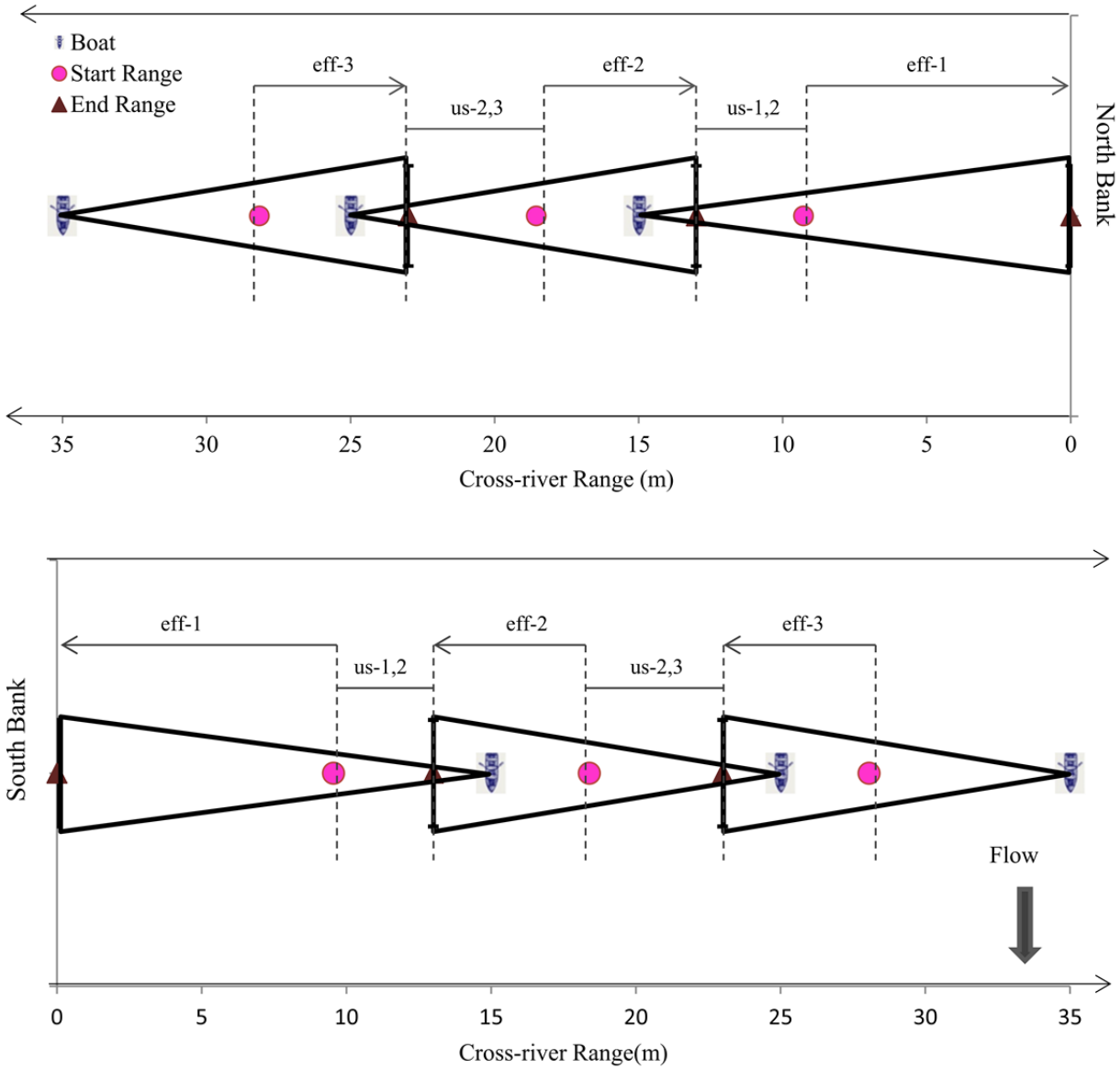

Note: Variables used for interpolating:

1. End Range (*er*) is the effective end range of the sonar based on where the river bottom ends in the DIDSON image.
2. Start Range (*sr*) is the effective start range of the sonar based on where the river bottom starts in the DIDSON image.
3. Effective sampling region (eff_1) of station 1; i.e., er_1-sr_1.
4. Unsampled region ($us_{1,2}$) between station 1 and station 2.
5. Mid-Range ($mr_{1,2}$) of the unsampled region between stations 1 and 2.

Figure 8.–The outermost cross-river stations at the Yentna River illustrating the effective sampling regions, unsampled regions, and the variables used for interpolating the unsampled regions between stations.

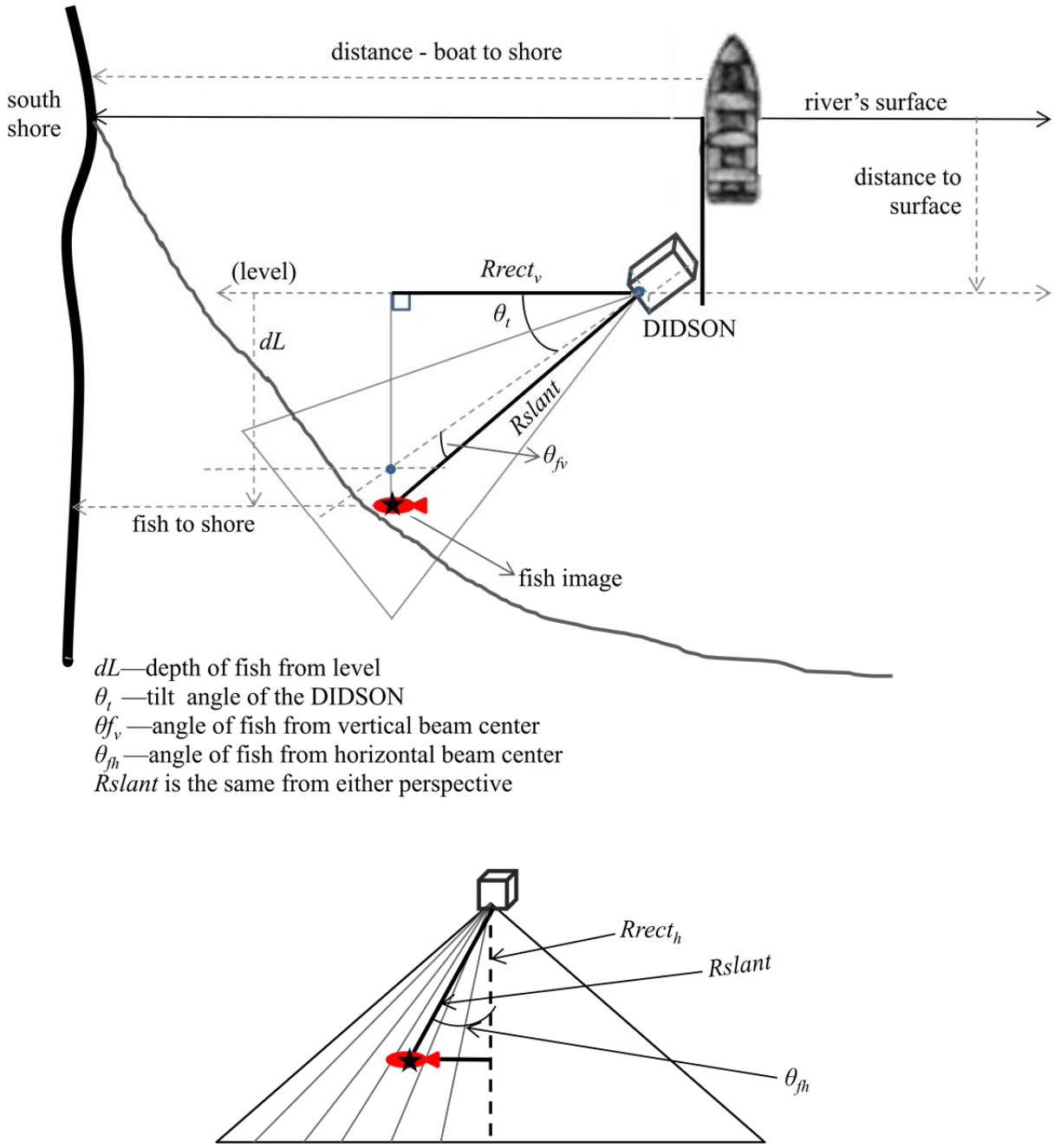

Note: For the north shore, the set up would be reversed with the DIDSON pointing away from shore.

Figure 9.–The Yentna River setup used for mobile surveys and the variables used to calculate the distance from shore to a fish observed in DIDSON images.

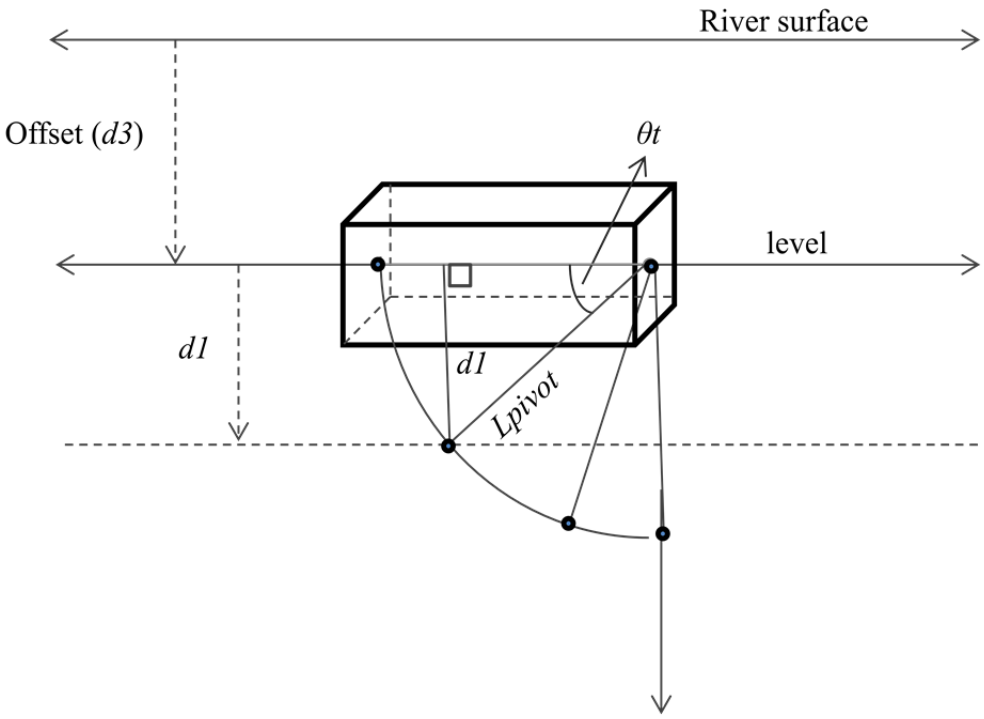

Note: $d1_t = Lpivot \times \sin\theta_{ti}$

Where: θ_{ti} is the pivoting transducer tilt angle, and *Lpivot* is the length from the pivot point to the edge of the DIDSON lens. In this diagram, the edge of the lens traces a circular path as it is tilted. This assumes the DIDSON itself is the pivoting arm. If the pivot point is distant from the DIDSON, which was the case in our set up, the length of the pivot arm needs to be taken into account.

Figure 10.–As the DIDSON changes tilt angle, the depth of the lens changes (d1).

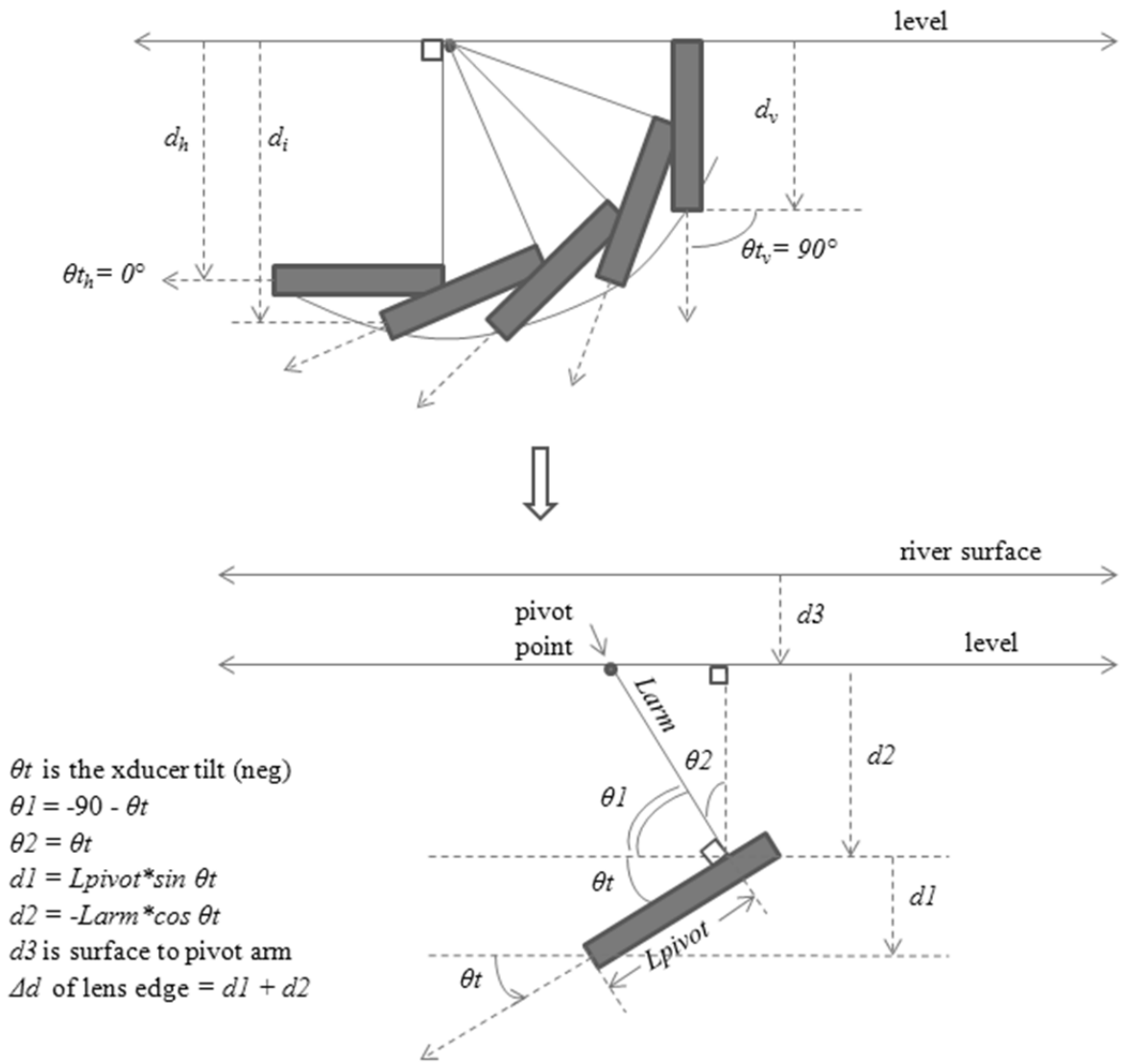

Note: The path traced by a short rotational arm is closer to a circular path. As the rotational arm is lengthened, the arc flattens, becoming more elliptical.

Figure 11.–Diagram showing the change in depth of a DIDSON lens based on the tilt angle and length of the rotational arm.

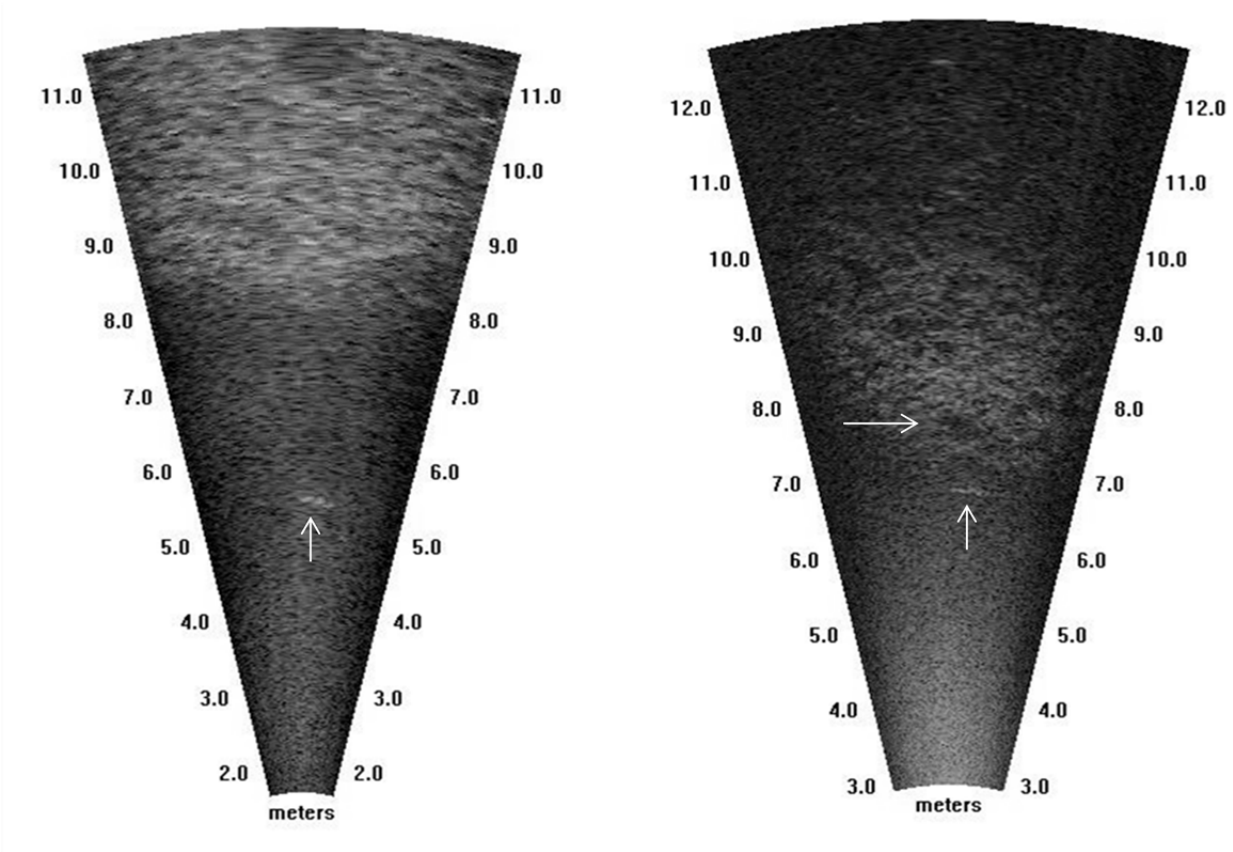

Note: Other dark shapes on the right image are shadows from rocks. In a still image, fish and rock shadows are similar. In video, the dark shadow moves across the beam. Fish traveling directly over the highly reflective river bottom were in most cases undetectable except for the moving shadow.

Figure 12.–Images from a mobile, horizontally oriented DIDSON at the Yentna River showing static river bottoms, likely composed of small gravel, with fish traces (up arrows) and the shadow of a fish (horizontal arrow).

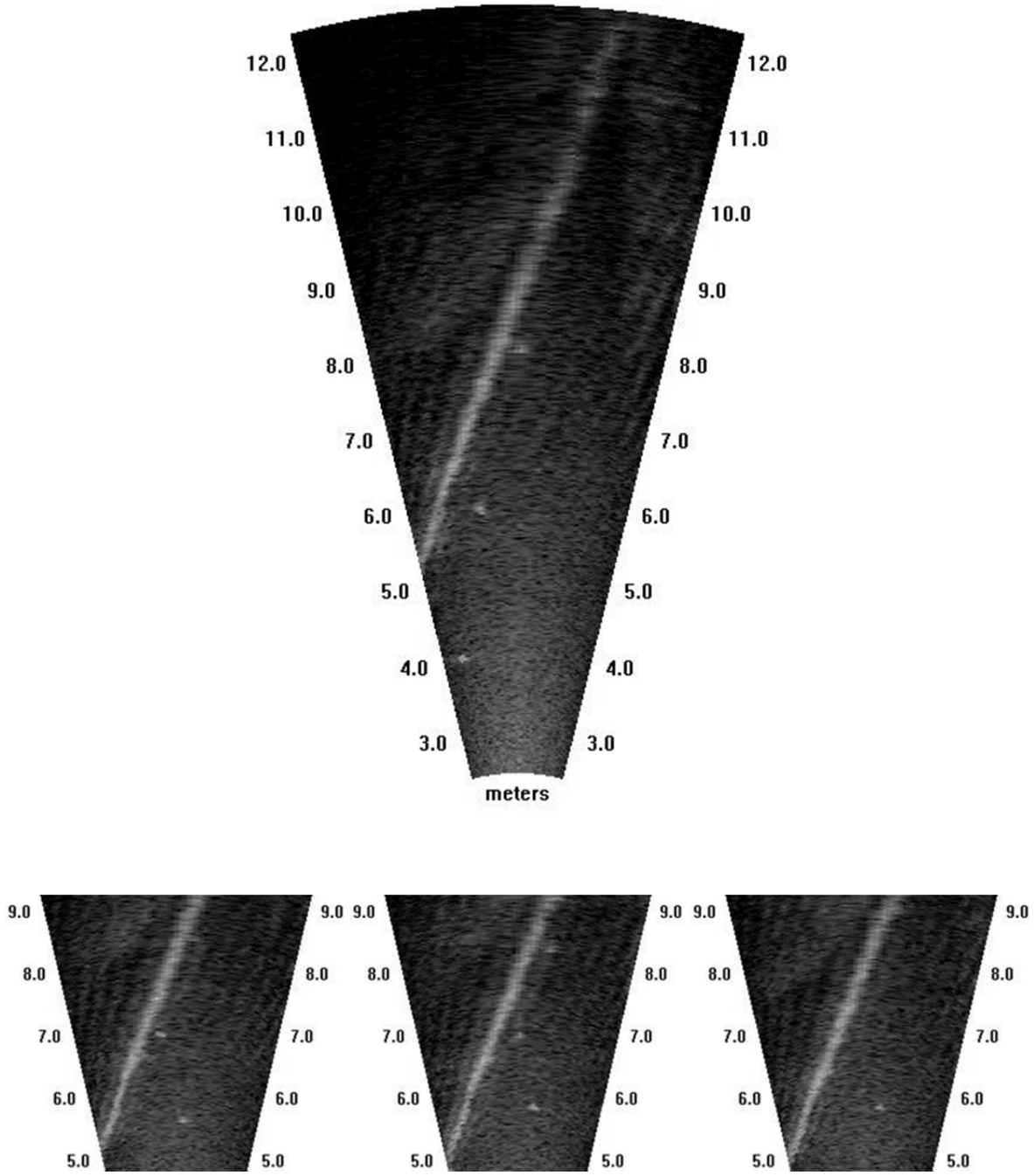

Note: The top image shows the diagonal line of the river bottom with 3 fish (round specs) just above the river bottom (to the right) and faint reflections off the bars from the weir. The bottom images are 3 successive frames showing fish specs disappearing rather than moving across the beam as they would in images from a horizontally positioned DIDSON.

Figure 13.–Yentna River images from a DIDSON oriented vertically, aimed sideways and down from a boat at the south bank station closest to shore.

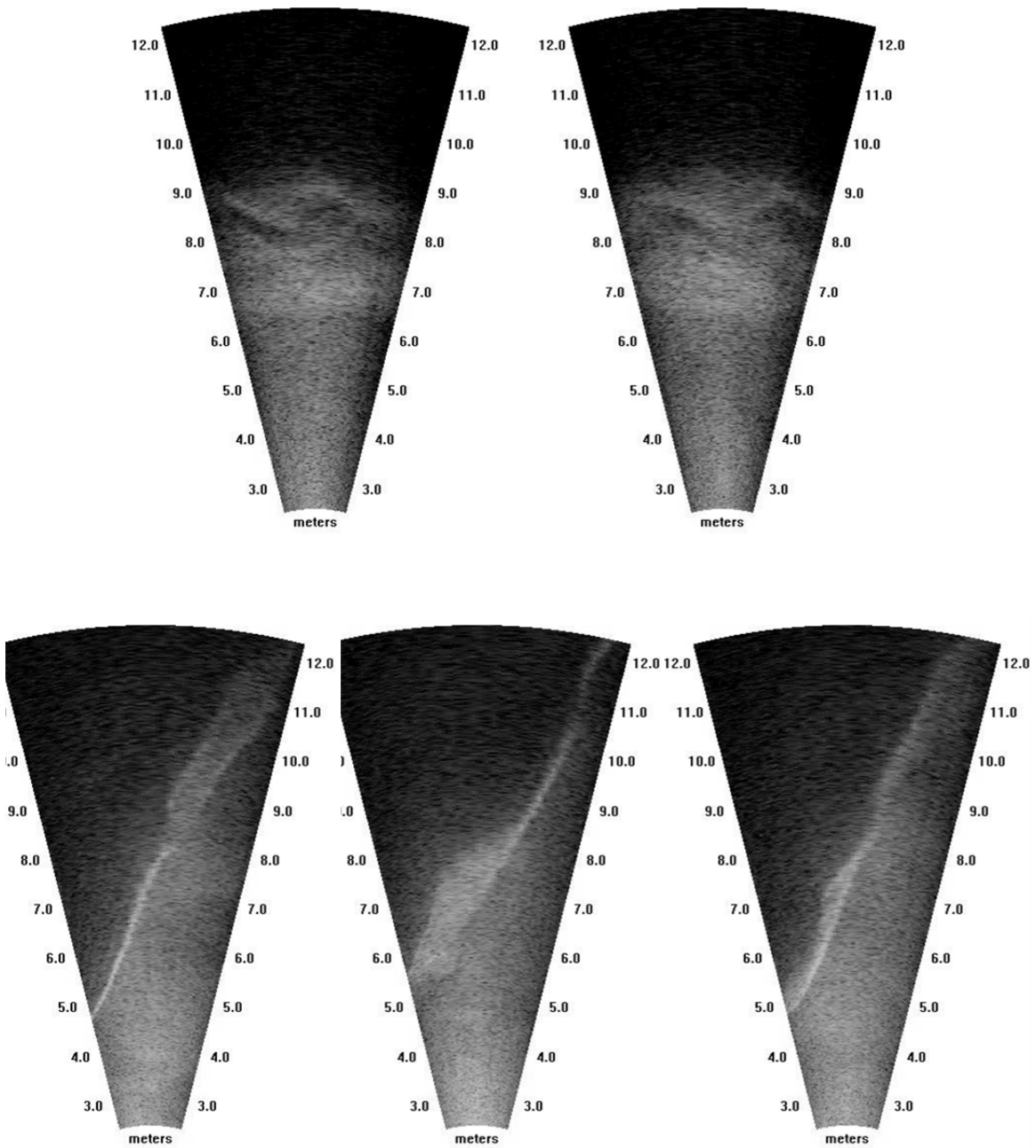

Note: The bottom 3 images show sand waves from a DIDSON oriented vertically where the rolling bottom appears to twist like a ribbon.

Figure 14.–Undulating sand waves along the river bottom from a mobile DIDSON positioned horizontally, aimed sideways and down from a boat at the Yentna River (top).

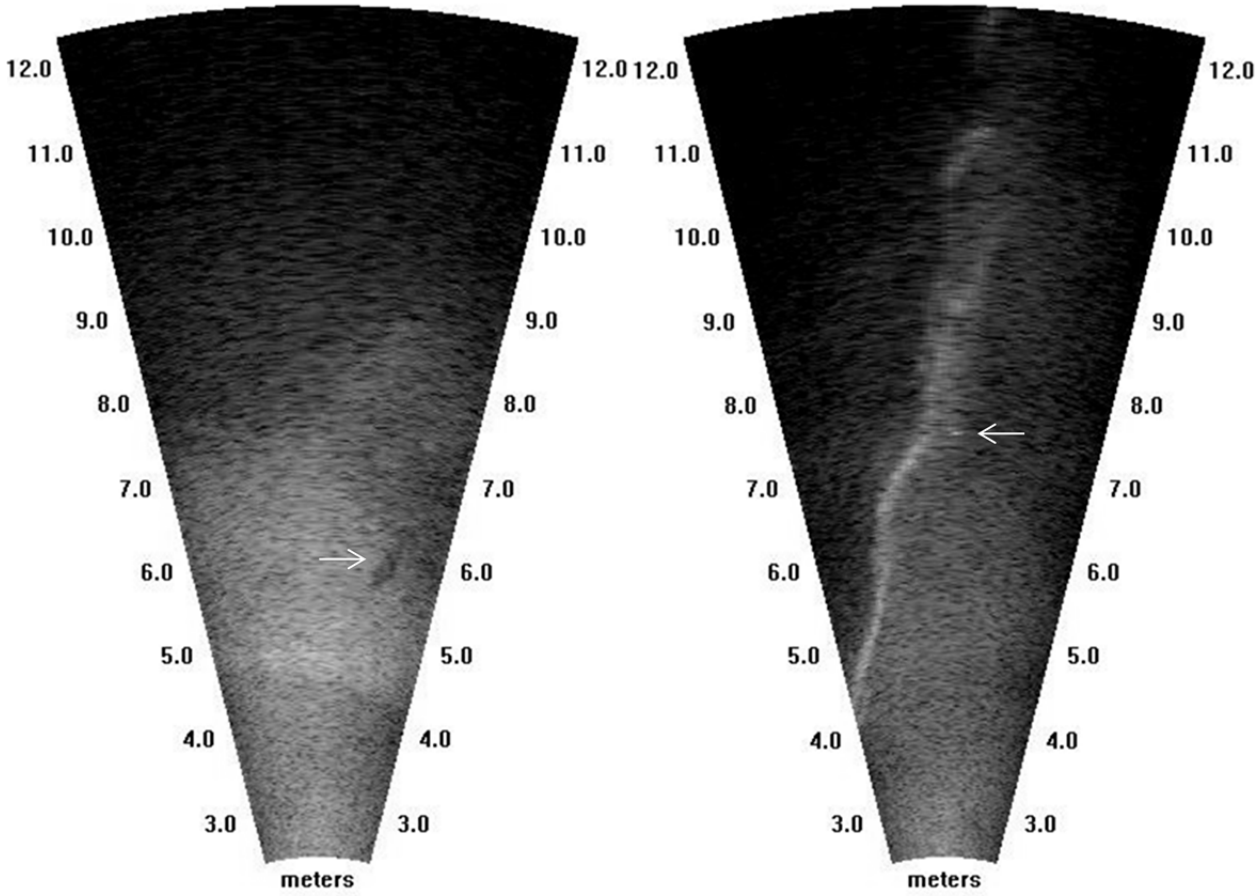

Figure 15.–Images of Yentna River fish detectable moving through clouds of silt from mobile DIDSONs positioned horizontally (left) and vertically (right).

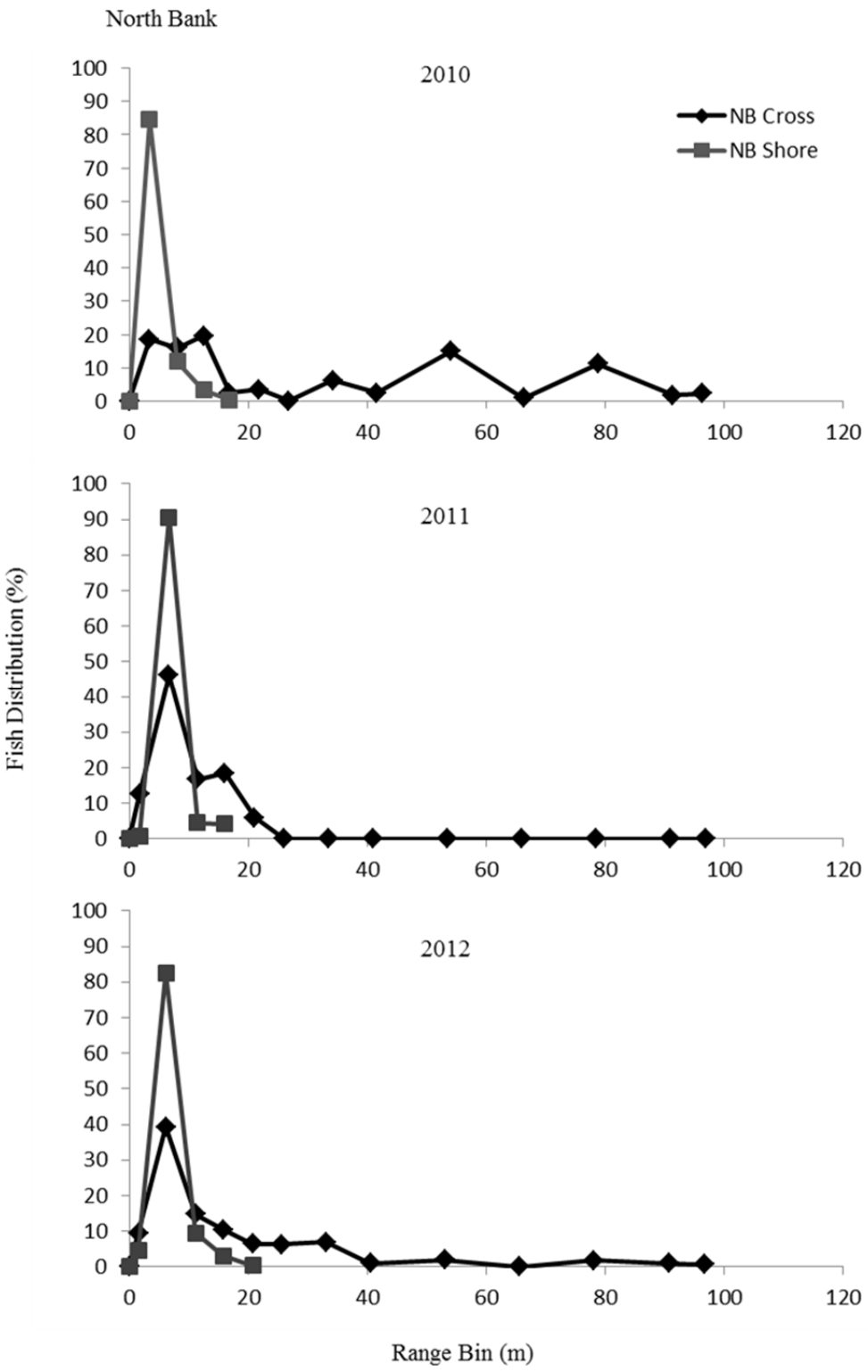

Figure 16.–Cross-river fish distributions by year from mobile, cross-river surveys and a fixed, shore-based sonar, both using DIDSONs, north bank Yentna River.

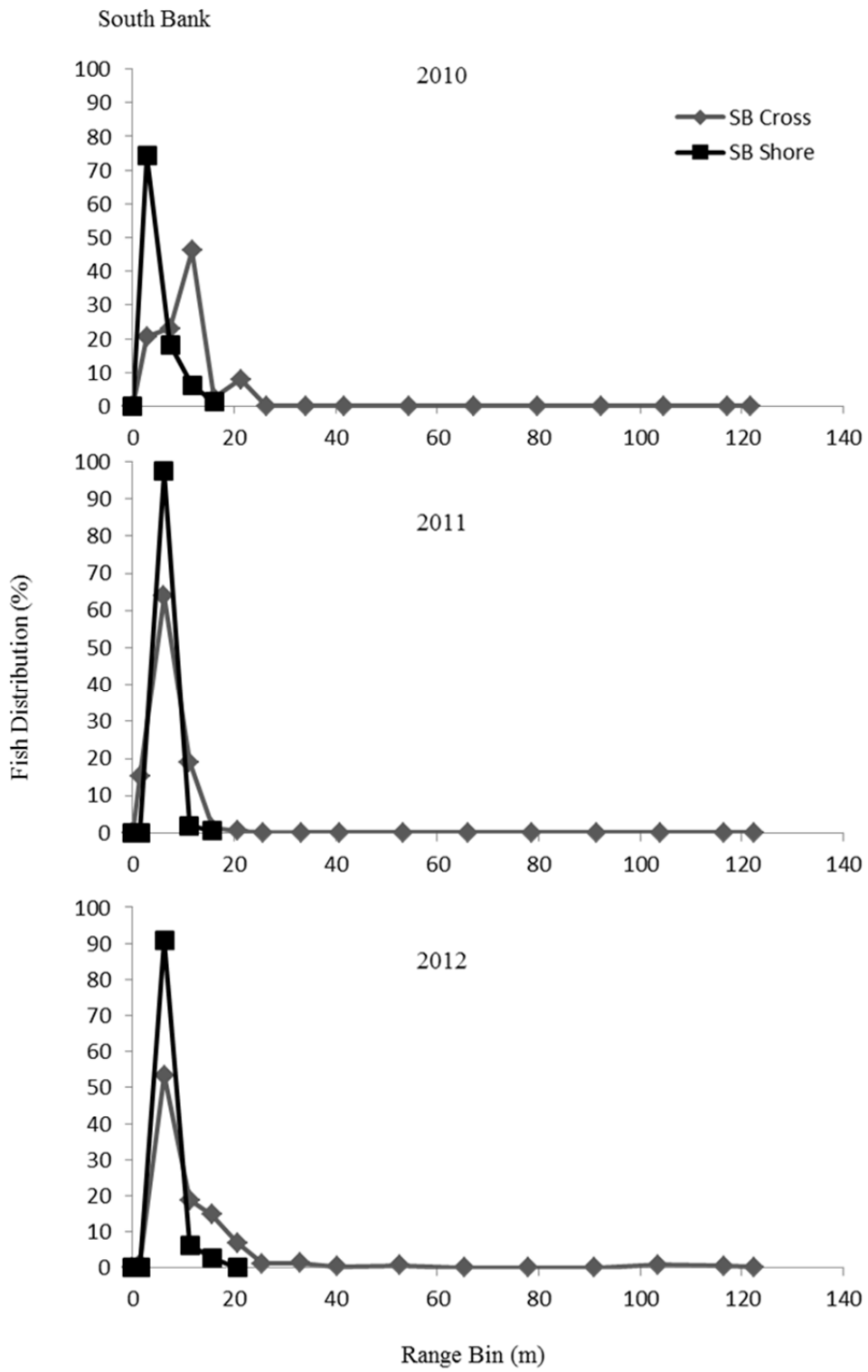

Figure 17.–Cross-river fish distributions by year from mobile, cross-river surveys and a shore-based sonar, both using DIDSONs, south bank Yentna River.

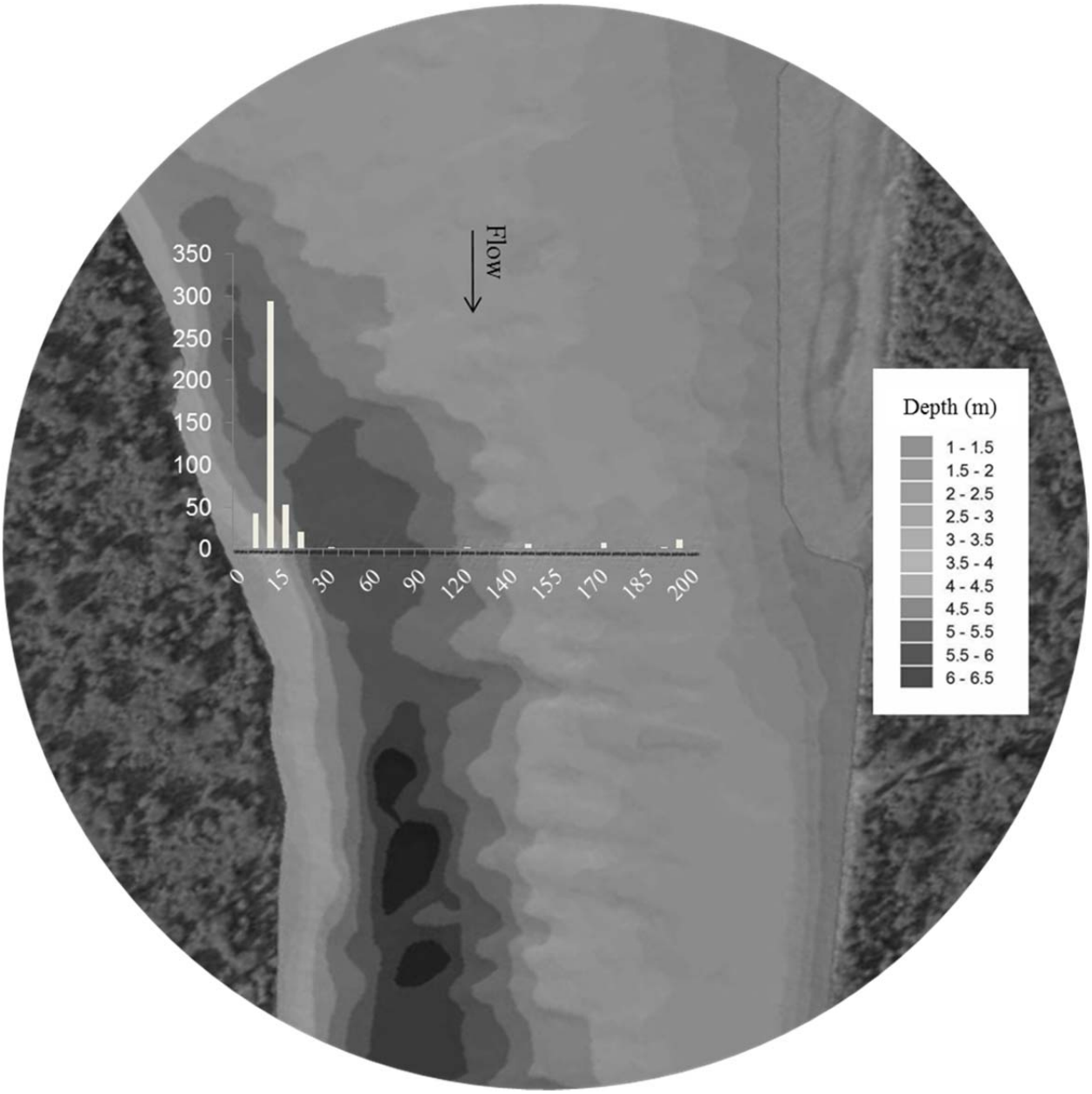

Figure 18.–South bank frequency distribution of fish averaged across all years of the cross-river study overlaid onto a contour map of the river bottom, Yentna River.

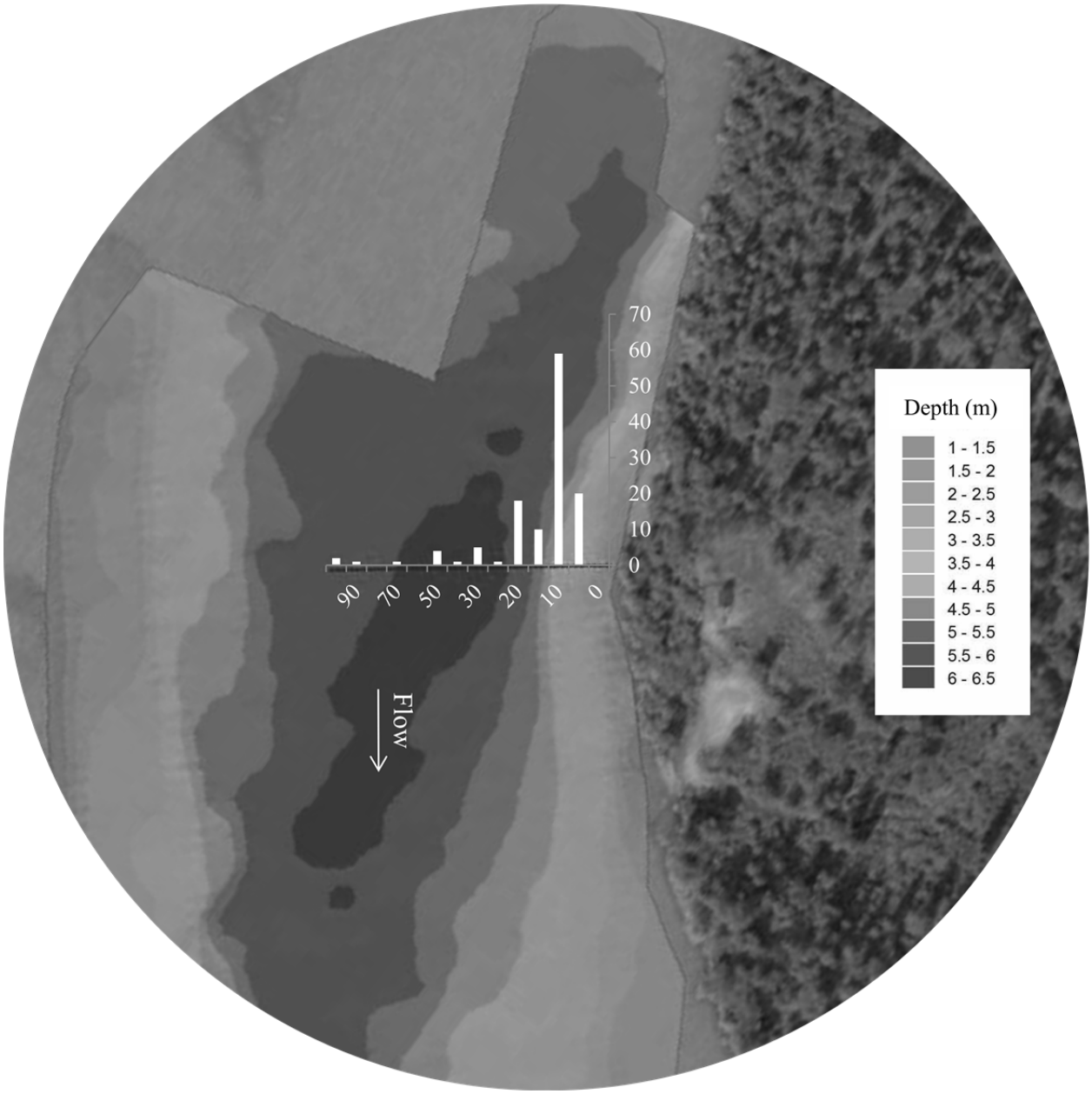

Figure 19.–North bank frequency distribution of fish averaged across all years of the cross-river study overlaid onto a contour map of the river bottom, Yentna River.

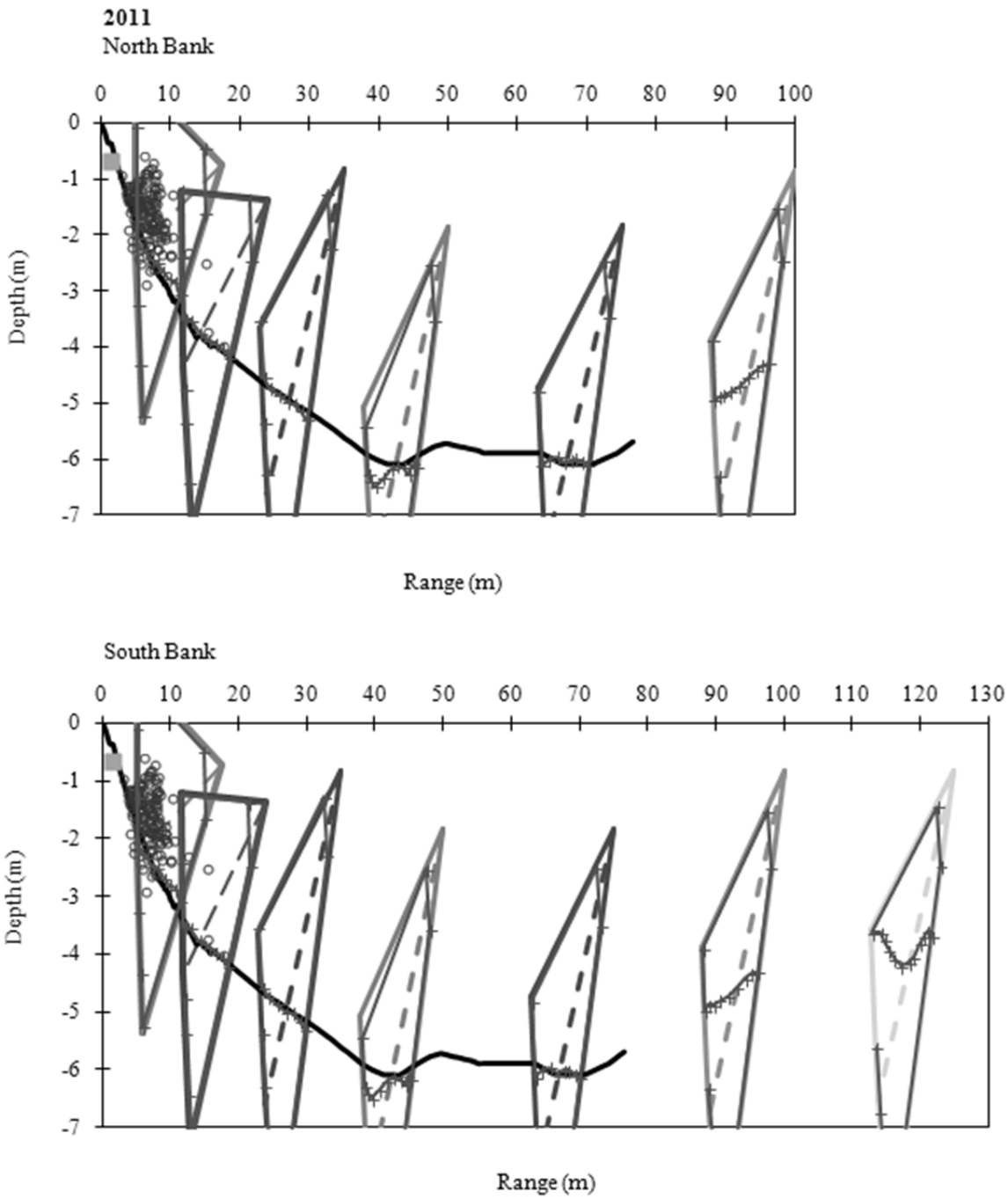

Note: The large downward triangles represent the transducer beam at each of the fixed cross-river stations, the partial tracings along these lines are beams outlined and exported from cross-river images. The circles represent fish positions, and the solid and cross-hatched lines are the river bottom.

Figure 20.–Yentna River range and depth of fish observed from a mobile, vertically positioned DIDSON, 2011.

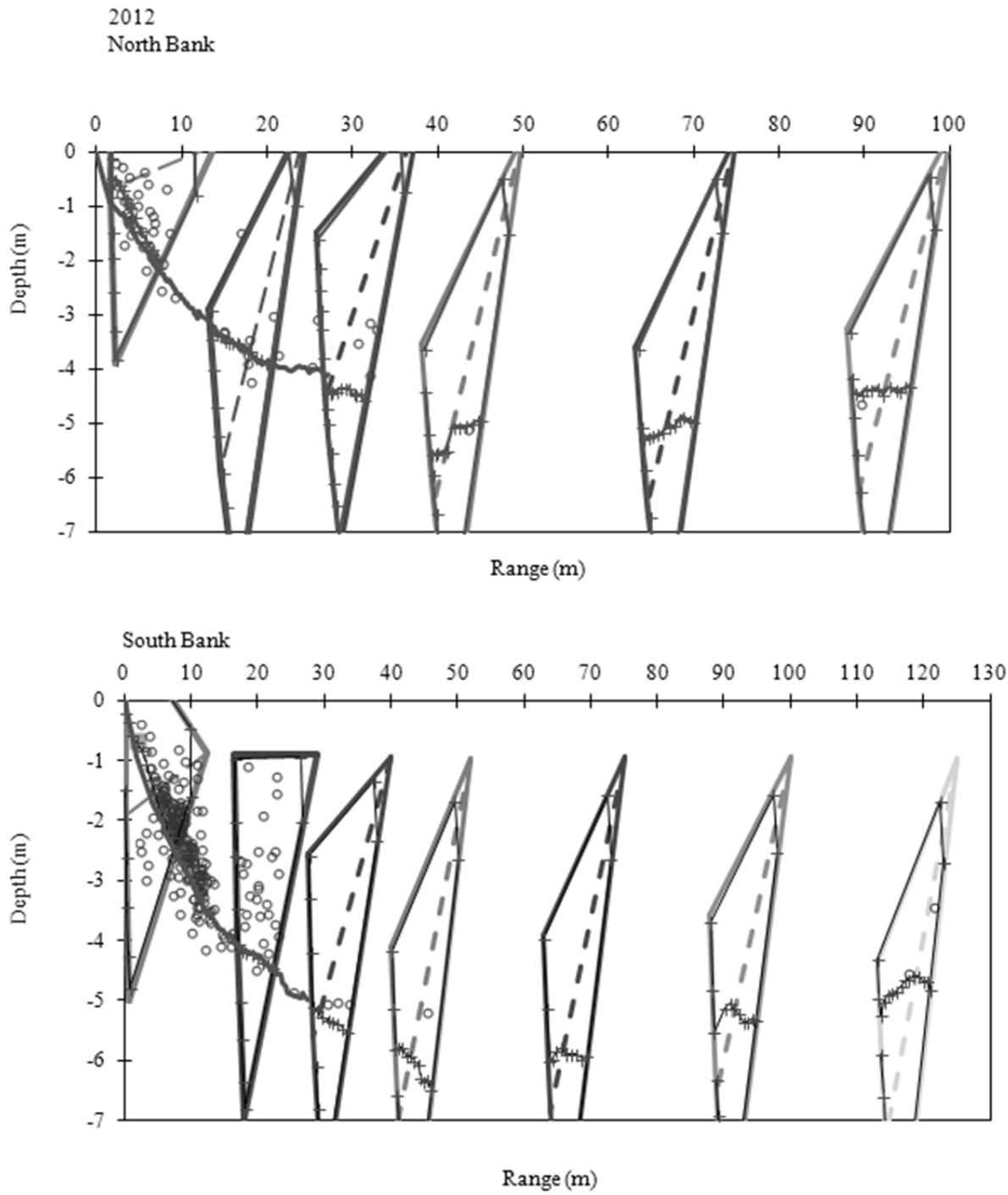

Note: The large downward triangles represent the transducer beam at each of the fixed cross-river stations, the partial tracings along these lines are beams outlined and exported from cross-river images. The circles represent fish positions, and the solid and cross-hatched lines are the river bottom.

Figure 21.–Yentna River range and depth of fish observed from a mobile, vertically positioned DIDSON, 2012.

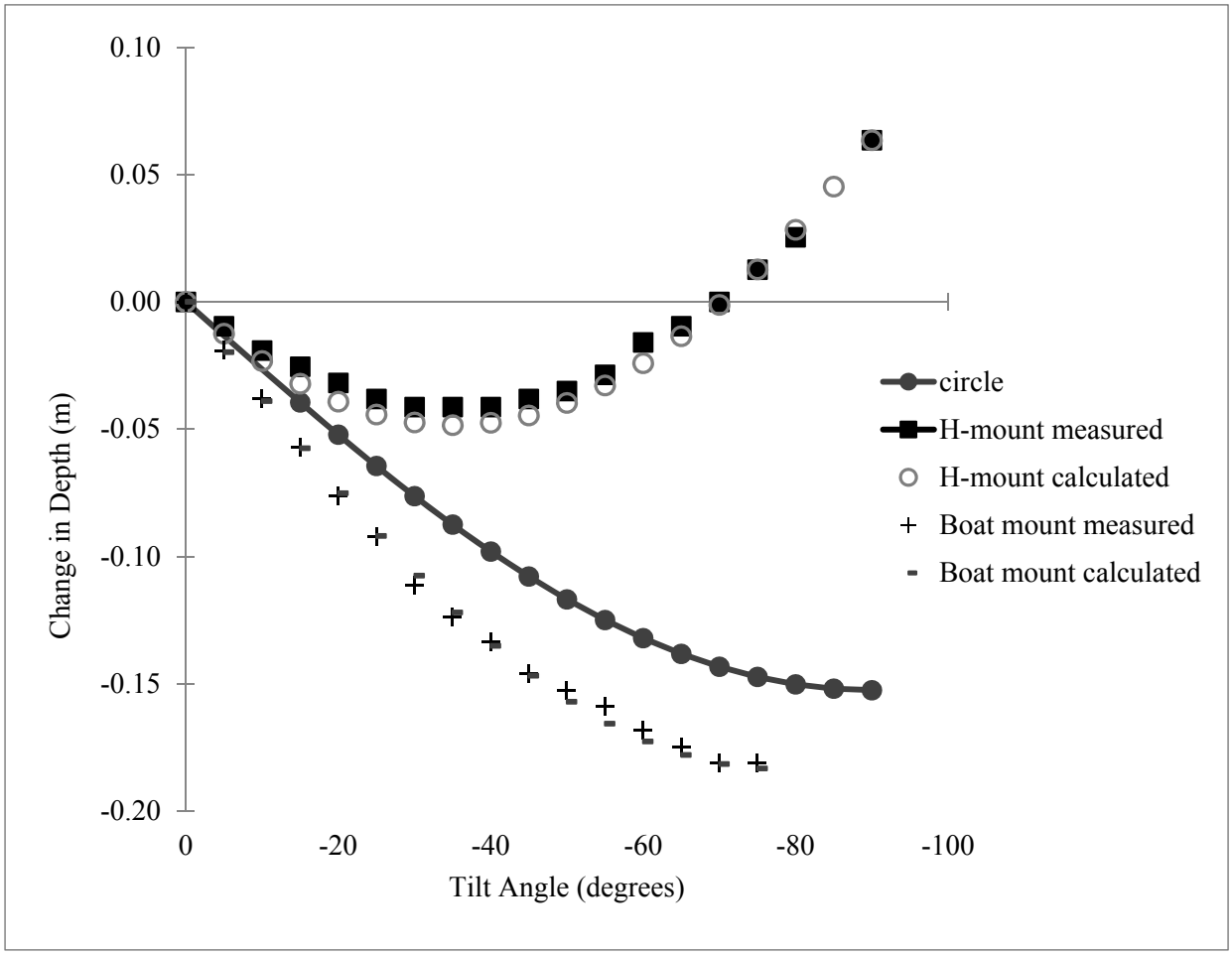

Note: The rotational arm of the boat mount arm (0.05 m) was shorter than the shore-based H-mount (0.216 m); and therefore, the arc traced by the end of the transducer was closer to that of a circle.

Figure 22.–A comparison of measured and calculated values for the changes in depth of the DIDSON transducer due to tilt angle for the shore-based H-mount and mobile boat mount.

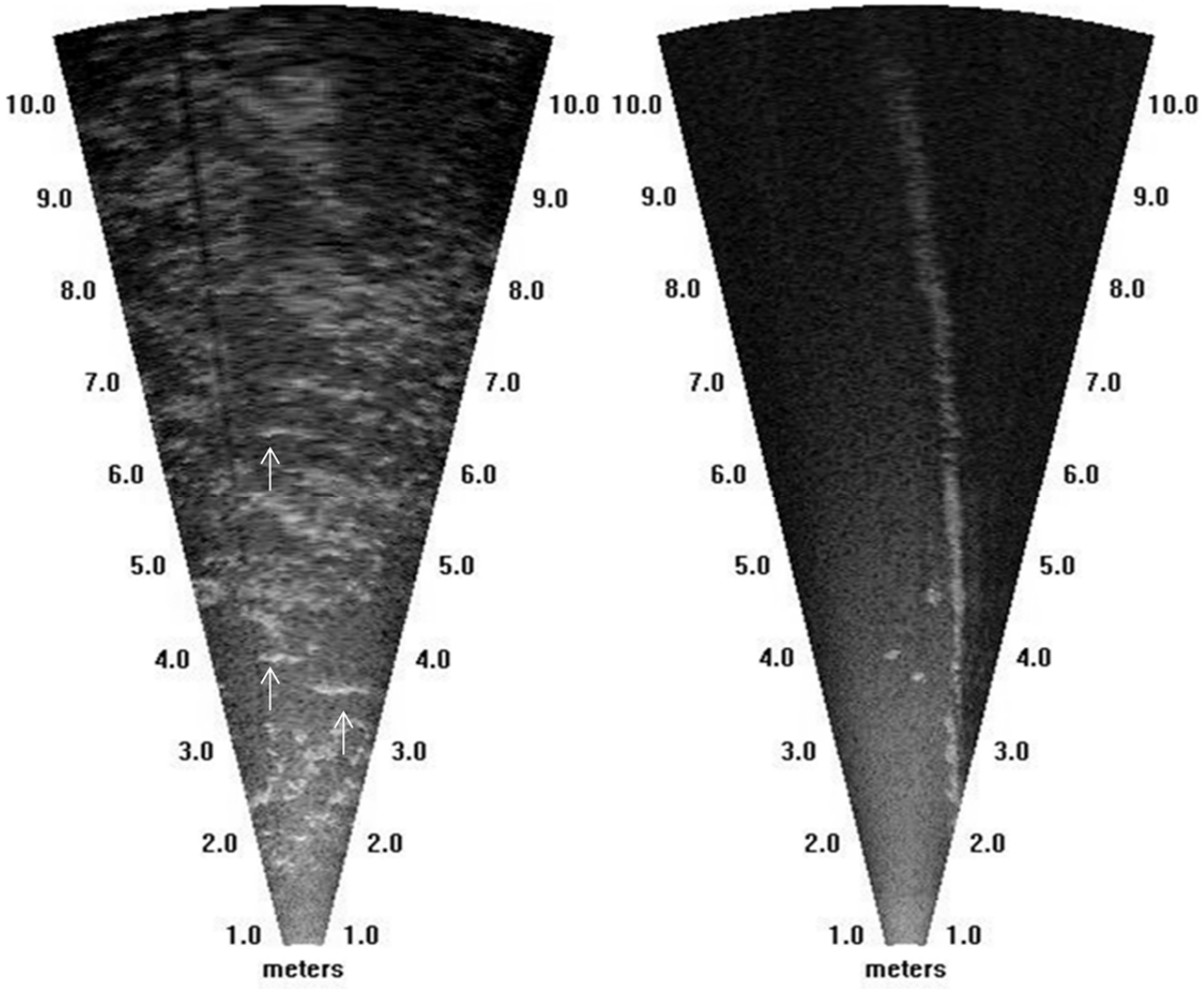

Note: The fish in the left bank image are more difficult to discern from the river bottom.

Figure 23.–Images from the horizontal (left) and vertical (right) DIDSONs showing 3 fish in each image, Yentna south bank, July 27, 2012.

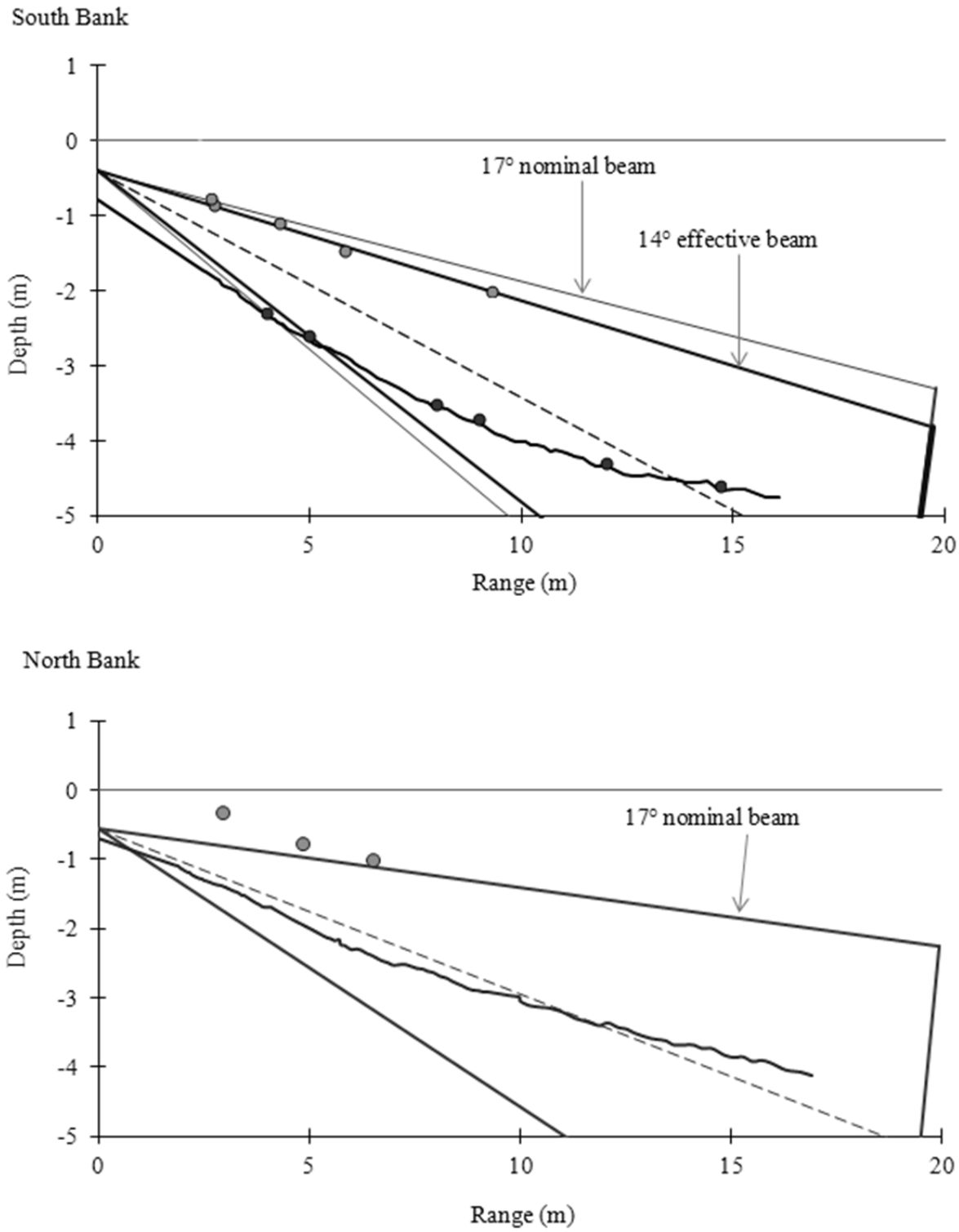

Note: The effective beams are based on the visual detection limits of an artificial target (circles) a 10.16 cm stainless steel sphere, which is similar in size acoustically to a sockeye salmon.

Figure 24.–Modeled nominal and effective beams for the horizontally oriented Yentna River DIDSONs.

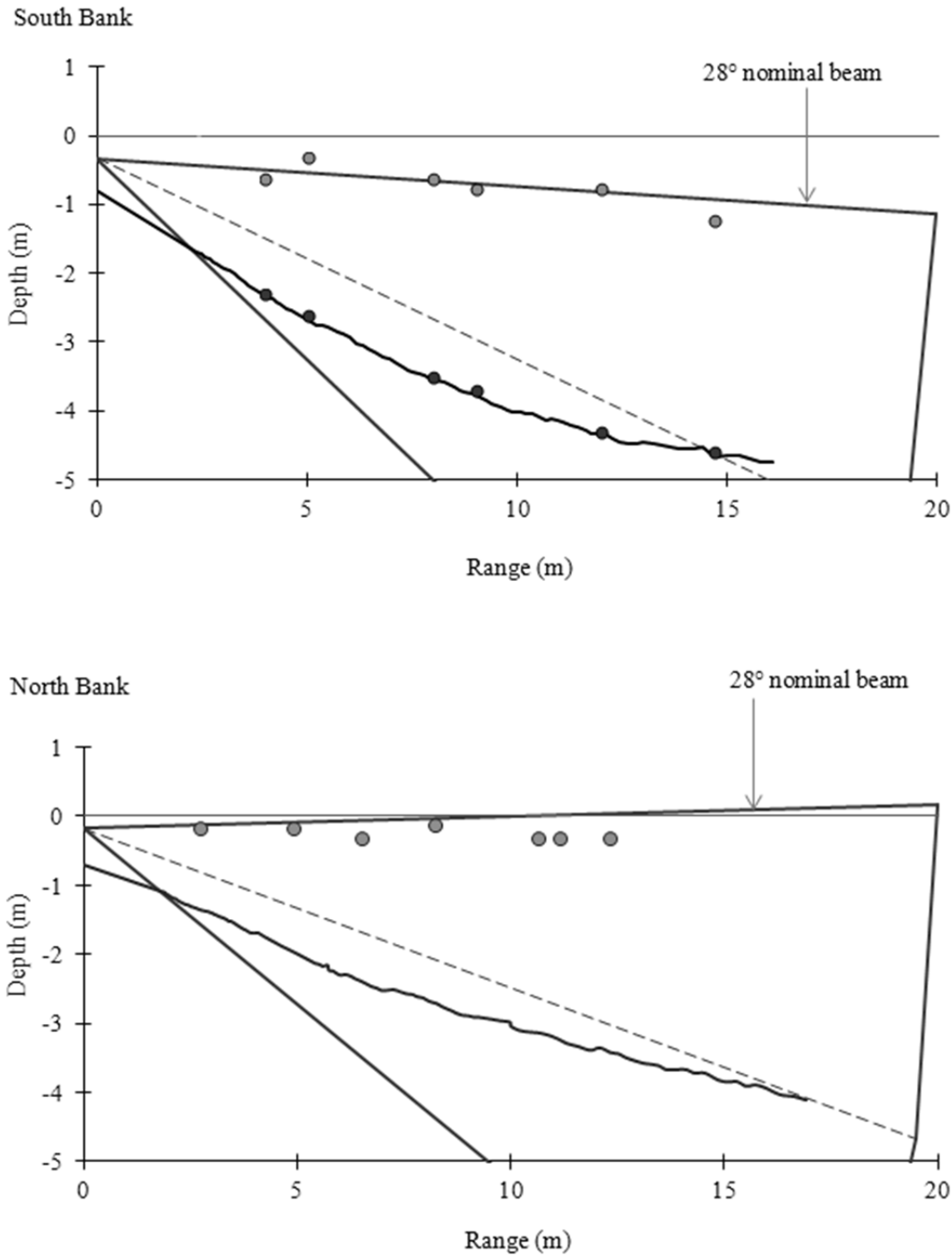

Note: The effective beams, the same size as the nominal beams, were based on the visual detection limits of an artificial target (circles) a 10.16 cm stainless steel sphere, which is similar in size acoustically to a sockeye salmon.

Figure 25.–Modeled nominal beams for the vertically oriented Yentna River DIDSONs.

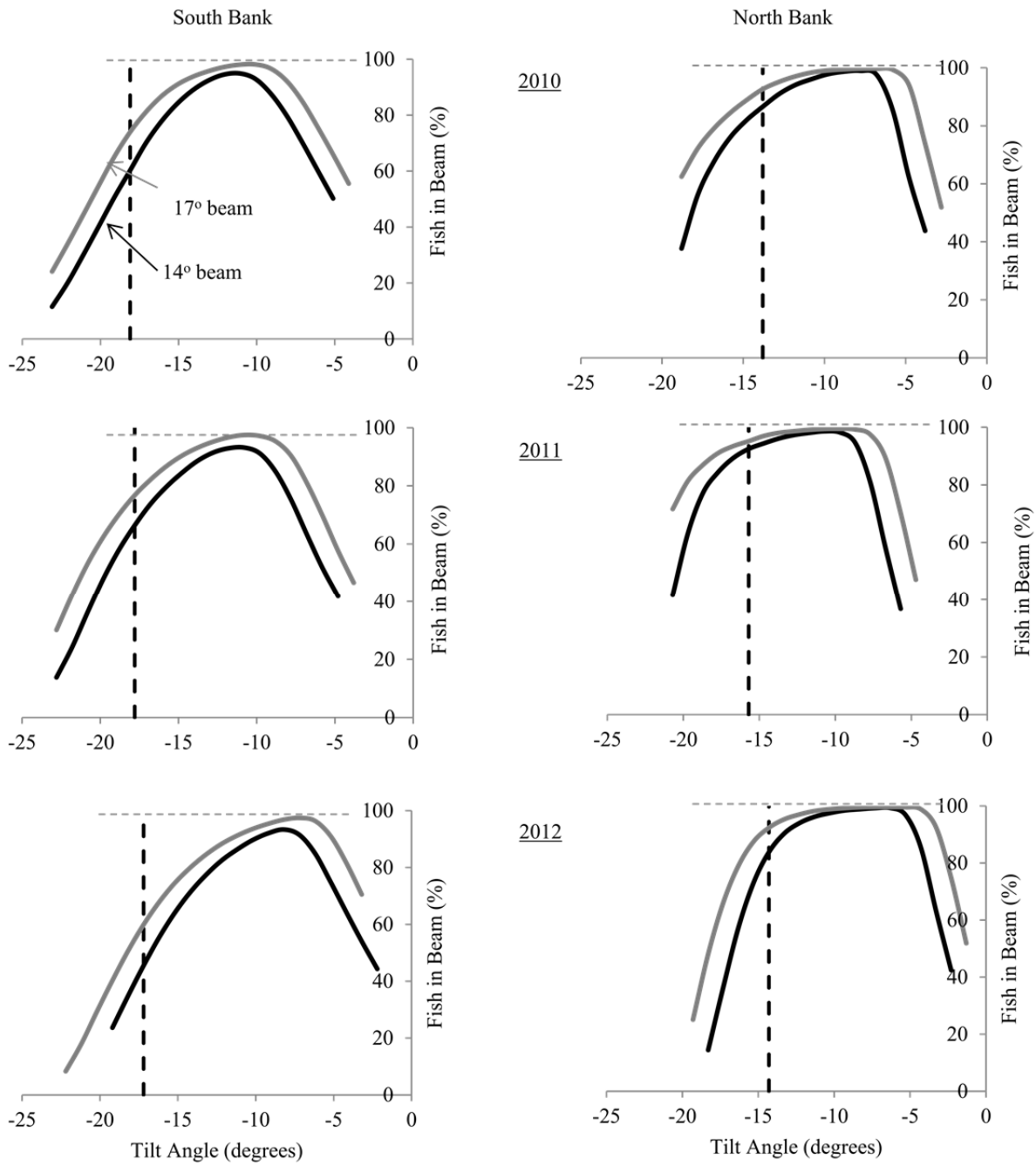

Note: The vertical dotted line marks the average tilt angle used to sample fish. The percentage of fish within the horizontal beam is increased by raising the transducer, particularly on the south bank of the Yentna River.

Figure 26.–The effect of changing the tilt angle on the percentage of migrating fish detectable to a horizontally positioned DIDSON (shown for 14º and 17º beams).

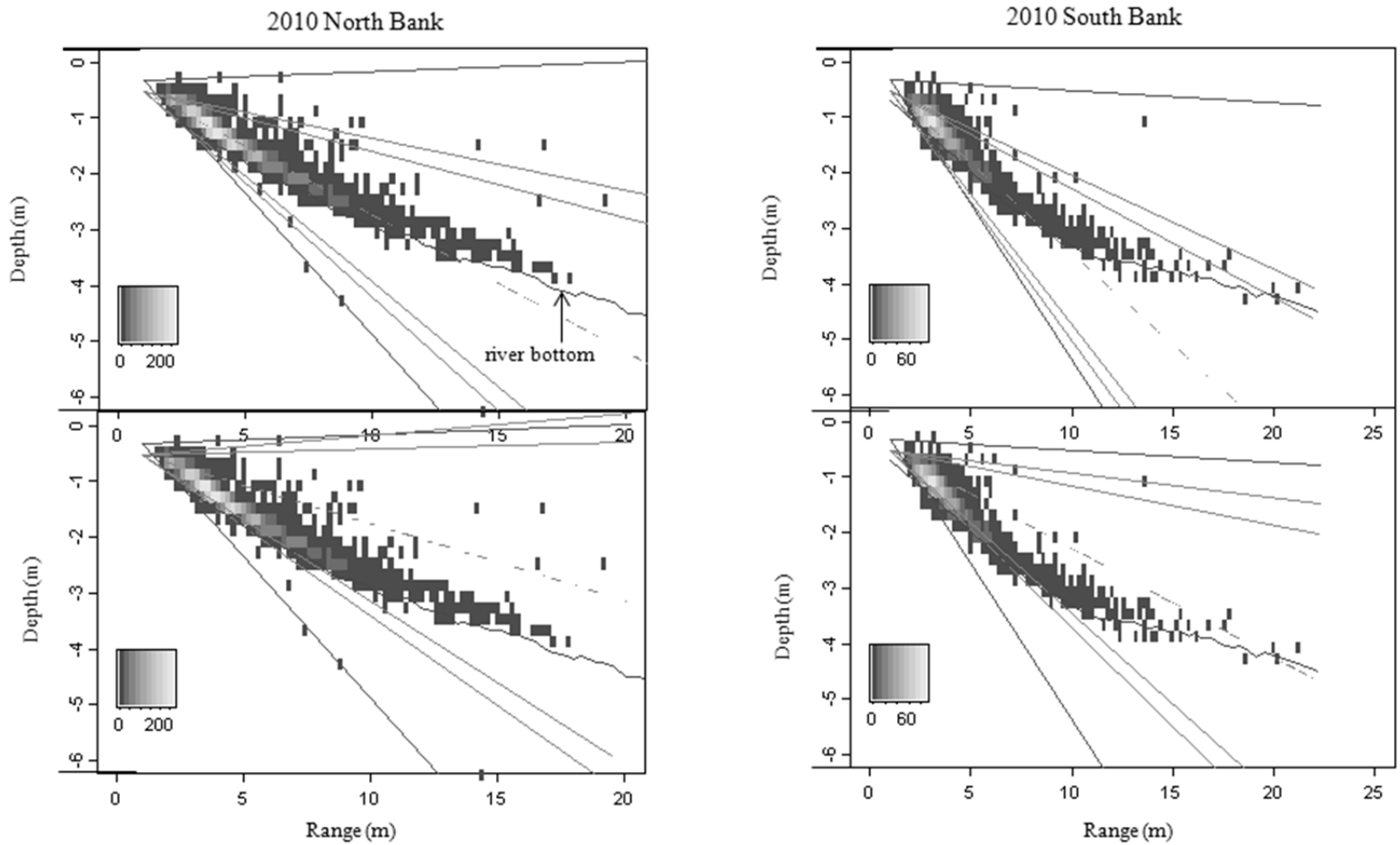

Note: Three modeled sonar beams are shown, the outermost beam triangle represents the composite beam oriented vertically, the innermost beams represent a horizontal orientation showing the nominal beam size (17°) and a more realistic beam size of 14° based on work using salmon-size targets.

Figure 27.–Yentna River, 2010, density plots of randomly selected fish coordinates with modeled sonar beams illustrating the traditional DIDSON tilt angle used at fish-counting sites (top) and the raised tilt angle that encompassed the largest number of fish (bottom).

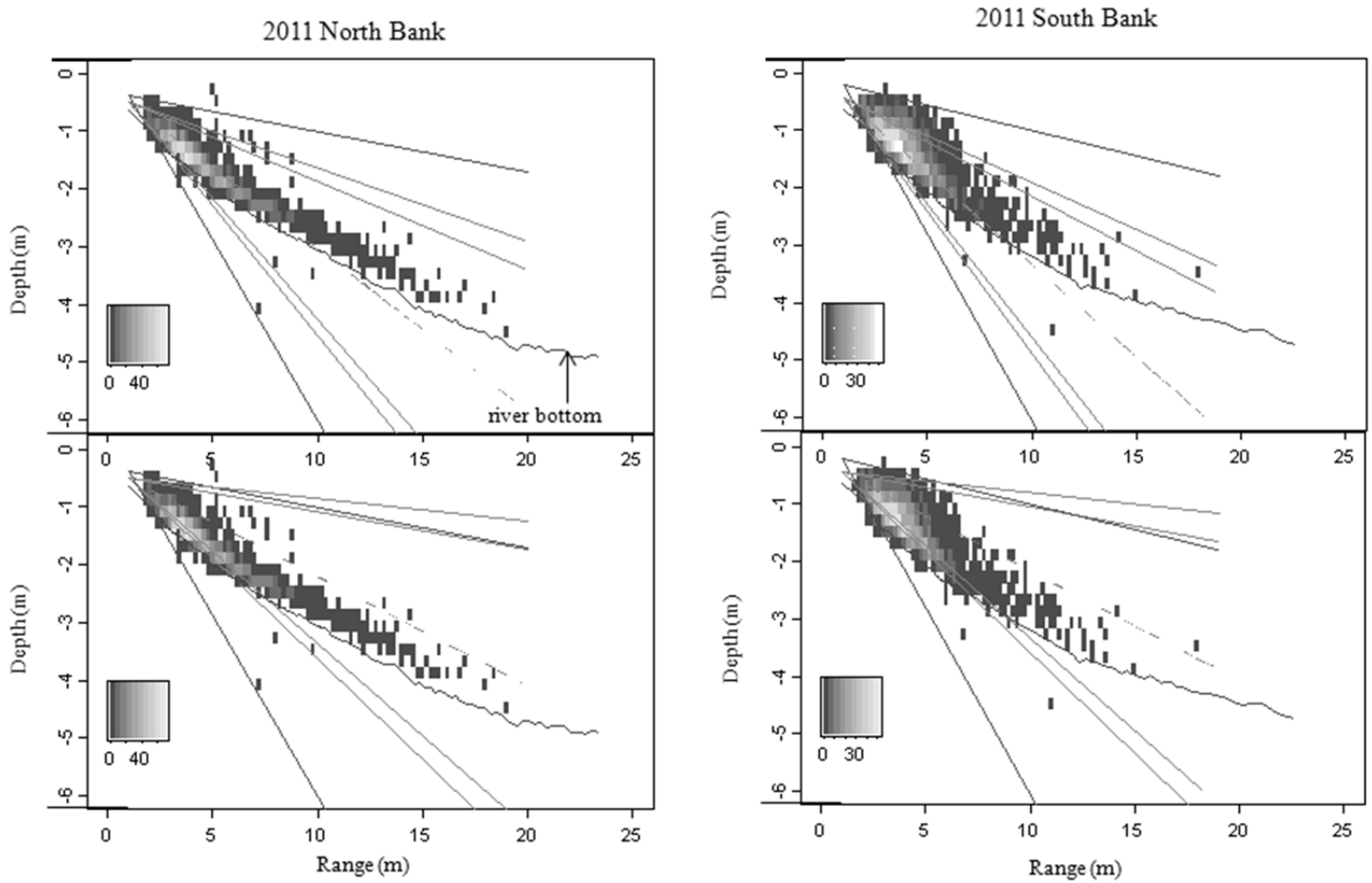

Note: Three modeled sonar beams are shown, the outermost beam triangle represents the composite beam oriented vertically, the innermost beams represent a horizontal orientation showing the nominal beam size (17°) and a more realistic beam size of 14° based on work using salmon-size targets.

Figure 28.–Yentna River, 2011, density plots of randomly selected fish coordinates with modeled sonar beams illustrating the traditional DIDSON tilt angle used at fish-counting sites (top) and the raised tilt angle that encompassed the largest number of fish (bottom).

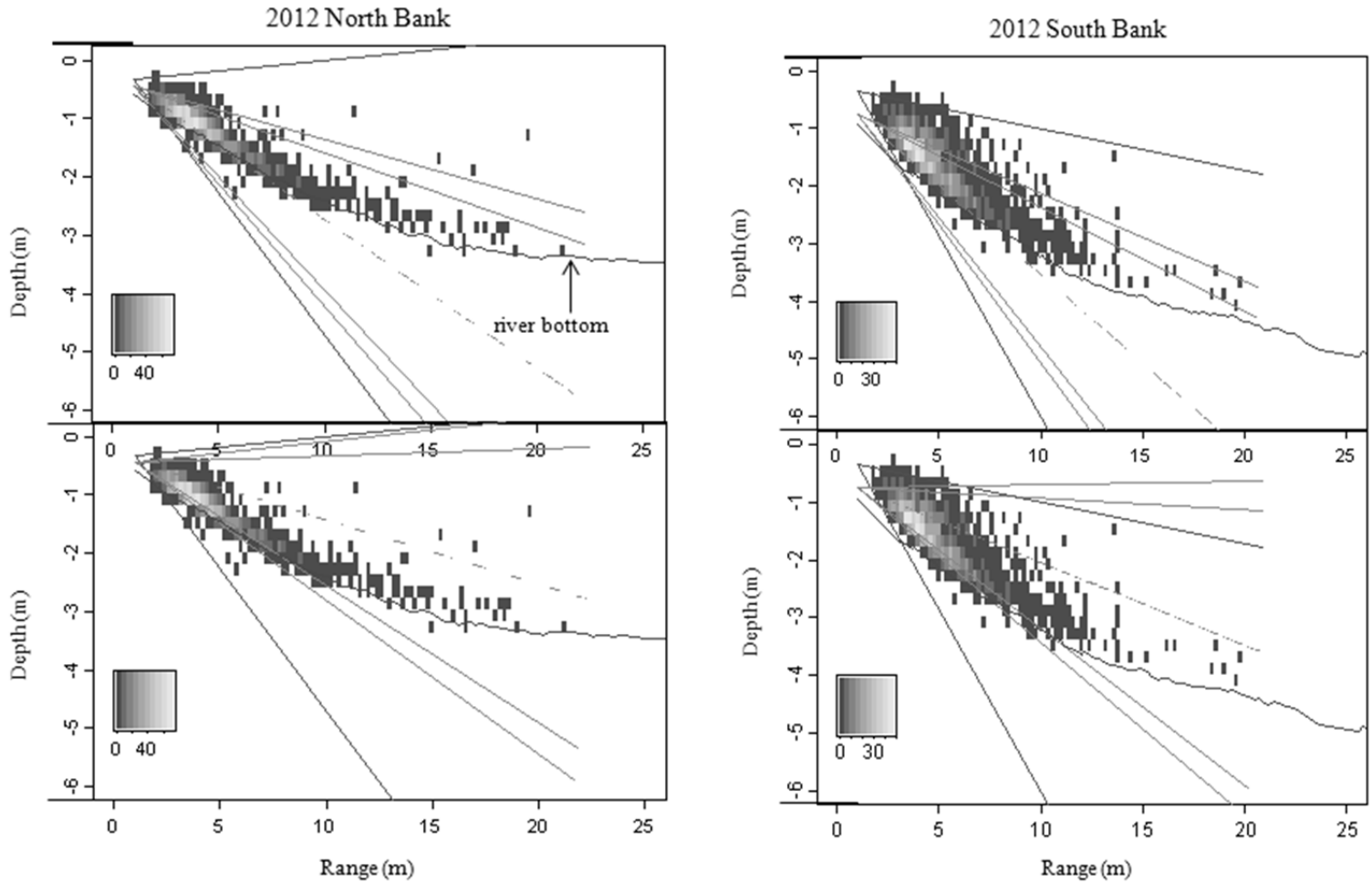

Note: Three modeled sonar beams are shown, the outermost beam triangle represents the composite beam oriented vertically, the innermost beams represent a horizontal orientation showing the nominal beam size (17°) and a more realistic beam size of 14° based on work using salmon-size target.

Figure 29.–Yentna River, 2012, density plots of randomly selected fish coordinates with modeled sonar beams illustrating the traditional DIDSON tilt angle used at fish-counting sites (top) and the raised tilt angle that encompassed the largest number of fish (bottom).

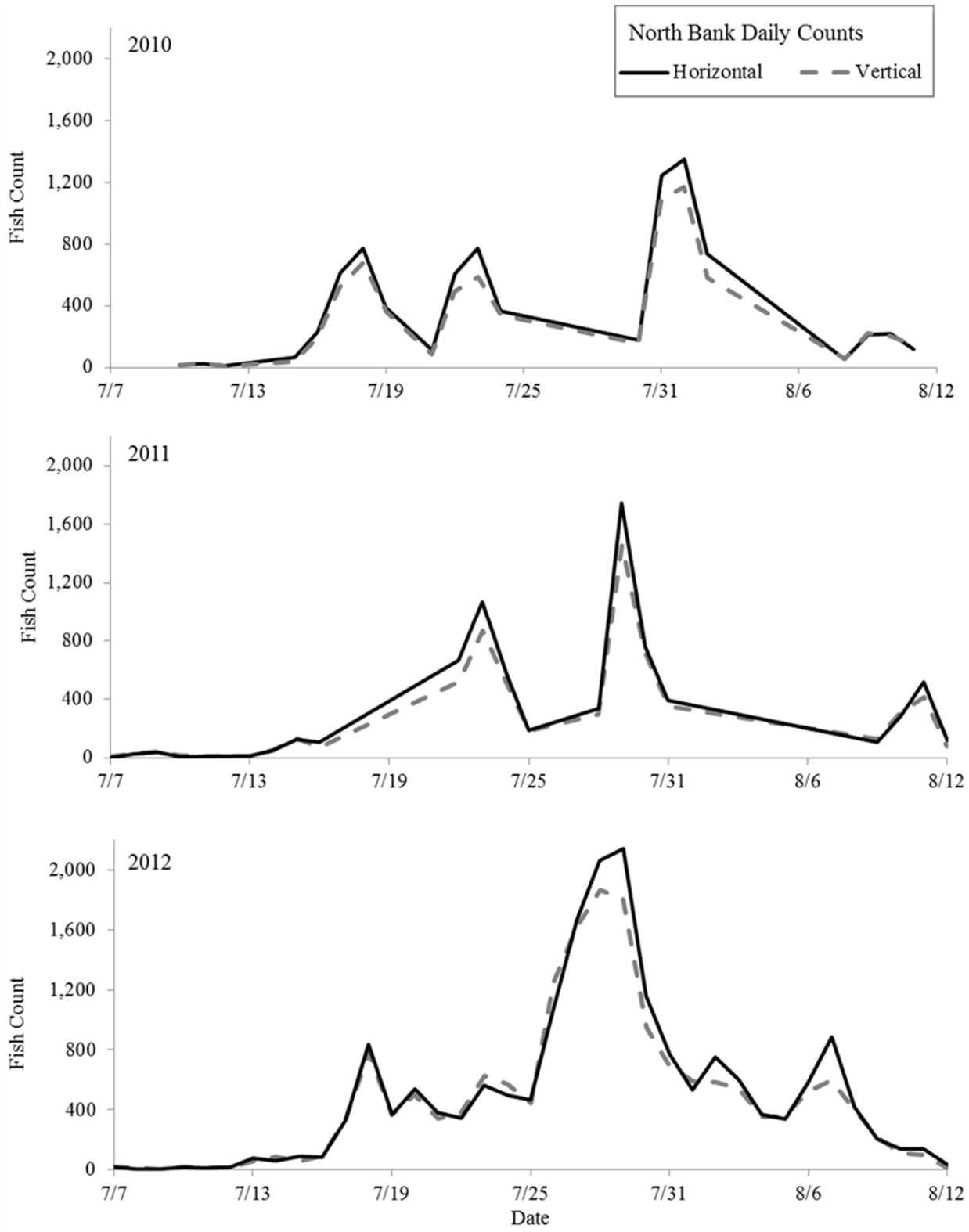

Figure 30.–Yentna River north bank paired daily fish counts from vertically and horizontally oriented DIDSONs.

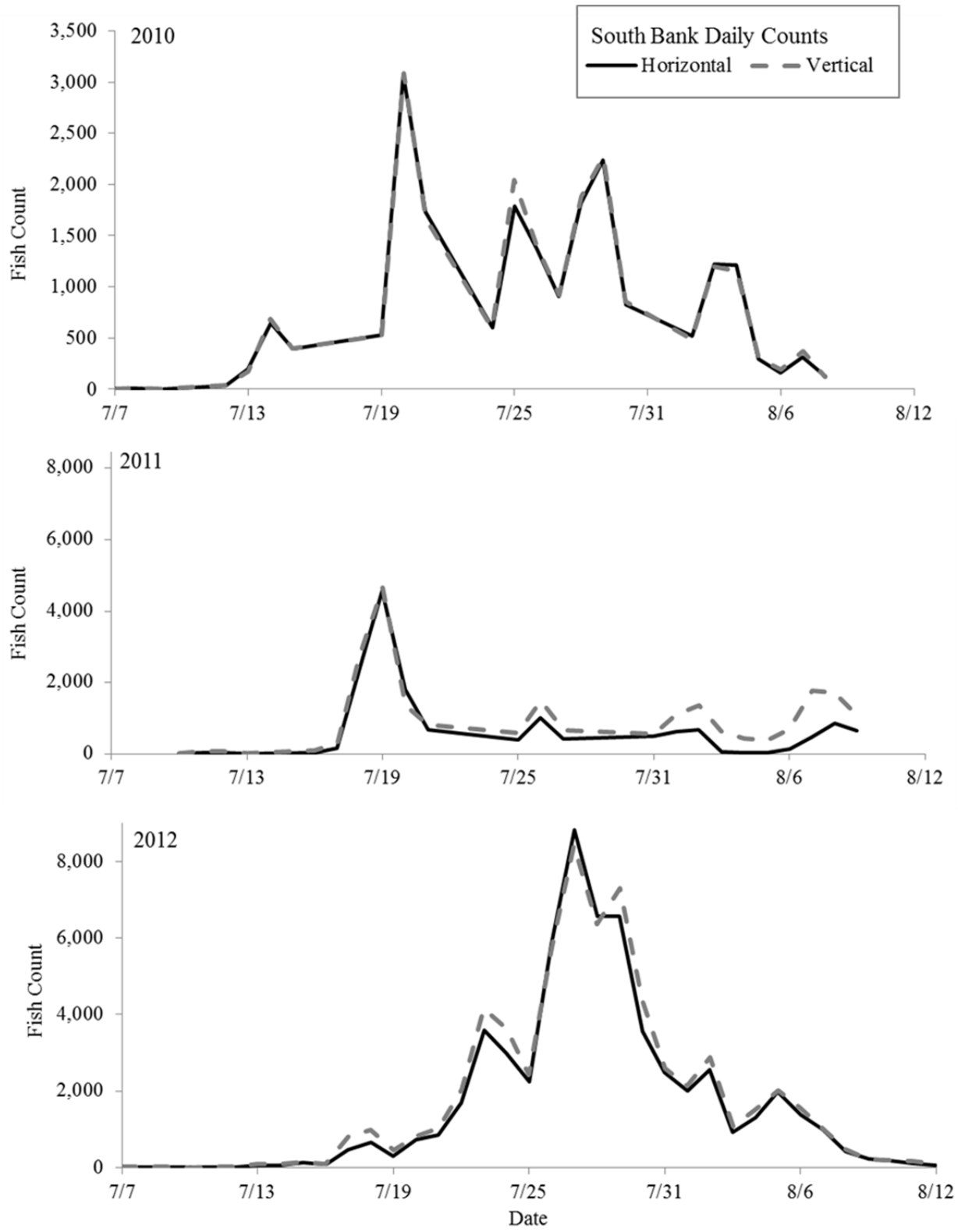

Figure 31.–Yentna River south bank paired daily fish counts from vertically and horizontally oriented DIDSONs.

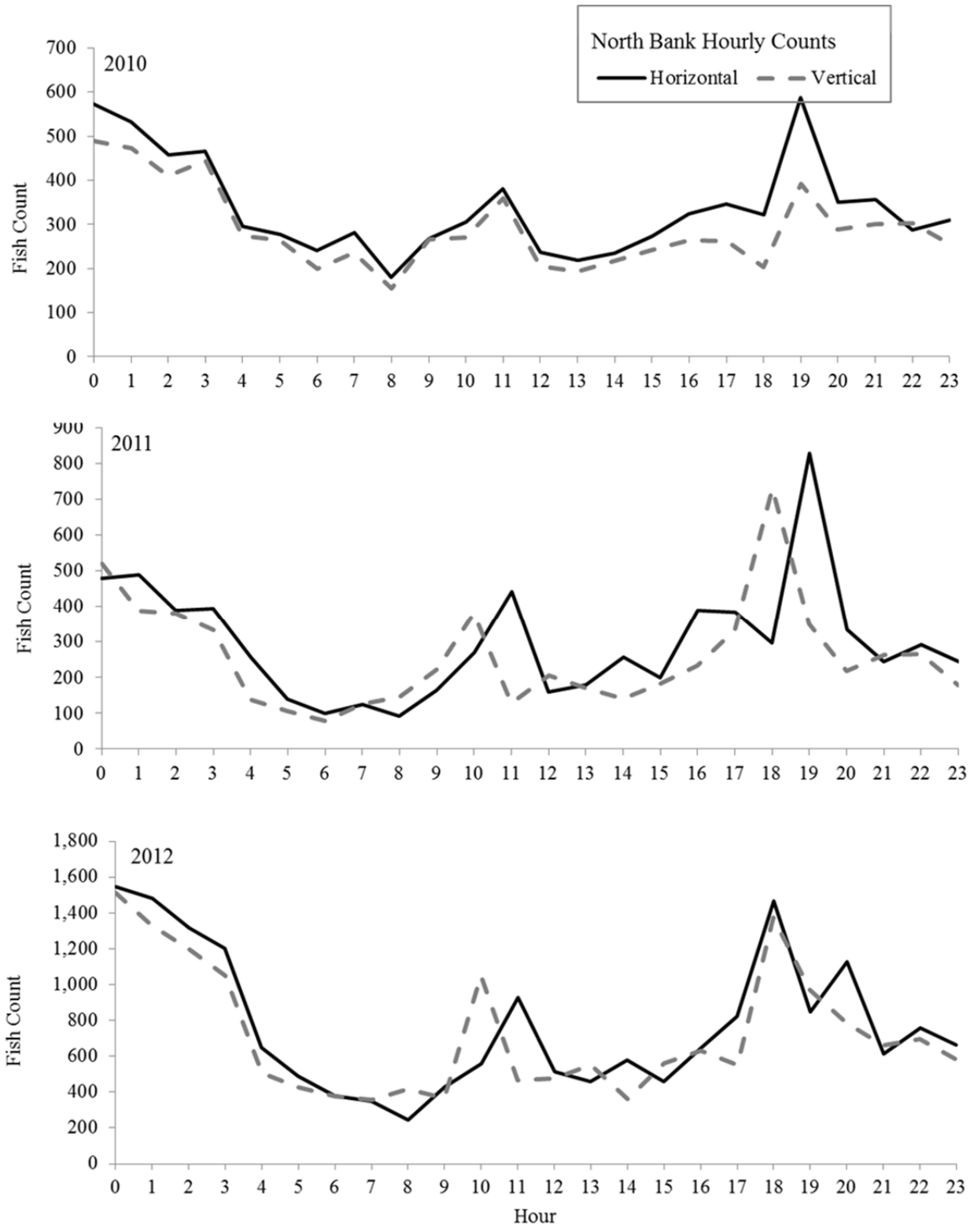

Figure 32.–Yentna River north bank paired hourly counts from vertically and horizontally oriented DIDSONs.

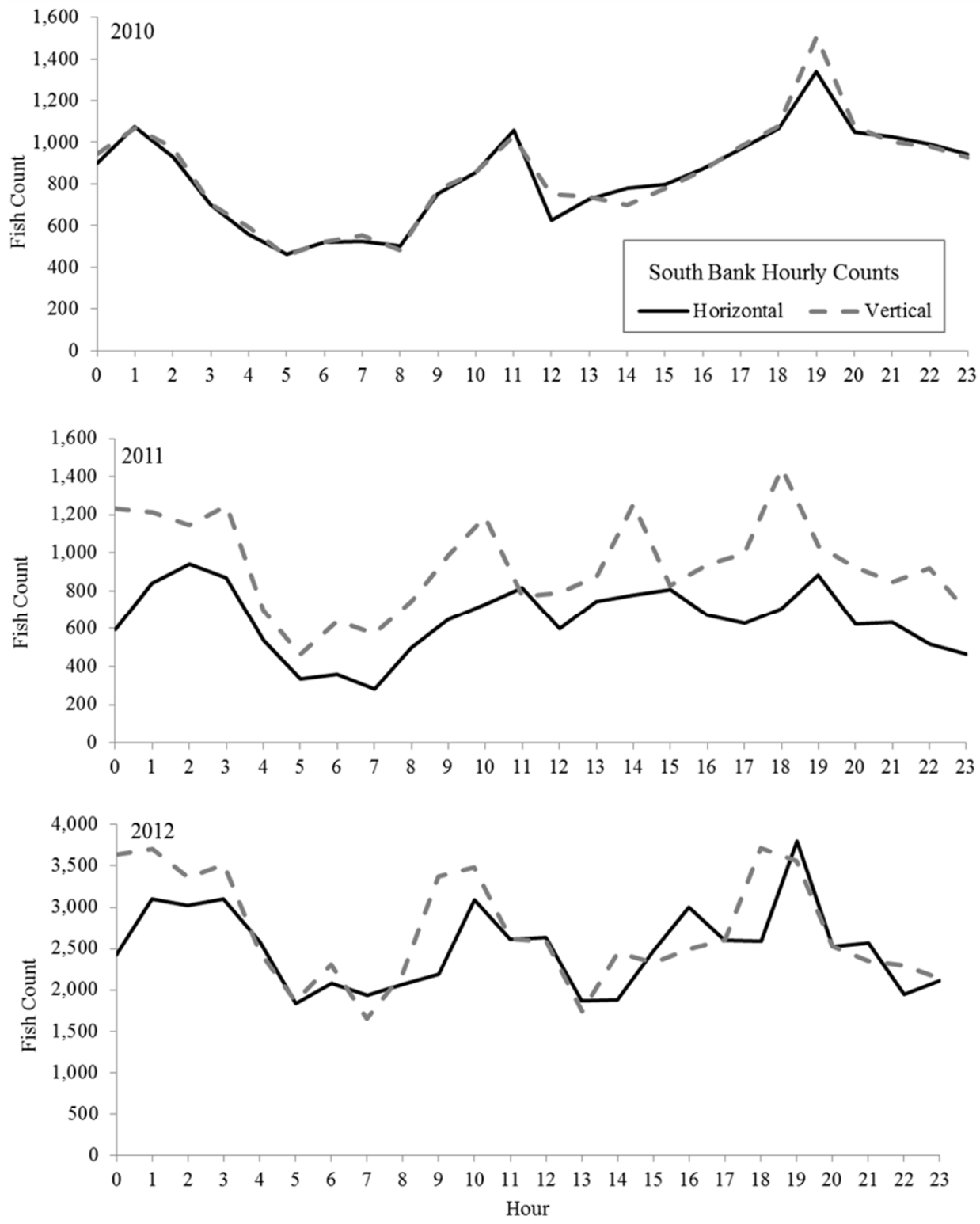

Figure 33.–Yentna River south bank paired hourly counts from vertically and horizontally oriented DIDSONs.

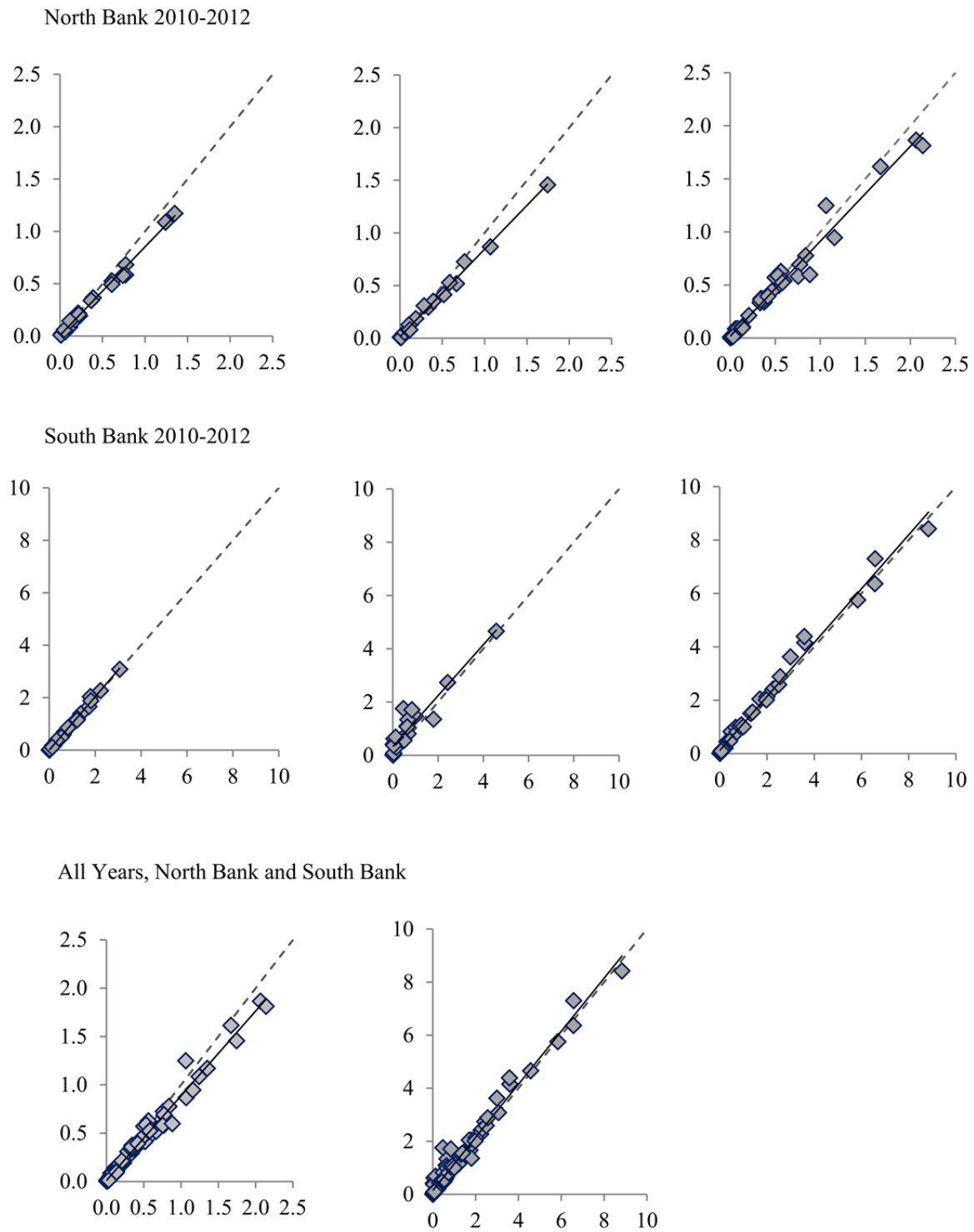

Note: The vertical position places the largest axis of the composite beam vertically in the water column leaving less room for fish to swim over the beam.

Figure 34.–A comparison of paired hourly fish counts from a DIDSON positioned horizontally (x-axis) and vertically (y-axis) by year and bank at the Yentna River.

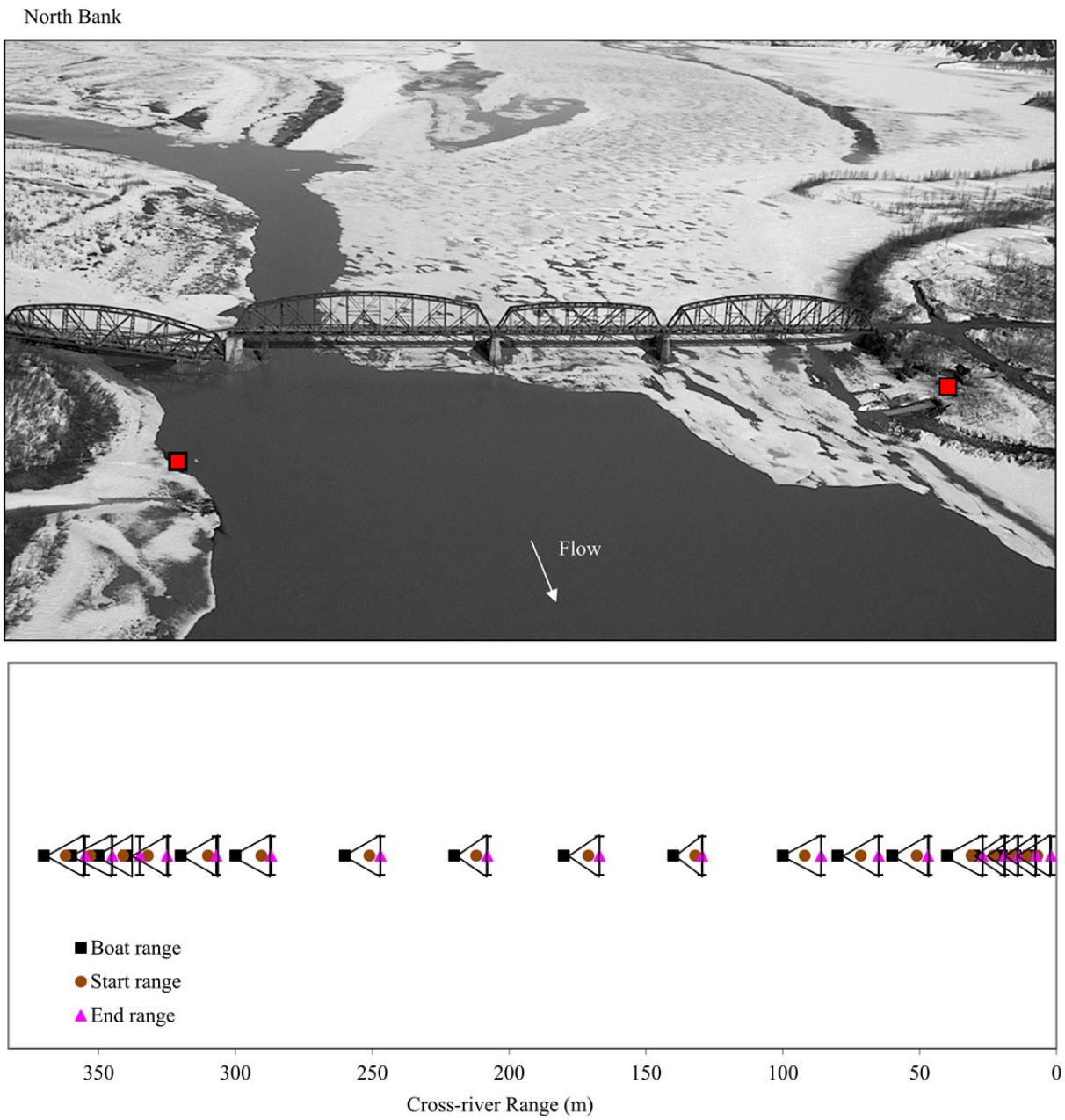

Note: Along the south bank, the sonar was placed on a concrete substrate that appears as a thin, gray rectangle. The spacing of the sampling stations used in 2006 (18 stations) for the cross-river transects are shown (bottom).

Figure 35.–The Copper River sonar sites, marked by square markers, below the Million Dollar Bridge at mile 48 of the Copper River Highway, May 15, 2002 (top).

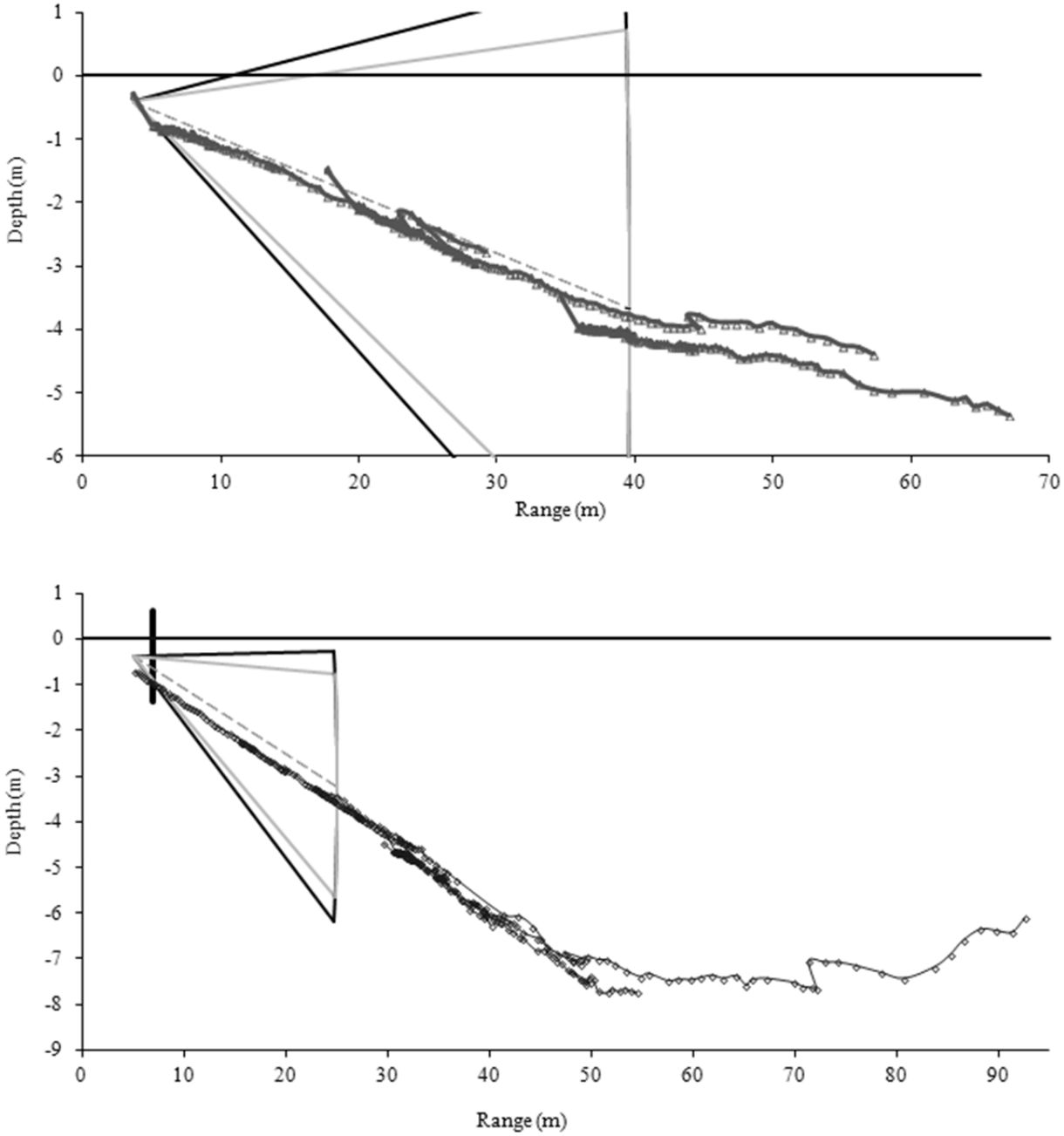

Figure 36.–River bottom profile of the 5° north bank slope (top) and 8.4° south bank slope (bottom) with a model of the sonar beam (shown with both 14° and 17° beams), Copper River.

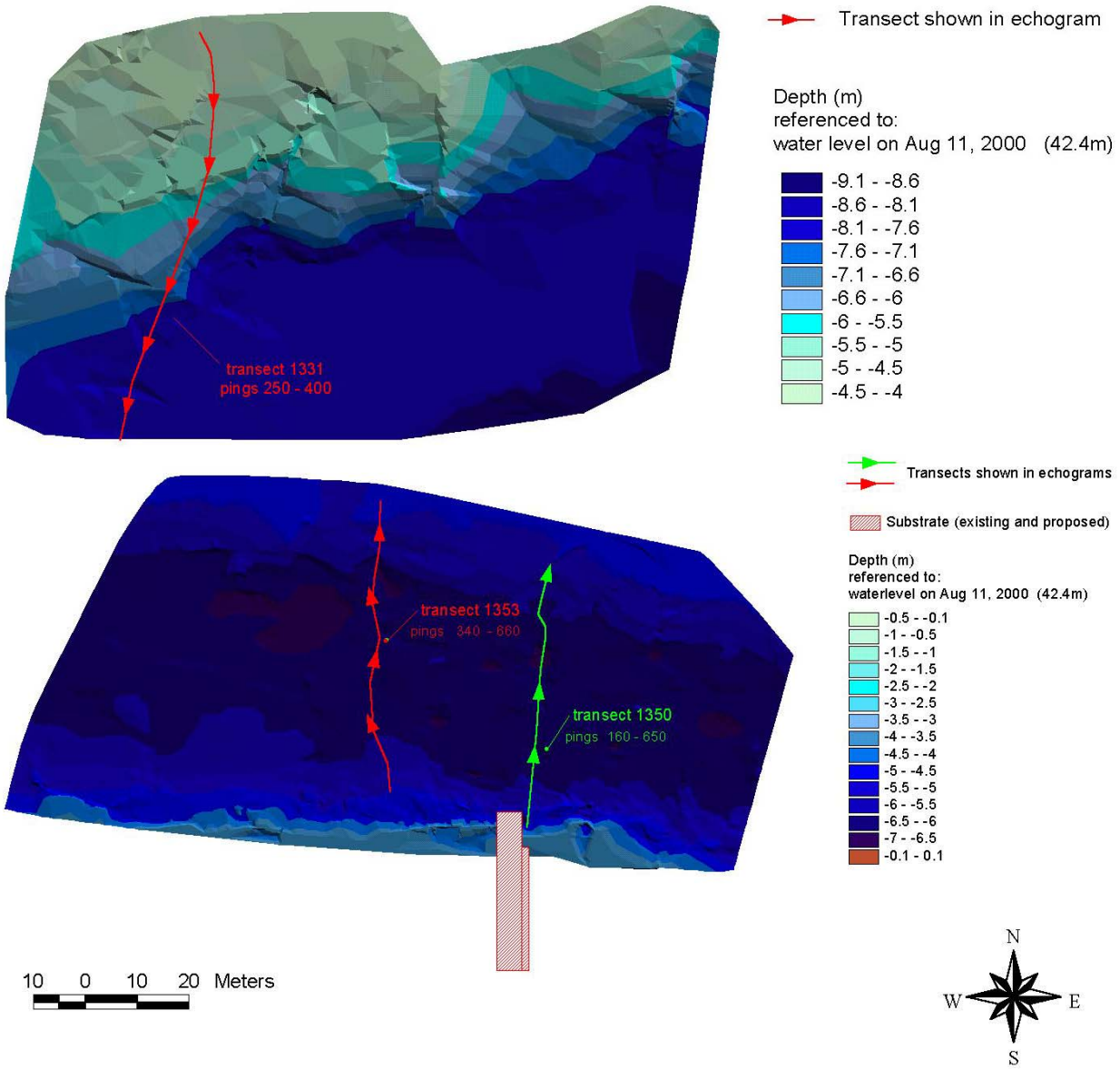

Figure 37.–Bathymetry map of the areas around the north (top) and south bank (bottom) sonar sites at the Copper River.

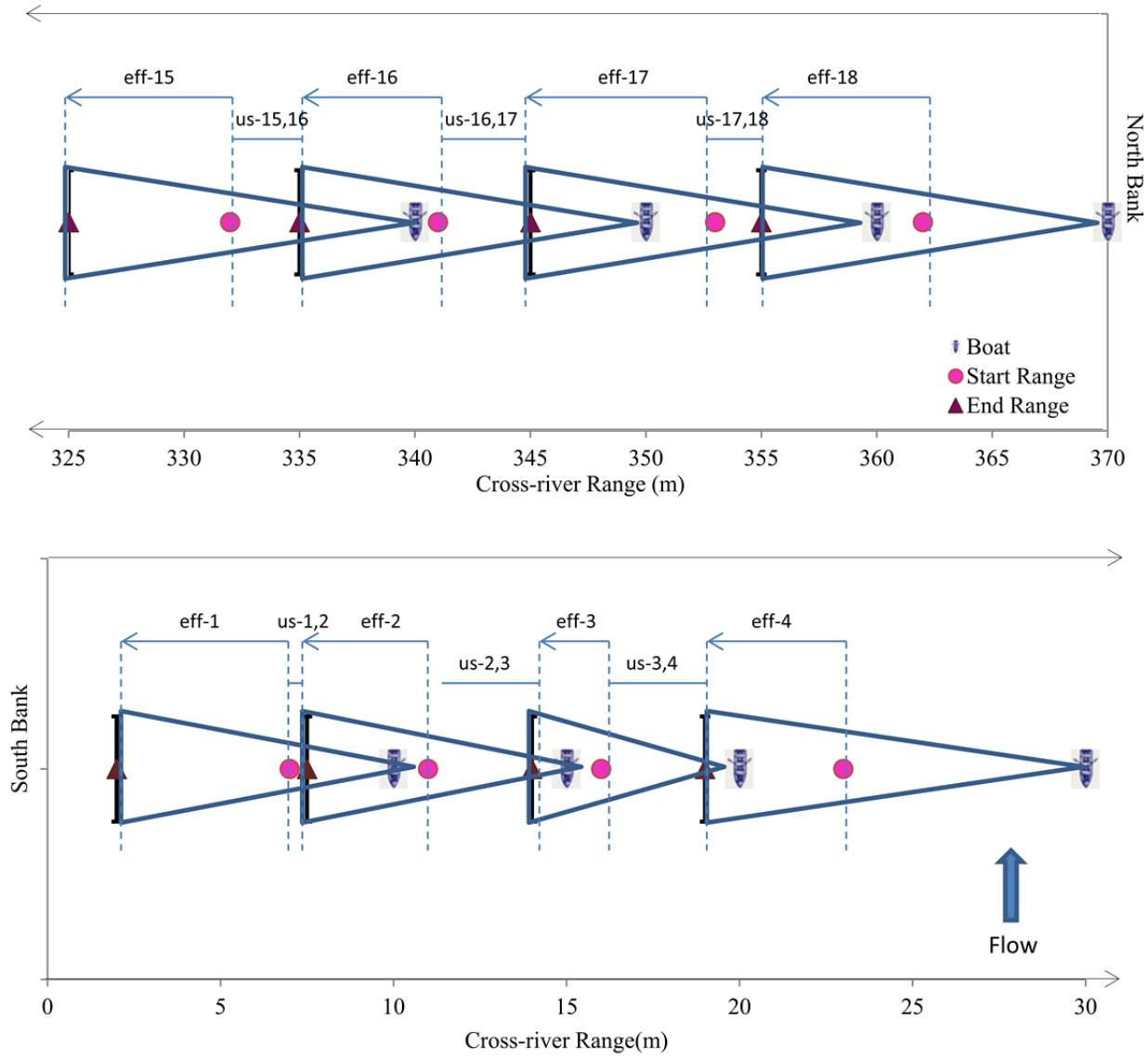

Note: Variables used for Interpolating:

1. End Range (*er*) is the effective end range of the sonar based on where the river bottom ends in the DIDSON image.
2. Start Range (*sr*) is the effective start range of the sonar based on where the river bottom starts in the DIDSON image.
3. Effective sampling region (eff_1) of station 1; i.e., er_1-sr_1.
4. Unsampled region ($us_{1,2}$) between station 1 and station 2.
5. Mid-Range ($mr_{1,2}$) of the unsampled region between stations 1 and 2.

Figure 38.–Cross-river transects starting from the Copper River north and south banks illustrating the effective sampling regions, unsampled regions, and the variables used for interpolating the unsampled regions between stations.

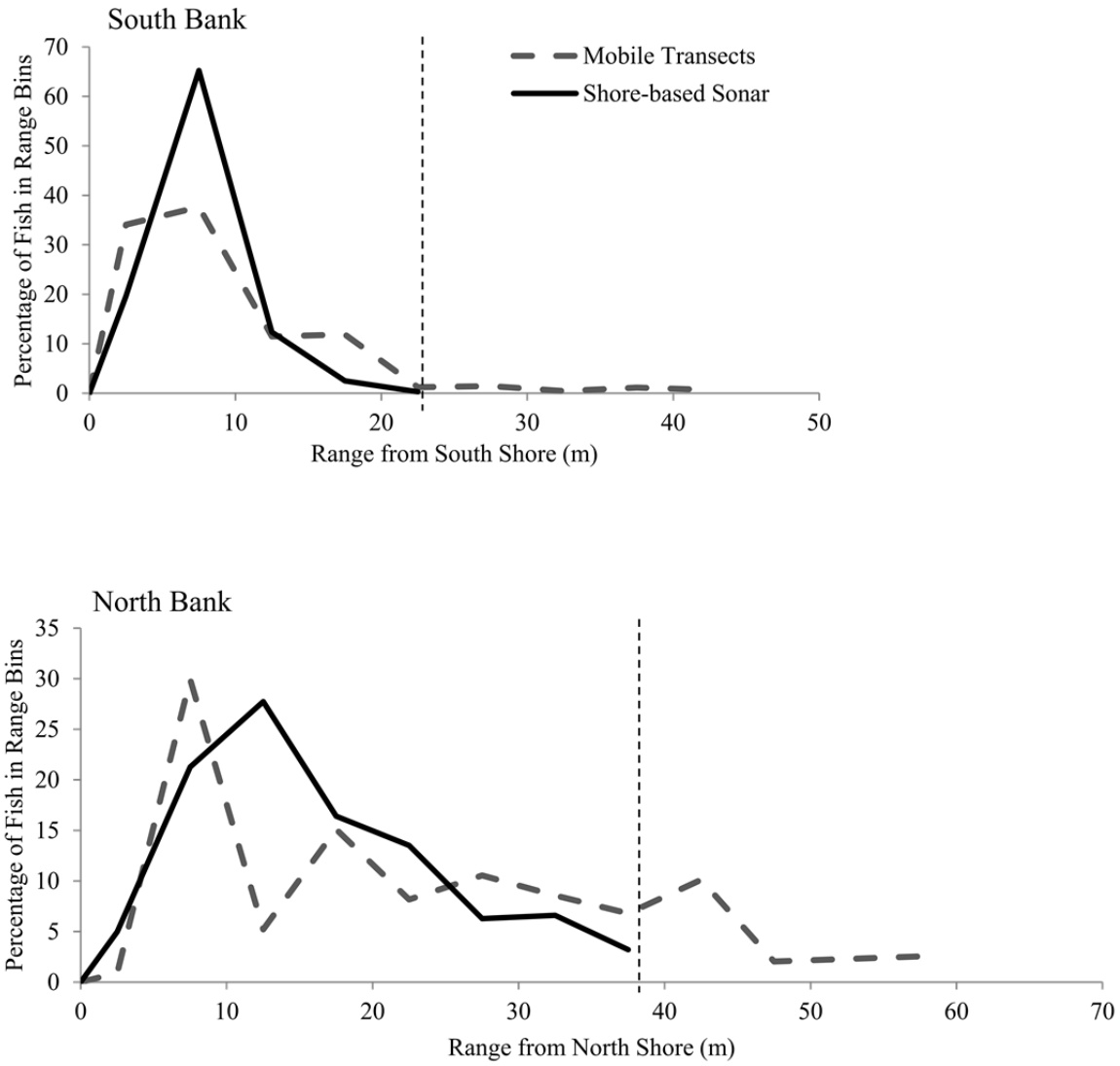

Figure 39.–A comparison of Copper River cross-river fish distributions from mobile and shore-based DIDSONs with vertical lines marking the approximate end ranges of the shore-based systems.

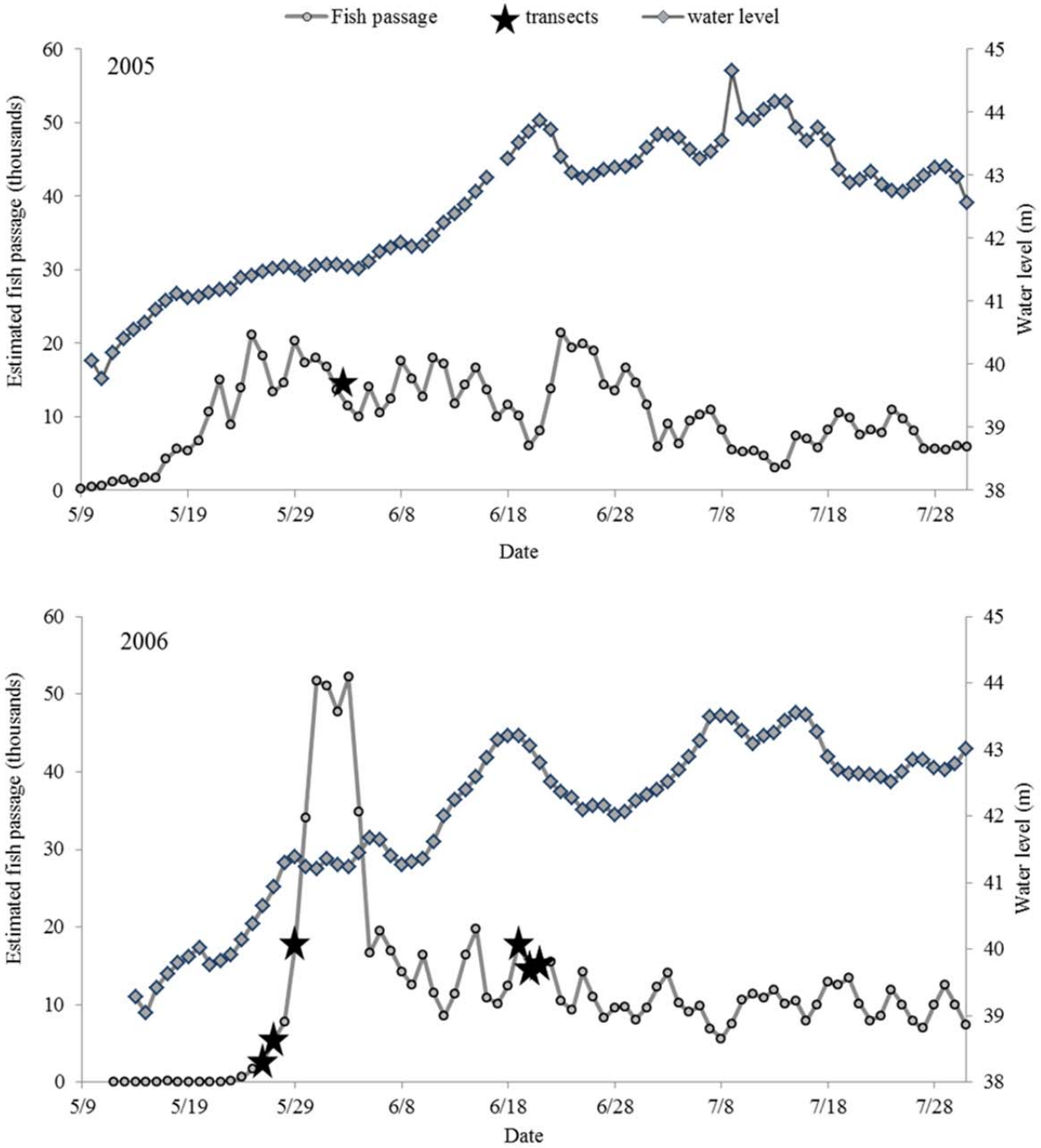

Note: The days transects were conducted are marked with a star. In 2006, 2 transects were completed on June 20 and 21.

Figure 40.–Copper River estimated salmon fish passage and water level for 2005 and 2006.

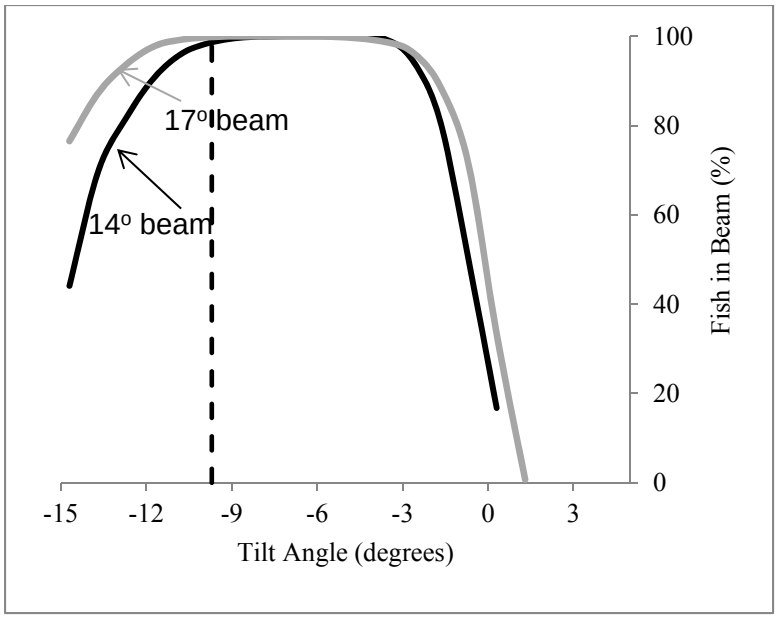

Note: The vertical dotted line marks the average tilt angle used to sample fish. The percentage of fish within the horizontal beam is increased slightly by raising the transducer, Copper River south bank, 2006.

Figure 41.–The effect of changing the tilt angle on the percentage of migrating fish detectable to a horizontally positioned DIDSON (shown for 14° and 17° beams).

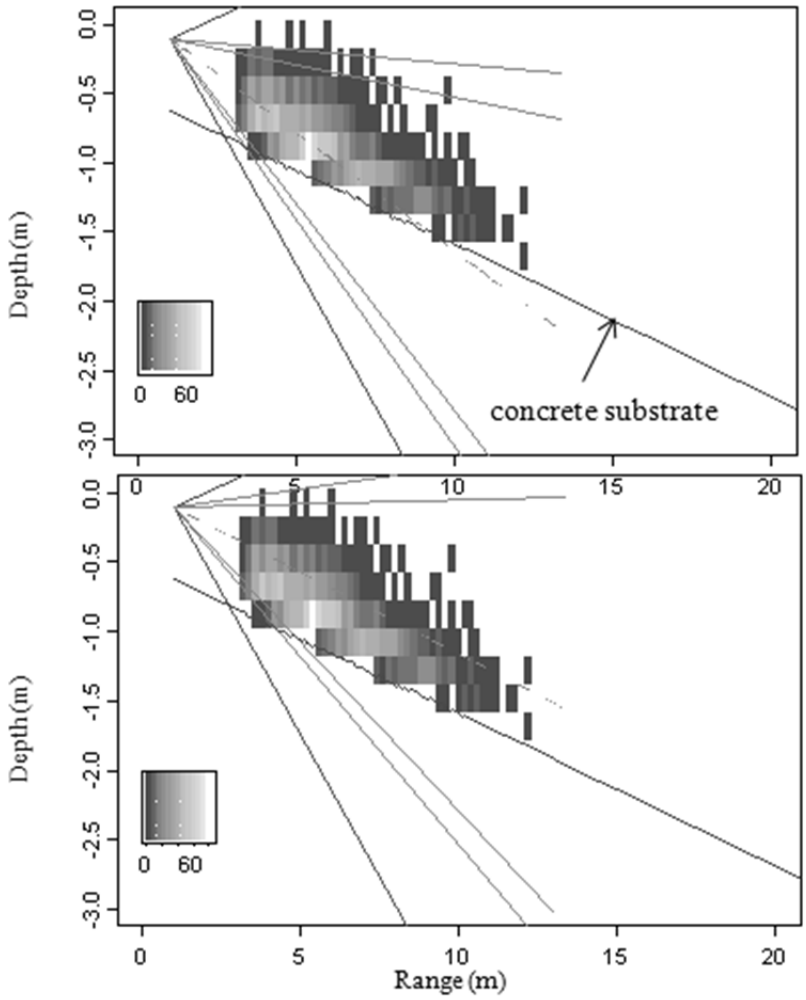

Note: Three modeled sonar beams are shown, the outermost beam triangle represents the composite beam oriented vertically, the innermost beams represent a horizontal orientation showing the nominal beam size (17°) and a more realistic beam size of 14° based on work using a salmon-size target.

Figure 42.–Copper River south bank, 2006, density plots of randomly selected fish coordinates with modeled sonar beams illustrating the traditional DIDSON tilt angle used at fish-counting sites (top) and the raised tilt angle that encompassed the largest number of fish (bottom).

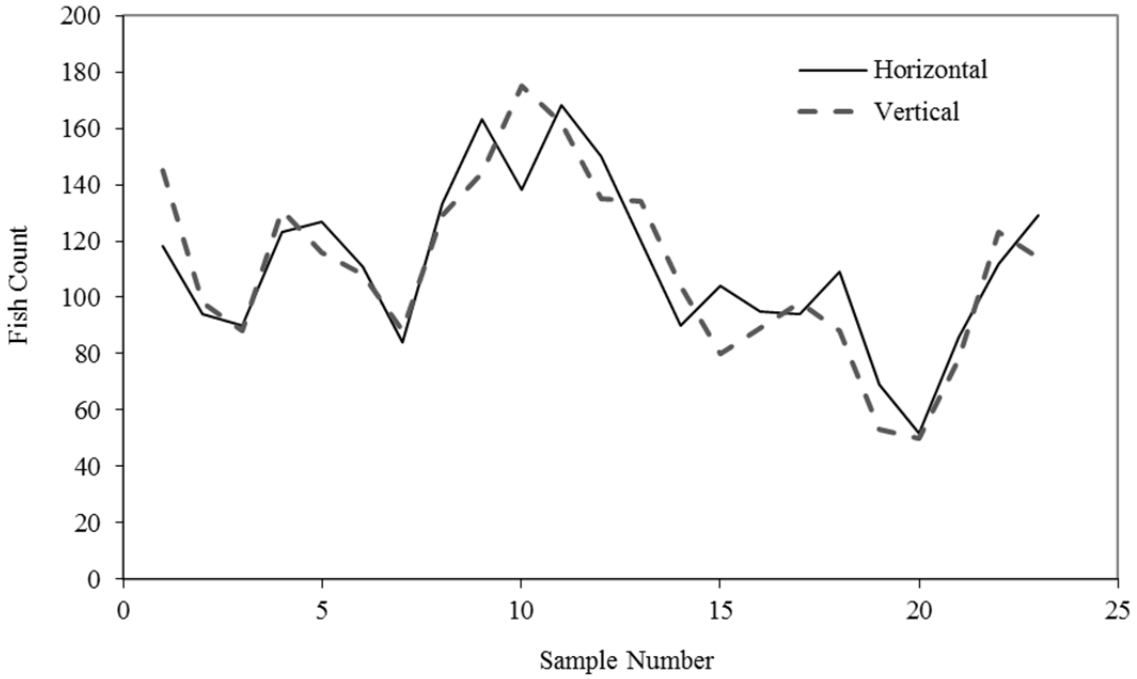

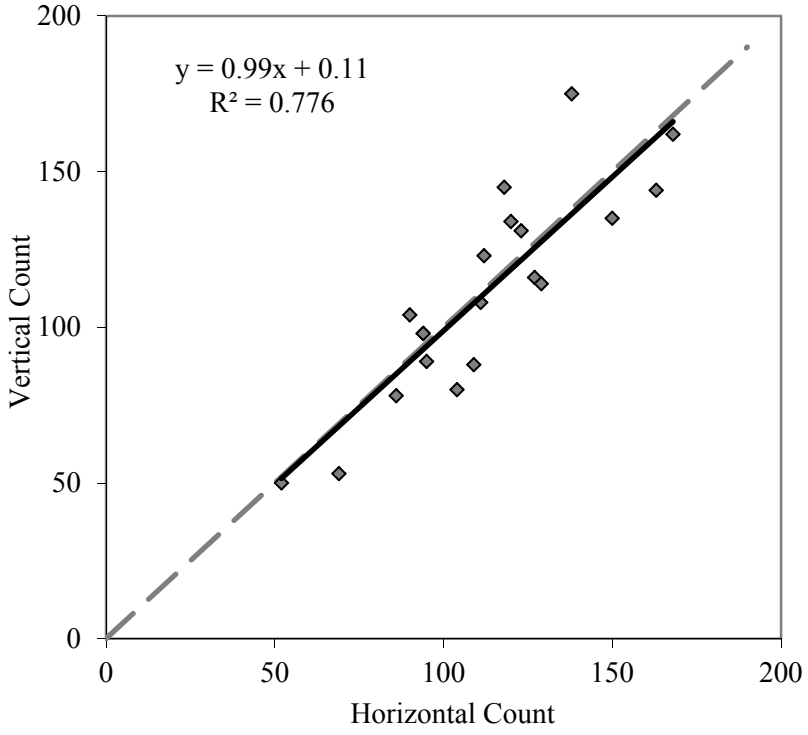

Note: Sampling alternated between them within an hour to avoid cross-talk, Copper River south bank, 2006.

Figure 43.–Paired 10 min fish counts by day (top) and linear regression comparison (bottom) obtained from DIDSONs, one with the composite beam positioned vertically and the other horizontally.

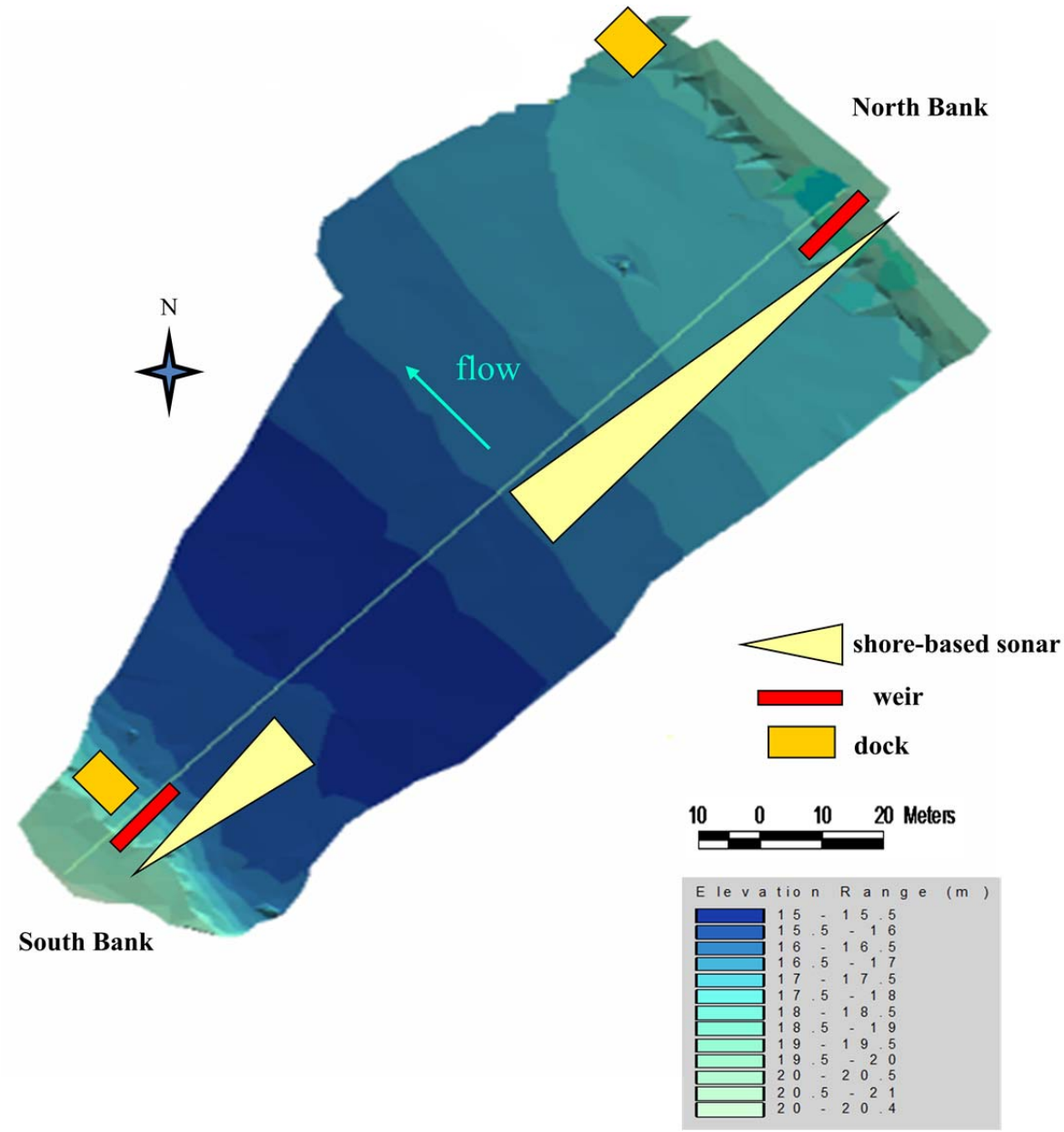

Figure 44.–Kenai River bathymetry of the sonar site showing locations of the shore-based DIDSONs, docks, and weirs.

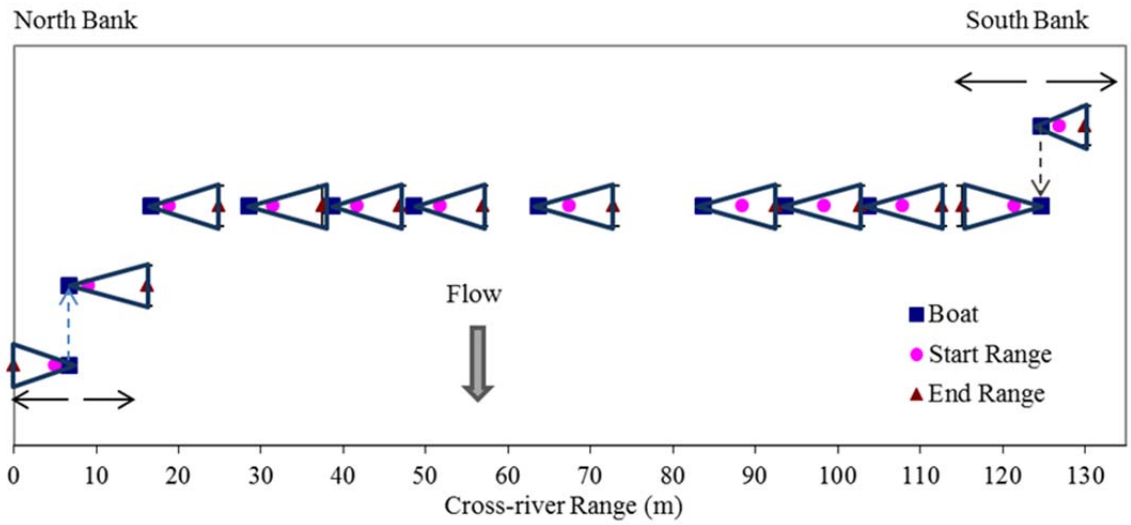

Note: The river width was divided into 12 stations. For the outer 2, the boat was tied at a dock and the DIDSON beam was directed first toward shore, and then away from shore, depicted with horizontal arrows.

Figure 45.–The spacing between stations for the 2007 July to August cross-river surveys at the Kenai River using a mobile DIDSON.

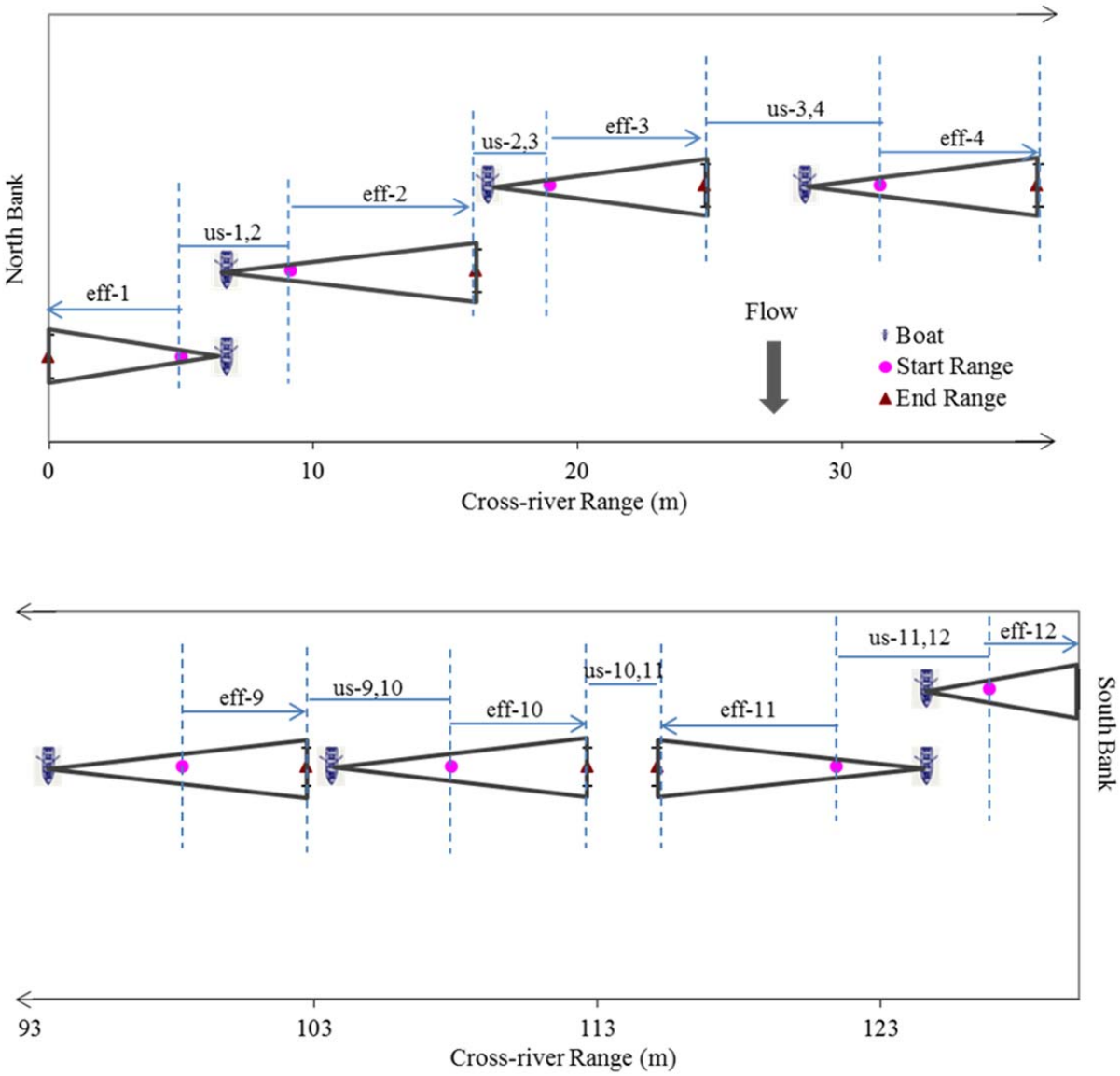

Note: Variables used for Interpolating:

1. End Range (*er*) is the effective end range of the sonar based on where the river bottom ends in the DIDSON image.
2. Start Range (*sr*) is the effective start range of the sonar based on where the river bottom starts in the DIDSON image.
3. Effective sampling region (eff_1) of station 1; i.e., er_1-sr_1.
4. Unsampled region ($us_{1,2}$) between station 1 and station 2.
5. Mid-Range ($mr_{1,2}$) of the unsampled region between stations 1 and 2.

Figure 46.–Diagram of the end stations of the 12 cross-river transects starting from the north and south banks illustrating the effective sampling regions, unsampled regions, and variables used for interpolating the unsampled regions, Kenai River, 2007.

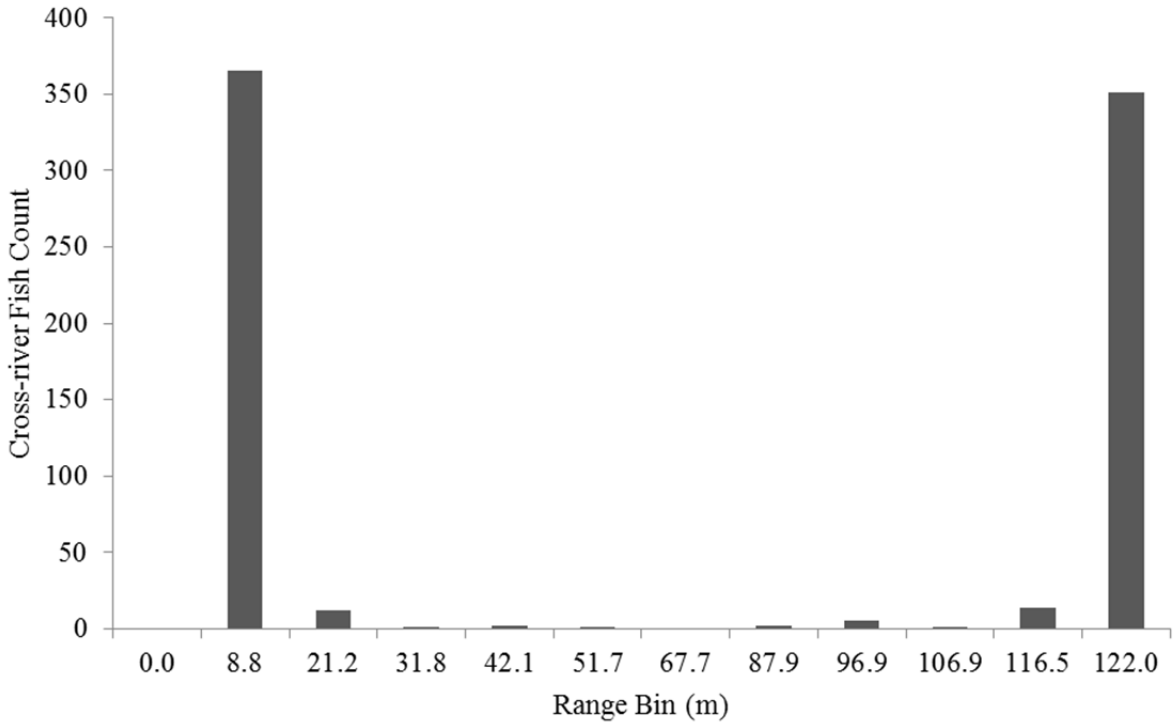

Note: Larger bins were used for the center of the river so the bin sizes are not equal across the transect.

Figure 47.–Fish counts summed by range bin from 2 cross-river surveys on July 26, 2006.

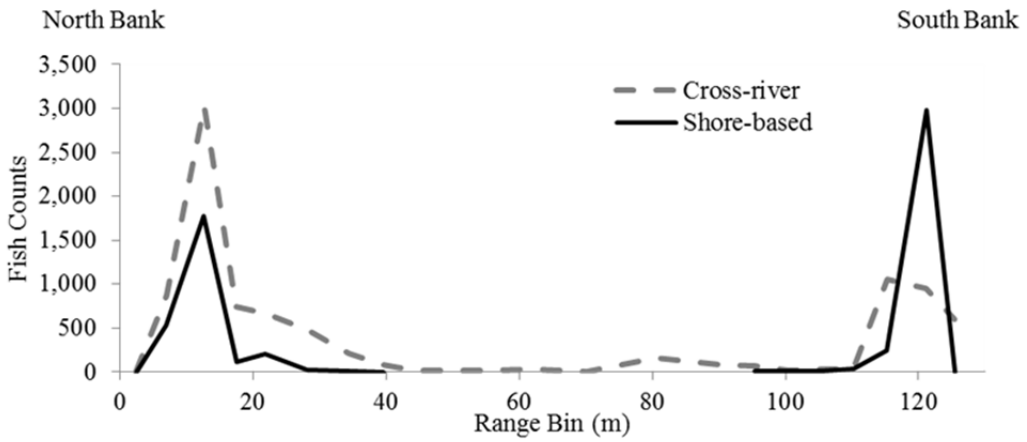

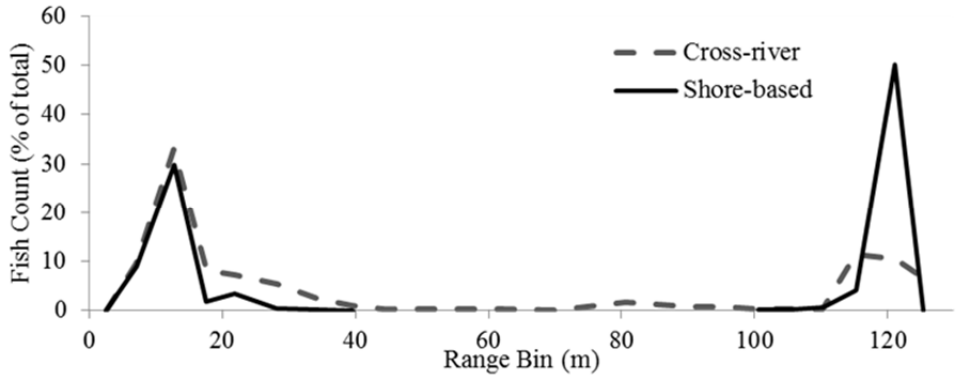

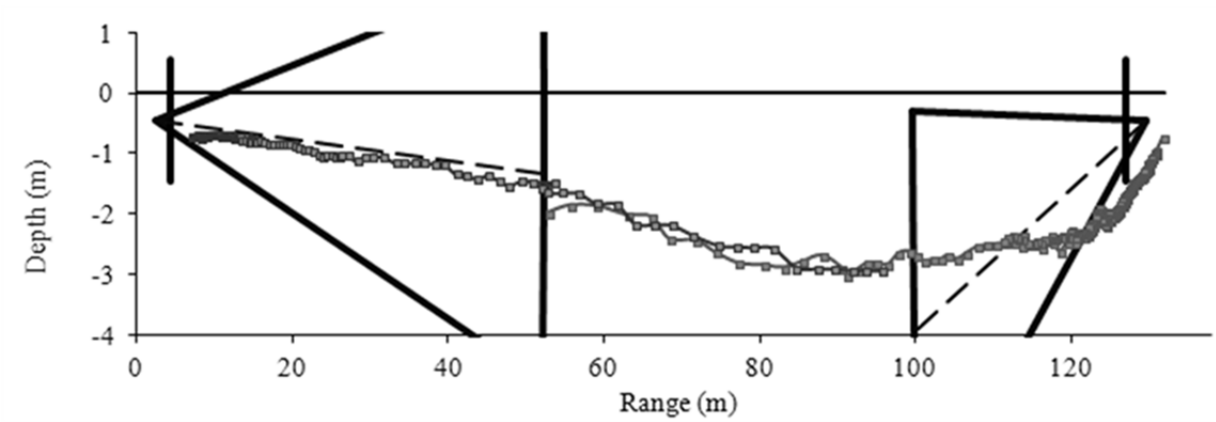

Note: A river bottom profile with modeled DIDSON beams showing the region ensonified by the shore-based DIDSONs (bottom).

Figure 48.–Kenai River cross-river fish distributions from shore-based and mobile surveys showing the raw counts (top) and the percent of total fish in each range bin (middle).

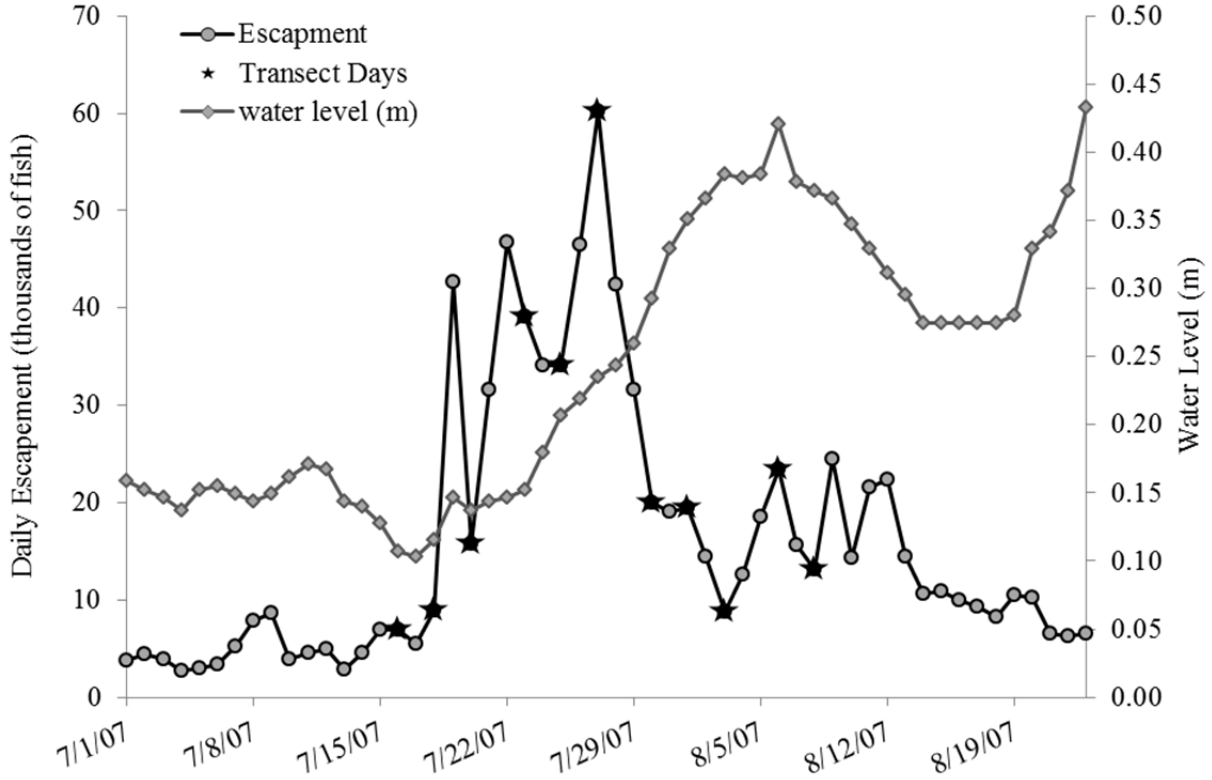

Figure 49.–Daily escapement and water level for the 2007 field season at the Kenai River with the cross-river sampling days marked with stars.

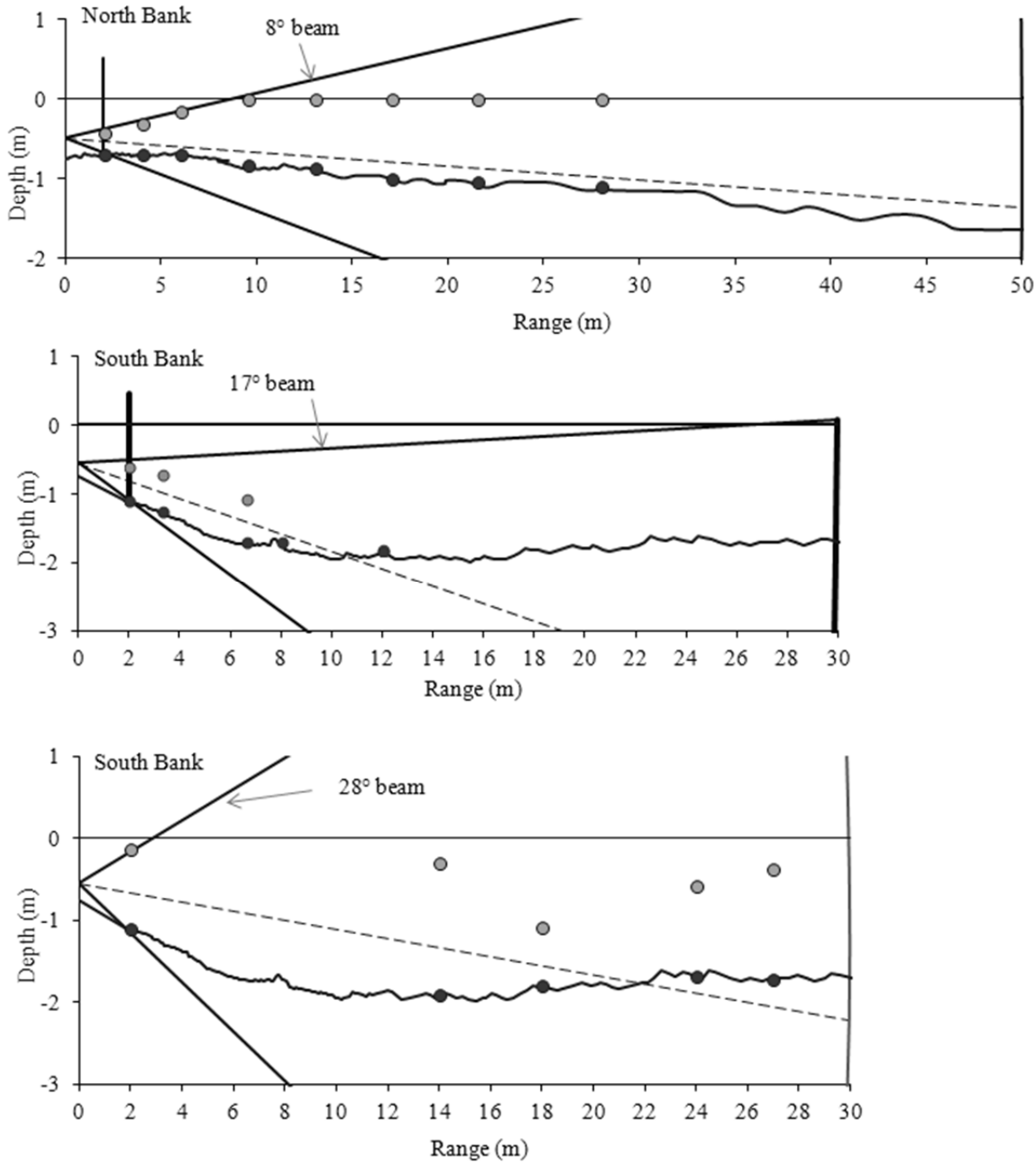

Figure 50.–Kenai River bottom profiles with modeled sonar beams representing horizontally positioned (top, middle) and vertically positioned (bottom) DIDSONs and the results from mapping the vertical detection limits of the beams using a stainless steel sphere along the north bank and a BB-filled plastic sphere along south bank (circles). The size of both targets is similar acoustically to a sockeye salmon.

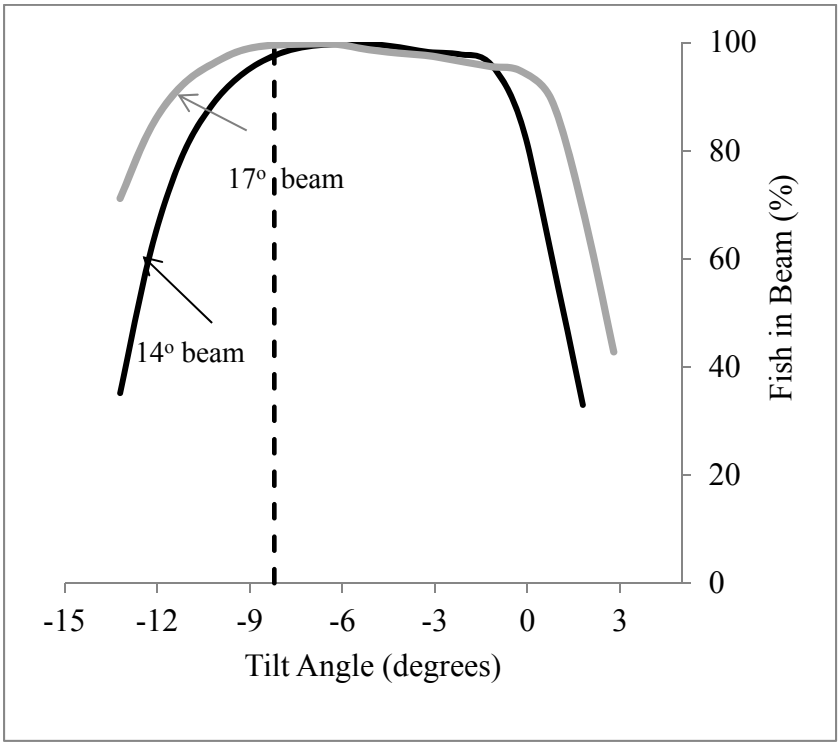

Note: The vertical dotted line marks the average tilt angle used to sample fish. The percentage of fish within the horizontal beam is increased slightly by raising the transducer, Kenai River south bank, 2007.

Figure 51.–The effect of changing the tilt angle on the percentage of migrating fish detectable to a horizontally positioned DIDSON (shown for 14º and 17º beams).

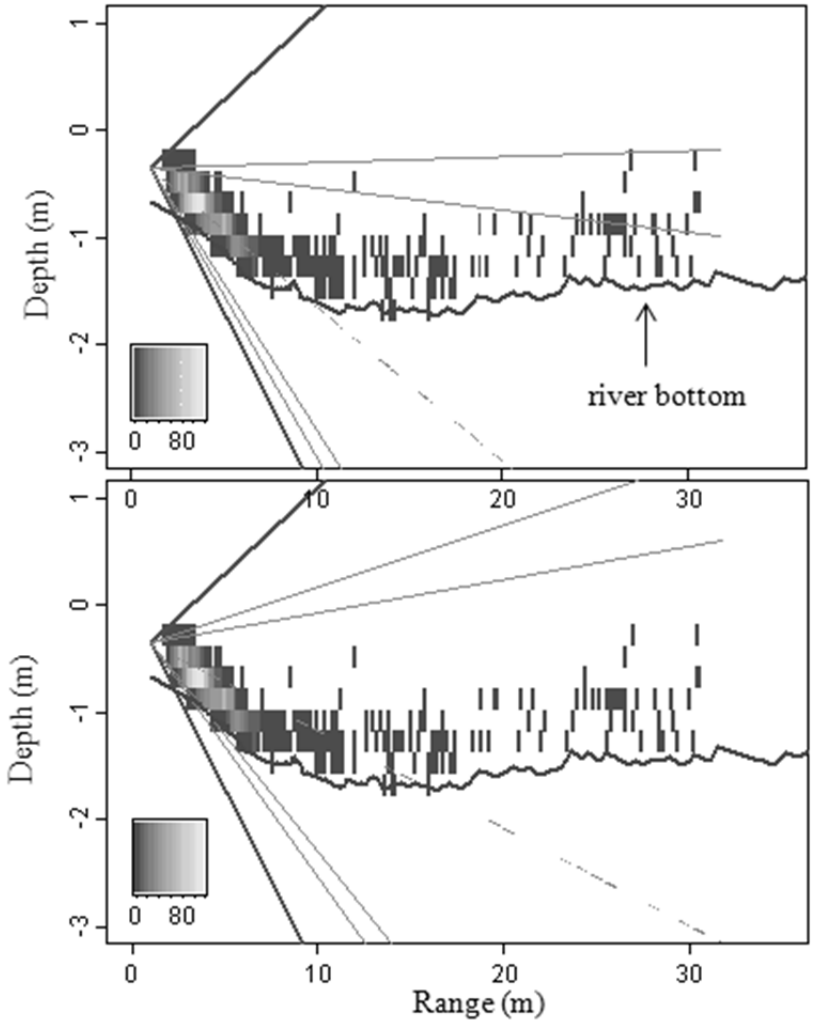

Note: Three modeled sonar beams are shown, the outermost beam triangle represents the composite beam oriented vertically, the innermost beams represent a horizontal orientation showing the nominal beam size (17°) and a more realistic beam size of 14° based on work using a salmon-size target.

Figure 52.–Kenai River south bank, 2006, density plots of randomly selected fish coordinates with modeled sonar beams illustrating the traditional DIDSON tilt angle used at fish-counting sites (top) and the raised tilt angle that encompassed the largest number of fish (bottom).

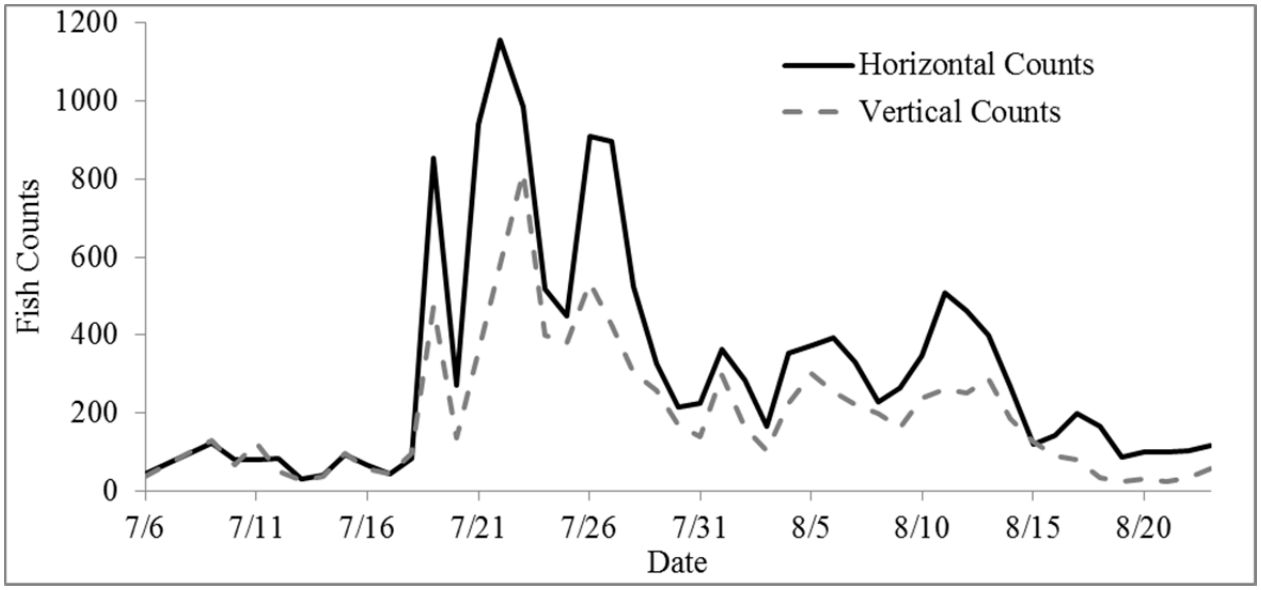

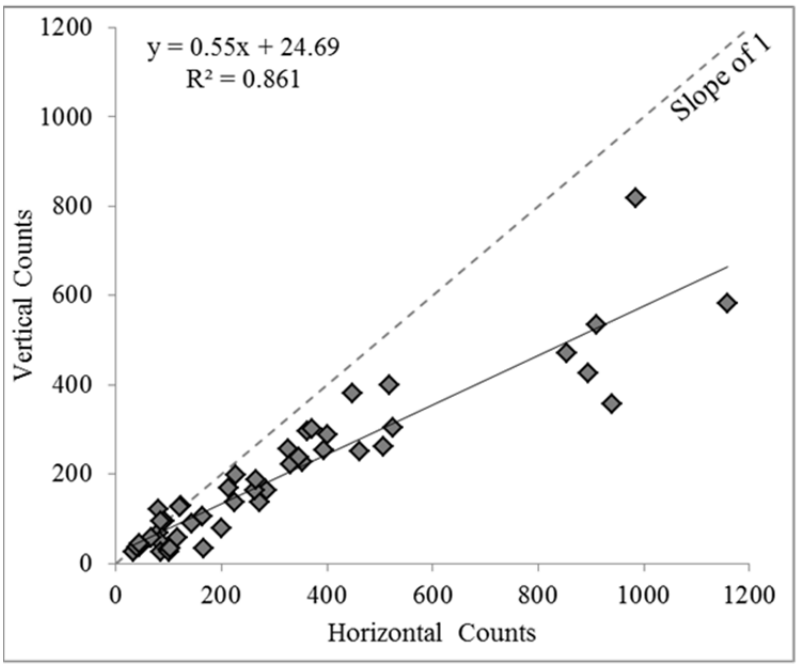

Note: Sampling alternated between them within an hour to avoid cross-talk, Kenai River south bank, 2007.

Figure 53.–Paired daily fish counts (top) and linear regression comparison (bottom) obtained from DIDSONs, one with the composite beam positioned vertically and the other horizontally.

APPENDIX A: YENTNA RIVER EQUIPMENT SETUP

Appendix A1.–Yentna River equipment setup for 2010.

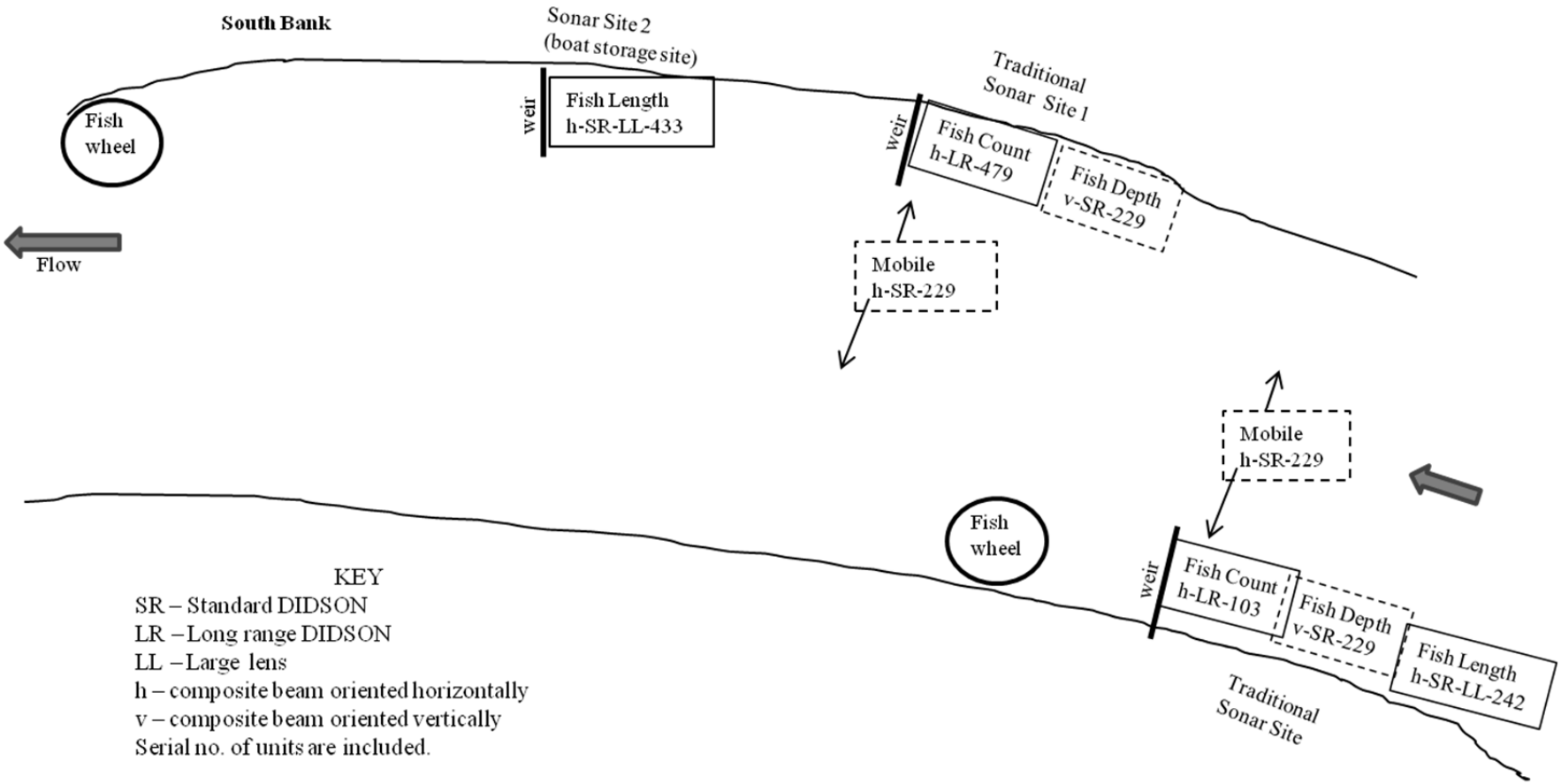

Appendix A2.–Yentna River equipment setup for 2011.

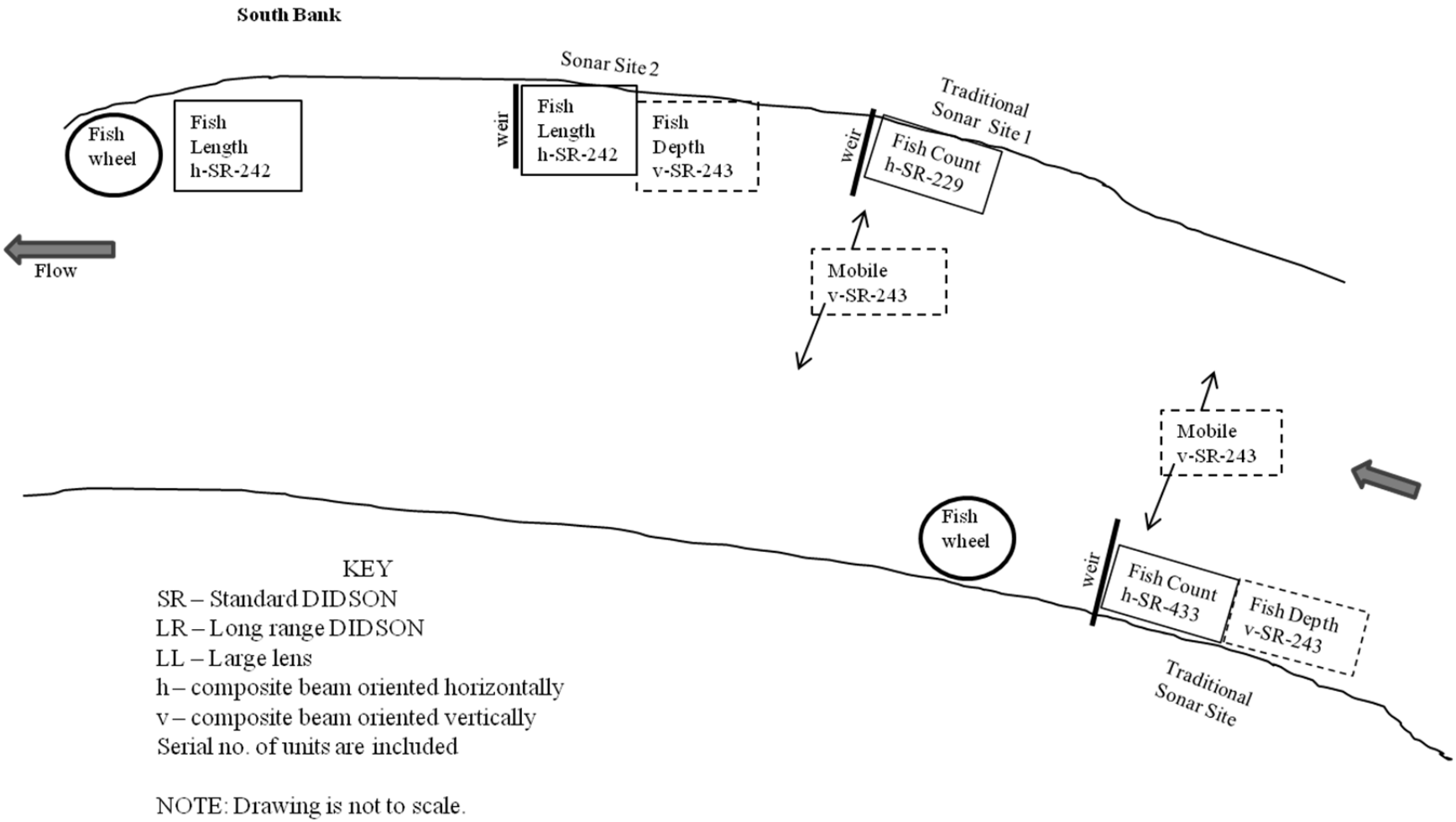

Appendix A3.–Yentna River equipment setup for 2012.

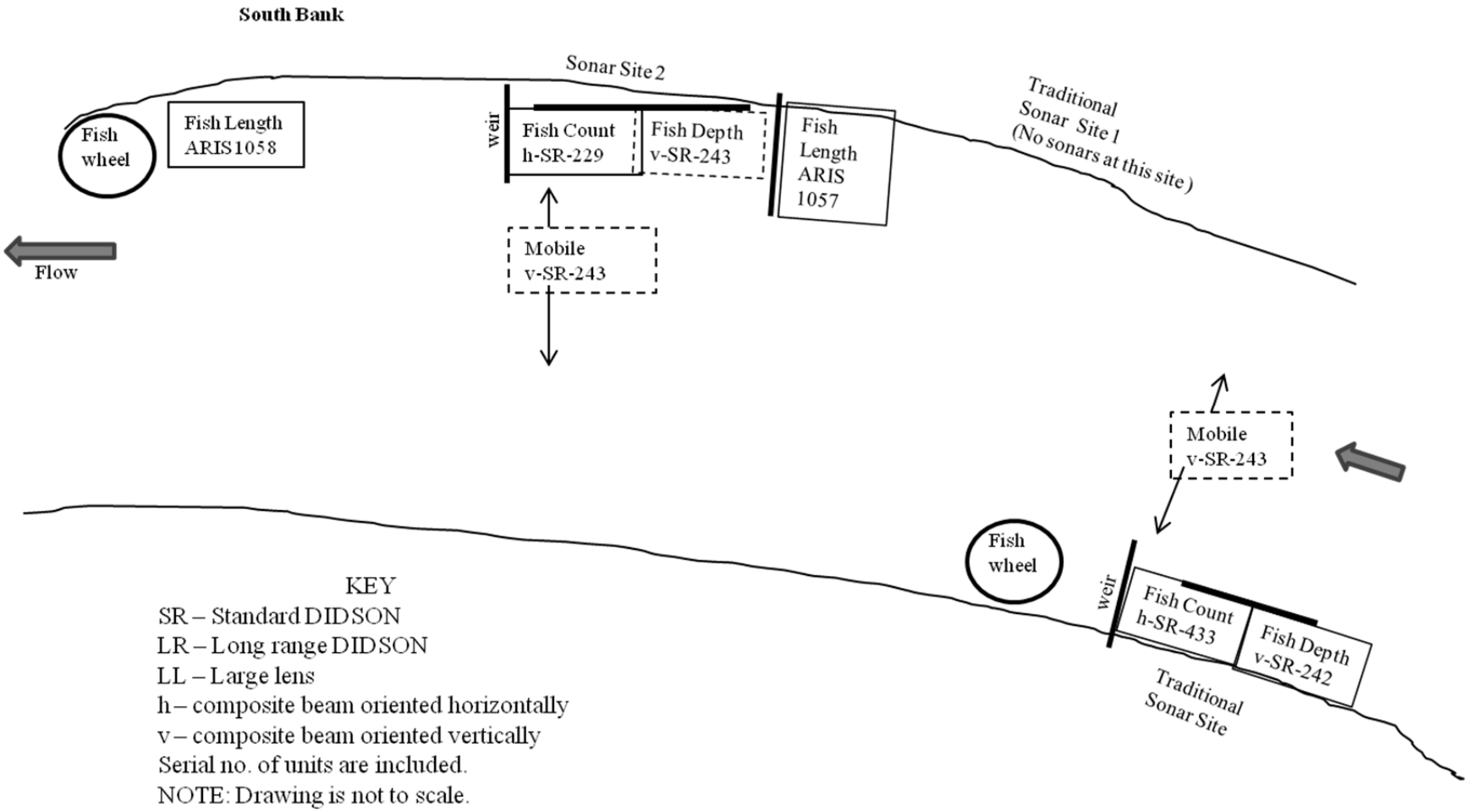

Appendix A4.–Satellite view of Yentna River sonar site, 2012 setup.

APPENDIX B: YENTNA RIVER WATER LEVEL CHANGES

Appendix B1.–Yentna River water level changes at the sonar site, 2011–2012.

Date	Difference (m)
2011	
7/13	0.000
7/16	-0.229
7/22	0.040
7/28	0.000
7/31	-0.082
8/9	-0.427
2012	
7/13	0.000
7/16	-0.064
7/19	0.037
7/22	-0.674
7/25	-0.698
7/28	-0.491
7/31	-0.911
8/6	-0.622
8/9	-0.155

APPENDIX C: CROSS-RIVER SURVEY INFORMATION

Appendix C1.–The number of transects, time sampled, and fish counted during the cross-river study.

Site	Stations (m from shore)	Year	DIDSON orientation	No. Transects[b]	Sample Time per station (min)	Total time sampled (all stations) (min)	Total Fish counted	Comments
Yentna NB	15, 25, 35, 50, 75, 100[a]	2009	horiz	4	5	120	3	not used
		2010	horiz	10	5	300	28	no stations omitted
		2010	vertical	2	5			not used
		2011	vertical	9	5	270	42	no stations omitted
		2012	vertical	9	5	270	56	no stations omitted
Yentna SB	15, 25, 35, 50, 75, 100, 125[a]	2009	horiz	3	5	105	9	not used
		2010	horiz	9	5	290	42	stations 1-5 omitted Aug 5 due to heavy debris
		2010	vertical	2	5			not used
		2011	vertical	9	5	315	141	no stations omitted
		2012	vertical	9	5	315	261	no stations omitted
Copper	10, 20, 30, 50, 70, 90, 110, 130, 262, 387, 317, 328, 340	2005	horiz	1	15	195	65	
	10, 20, 30, 40, 60, 80, 100, 140, 180, 220, 260, 280, 300, 310, 320, 330, and 340	2006	horiz	8	10 & 5	1040	292	
Kenai	7, 7, 17, 29, 39, 49, 64, 84, 94, 104, 122, 122	2007	horiz	22	5	1430	1661	

[a] Additional stations were sampled but the data were truncated to halfway across the river to avoid double counting fish.

[b] Transects were also conducted on Aug 11, 2010, and July 7 and 10, 2011, but resulted in no fish at any station and were excluded from this table.

APPENDIX D: YENTNA RIVER FISH COUNTS FROM VERTICAL AND HORIZONTAL DIDSONS

Appendix D1.–Yentna River north bank daily fish counts from vertically and horizontally oriented DIDSONs.

	2010			2011			2012		
Date	vertical	horizontal	h/v %	vertical	horizontal	h/v %	vertical	horizontal	h/v %
7/7/12				8	4	50	17	19	112
7/8/12				28	29	104	11	5	45
7/9/12				41	36	88	3	4	133
7/10/12	15	21	140	16	10	63	21	16	76
7/11/12	26	23	88				15	12	80
7/12/12	9	13	144				13	15	115
7/13/12				6	13	217	56	76	136
7/14/12				54	54	100	88	59	67
7/15/12	40	63	158	132	125	95	57	87	153
7/16/12	192	229	119	74	108	146	90	81	90
7/17/12	524	614	117				333	333	100
7/18/12	681	773	114				777	838	108
7/19/12	365	391	107				367	367	100
7/20/12							497	540	109
7/21/12	86	115	134				339	378	112
7/22/12	494	610	123	518	667	129	375	345	92
7/23/12	585	772	132	868	1,068	123	628	562	89
7/24/12	339	368	109	528	585	111	571	499	87
7/25/12				186	187	101	443	463	105
7/26/12							1,249	1,064	85
7/27/12							1,616	1,669	103
7/28/12				295	335	114	1,865	2,065	111
7/29/12				1,457	1,744	120	1,813	2,139	118
7/30/12	154	177	115	726	762	105	947	1,158	122
7/31/12	1,087	1,242	114	351	393	112	693	772	111
8/1/12	1,171	1,351	115				588	530	90
8/2/12	579	740	128				582	754	130
8/3/12							540	597	111
8/4/12							356	367	103
8/5/12							359	337	94
8/6/12							524	580	111
8/7/12							599	883	147
8/8/12	59	51	86				393	419	107
8/9/12	219	214	98	127	105	83	213	207	97
8/10/12	205	221	108	308	285	93	108	136	126
8/11/12	144	118	82	414	518	125	98	135	138
8/12/12				80	117	146	15	32	213
Total	6,974	8,106	116	6,217	7,145	115	17,259	18,543	107
All years	30,450	33,794	111						

Appendix D2.–Yentna River south bank daily fish counts from vertically and horizontally oriented DIDSONs.

	2010			2011			2012		
Date	vertical	horizontal	h/v %	vertical	horizontal	h/v %	vertical	horizontal	h/v %
7/7/12	2	9	450				14	14	100
7/8/12	13	10	77				14	17	121
7/9/12	1	0	0				13	8	62
7/10/12				17	15	88	10	12	120
7/11/12				71	29	41	21	10	48
7/12/12	37	32	86	55	35	64	31	20	65
7/13/12	178	196	110	16	9	56	90	49	54
7/14/12	685	649	95				88	66	75
7/15/12	395	394	100				150	128	85
7/16/12				86	39	45	99	75	76
7/17/12				306	152	50	827	480	58
7/18/12				2,738	2,422	88	987	670	68
7/19/12	524	533	102	4,658	4,571	98	449	303	67
7/20/12	3,083	3,068	100	1,359	1,801	133	812	728	90
7/21/12	1,665	1,733	104	810	676	83	1,029	845	82
7/22/12							2,044	1,701	83
7/23/12							4,155	3,595	87
7/24/12	596	604	101				3,628	2,995	83
7/25/12	2,041	1,789	88	579	394	68	2,416	2,253	93
7/26/12	1,390	1,372	99	1,469	990	67	5,758	5,839	101
7/27/12	916	903	99	647	424	66	8,421	8,835	105
7/28/12	1,880	1,814	96				6,367	6,568	103
7/29/12	2,270	2,232	98				7,303	6,579	90
7/30/12	861	822	95				4,390	3,579	82
7/31/12				563	494	88	2,587	2,494	96
8/1/12				1,097	623	57	2,131	2,001	94
8/2/12	487	523	107	1,337	664	50	2,886	2,560	89
8/3/12	1,200	1,225	102	621	49	8	1,078	923	86
8/4/12	1,149	1,212	105	414	20	5	1,507	1,314	87
8/5/12	296	293	99	376	35	9	2,010	1,979	98
8/6/12	188	158	84	686	122	18	1,554	1,387	89
8/7/12	370	317	86	1,761	468	27	1,003	998	100
8/8/12	117	126	108	1,714	843	49	472	426	90
8/9/12				1,073	637	59	210	233	111
8/10/12							187	180	96
8/11/12							163	117	72
8/12/12							95	70	74
Total	20,344	20,014	98	22,453	15,512	69	64,999	60,051	92
All years	107,796	95,577	89						

Appendix D3.–Yentna River north bank hourly fish counts from vertically and horizontally oriented DIDSONs.

	No.	2010		No.	2011		No.	2012	
Hour	of hours	vertical	horizontal	of hours	vertical	horizontal	of hours	vertical	horizontal
0	15	490	573	14	519	480	37	1,513	1,548
1	15	473	533	14	387	489	36	1,329	1,482
2	15	411	458	14	381	390	35	1,201	1,318
3	15	445	466	14	334	394	34	1,050	1,201
4	15	275	295	14	138	257	35	507	650
5	15	264	277	14	105	139	35	427	487
6	15	200	241	13	79	100	34	378	380
7	15	236	282	15	125	124	31	358	350
8	15	154	181	14	145	91	29	418	247
9	15	266	268	14	223	165	35	368	428
10	15	271	306	13	380	269	37	1,049	559
11	14	360	380	13	128	441	36	469	930
12	13	206	237	11	206	159	35	475	516
13	11	193	218	10	171	179	34	553	460
14	11	218	234	10	142	256	35	362	581
15	11	242	274	10	183	200	33	559	458
16	13	265	323	12	234	390	34	629	642
17	14	263	347	12	332	383	34	550	821
18	15	203	322	13	729	297	36	1,375	1,467
19	15	391	587	14	350	828	36	969	849
20	15	288	350	14	219	334	35	784	1,129
21	15	301	357	15	262	244	36	659	615
22	15	302	287	15	266	292	36	694	760
23	15	257	310	14	179	244	36	583	665
Total	342	6,974	8,106	316	6,217	7,145	834	17,259	18,543

Appendix D4.–Yentna River south bank hourly fish counts from vertically and horizontally oriented DIDSONs.

	No.	2010		No.	2011		No.	2012	
Hour	of hours	vertical	horizontal	of hours	vertical	horizontal	of hours	vertical	horizontal
0	18	946	899	19	1,230	593	37	3,642	2,427
1	17	1,069	1,075	19	1,212	842	37	3,701	3,097
2	17	976	931	19	1,148	941	36	3,356	3,027
3	14	702	700	19	1,245	868	35	3,512	3,095
4	14	594	561	18	697	539	35	2,468	2,574
5	14	457	461	18	460	337	34	1,863	1,839
6	19	524	518	19	641	361	35	2,309	2,078
7	17	554	524	19	571	282	35	1,654	1,935
8	18	483	502	18	748	497	36	2,200	2,074
9	18	774	754	19	986	647	37	3,376	2,191
10	18	858	854	18	1,190	730	37	3,486	3,094
11	18	1,030	1,059	17	769	817	37	2,614	2,608
12	15	749	626	14	788	600	35	2,583	2,637
13	13	736	727	16	878	746	27	1,746	1,874
14	12	699	779	16	1,256	779	26	2,456	1,876
15	14	777	795	15	829	805	25	2,327	2,468
16	14	867	873	17	937	671	33	2,495	3,001
17	15	979	967	17	997	630	35	2,606	2,604
18	18	1,075	1,064	19	1,445	705	35	3,714	2,585
19	18	1,508	1,339	19	1,036	882	35	3,565	3,801
20	18	1,076	1,046	19	925	624	35	2,533	2,528
21	17	1,004	1,024	18	848	633	36	2,356	2,570
22	18	978	992	18	921	520	36	2,300	1,951
23	18	929	944	19	696	463	36	2,137	2,117
Total	392	20,344	20,014	429	22,453	15,512	825	64,999	60,051